New excavations in old sites. The Late Neolithic necropolis from Iclod, Cluj County, Romania (I)[1]

Mihai GLIGOR[2]*, Ana FETCU[3], Doru BOGDAN[4], Marian-Bogdan CONDURĂȚEANU[5]

Abstract. The aim of this paper is to present the results of the archaeological excavations conducted between 2015–2017 in the Late Neolithic necropolis from Iclod (Cluj County, Romania). Initiated by contemporary infrastructure projects, the investigations targeted a previously unexplored southeastern sector of the site. A total of 24 new graves were identified, enriching the osteoarchaeological record of this Late Neolithic necropolis. Historically, systematic research at the Iclod site began in 1973 under the supervision of Gh. Lazarovici, revealing a complex Neolithic settlement comprising habitation areas, defensive structures, and burial zones, distributed across four distinct sectors (A, B, C, and D). Iclod A, severely impacted by soil erosion due to fluctuations in the course of the Someşul Mic River, has yielded around 40 graves, whereas Iclod B, the main habitation area, with its funerary area – Cemetery B, has produced around 74 graves over several decades of archaeological research. Sex determination was possible for 15 adult individuals (62.5% of the total sample of 24). Of these, eight were female (53.3% of the sexed adults, 33.3% of the total sample), and seven were male (46.7% of the sexed adults, 29.2% of the total sample). Age-at-death assessment shows that young adults comprise the largest proportion of the sample (33.3%), followed by middle adults (25%). Adolescents represent 16.7% of the individuals, children account for 12.5%, and old adults are represented by a single case (4.2%). The deceased were predominantly buried in dorsal decubitus, with variations in limb positioning, mostly oriented along the W-E axis.

[1] The present study (Part I) focuses on the archaeological and anthropological investigation of the Iclod necropolis (2015–2017 excavations), encompassing the research history of the site, the osteoarchaeological analysis of the skeletal remains, radiocarbon dating results, and an interpretative synthesis of the results in the broader context of Neolithic and Eneolithic burial practices in Transylvania and Crișana.

[2] History, Archaeology and Patrimony Department, "1 Decembrie 1918" University of Alba Iulia, Alba Iulia, Romania; mihai.gligor@uab.ro.

[3] Independent researcher, Alba Iulia, Romania; fetcuana@gmail.com.

[4] Independent researcher, Cluj-Napoca, Romania; dorubogdan@yahoo.com.

[5] Doctoral School of History, "1 Decembrie 1918" University of Alba Iulia, Alba Iulia, Romania; condurateanu.marian.sdi20@uab.ro.

* Corresponding author: mihai.gligor@uab.ro.

CC BY NC SA

Anthropological analyses for our subset suggest high mortality rates among young adults, particularly females, most likely indicative of gender-related risks and occupational hazards. The proportion of non-adults highlights juvenile vulnerability typical of Neolithic populations. Palaeopathological assessment identified common health issues, specific for prehistoric populations, such as metabolic stress indicators, dental pathologies, degenerative joint diseases, and signs of infections. Radiocarbon dating, conducted on selected non-adult bone fragments, provided crucial chronological reference points, facilitating a clearer understanding of the site's temporal context and enabling a more accurate integration of the recent findings with previously documented research.
Keywords*:* prehistoric population structure; palaeopathology; biological profile; prehistoric cemeteries; radiocarbon dating.

Săpături noi în situri vechi. Necropola aparținând neoliticului târziu de la Iclod, județul Cluj, România (I). Scopul acestei lucrări este de a prezenta rezultatele cercetărilor arheologice realizate între anii 2015–2017 la situl neolitic de la Iclod (județul Cluj, România), inițiate ca urmare a unor proiecte de dezvoltare, care au avut drept obiectiv cercetarea unui sector sud-estic, neexplorat anterior. Au fost identificate în total 24 de morminte noi, îmbogățind registrul osteoarheologic al acestei necropole. Din punct de vedere istoric, cercetările sistematice de la Iclod au început în anul 1973, sub coordonarea lui Gh. Lazarovici, și au relevat o așezare complexă, formată din zone de locuire, structuri defensive și spații funerare, repartizate în patru sectoare distincte (A, B, C, D). Iclod A, afectat sever de modificările cursului Someșului Mic, a relevat până acum 40 de morminte, în timp ce Iclod B, zonă centrală de locuire și spațiu funerar – Cimitirul B, a oferit circa 74 de morminte descoperite pe parcursul mai multor decenii. Determinarea sexului a fost posibilă pentru 15 indivizi adulți (62,5% din totalul eșantionului de 24), dintre care opt sunt femei (53,3% dintre adulții determinați, 33,3% din total) și șapte sunt bărbați (46,7% dintre adulții determinați, 29,2% din total). Evaluarea vârstei la deces arată că adulții tineri reprezintă cea mai mare proporție a eșantionului (33,3%), urmați de adulții de vârstă mijlocie (25%). Adolescenții constituie 16,7% dintre indivizi, copiii însumează 12,5%, iar adulții vârstnici sunt reprezentați de un singur caz (4,2%). Scheletele au fost descoperite predominant în decubit dorsal, cu variații ale poziției membrelor și orientare majoritară pe axa V-E. Pentru lotul în discuție, analizele antropologice sugerează o mortalitate ridicată printre adulții tineri, în special femei, indicând potențiale riscuri asociate genului și activităților ocupaționale. Proporția mare de non-adulți reflectă vulnerabilitatea juvenilă specifică populațiilor neolitice. Evaluările paleopatologice au evidențiat afecțiuni comune, precum stres metabolic, patologii dentare, boli degenerative articulare și semne ale unor procese infecțioase. Datarea cu radiocarbon, realizată pe schelete selectate din rândul non-adulților, oferă repere cronologice importante, contribuind la clarificarea cadrului temporal al sitului și permițând o mai bună integrare a noilor descoperiri în contextul general al celor precedente.
Cuvinte cheie: demografie preistorică; paleopatologie; profil biologic; cimitire preistorice; datare radiocarbon.

Site background

The archaeological site of Iclod (Cluj County, Romania) is located in the northwestern part of the Transylvanian Depression, on the low left terrace of the Someșul Mic River, just east of the modern village of Iclod (**Pl. I/1**). The site first entered the archaeological record over a century ago, following the discovery of

two inhumation graves by M. Roska. The area in which the graves were initially uncovered was designated as **Iclod A** (Roska 1942, p. 193–195, fig. 234–235; Lazarovici 1977, p. 212–213; 1983, p. 50; 1991, p. 5–6; Lazarovici, Bulbuc 1983, p. 161; Mischka 2012, p. 155) and since then, the site has come to occupy a key position in understanding the transition between the Late Neolithic and the Early Copper Age in Transylvania (Maxim 1999, p. 131–133; Mischka 2012, p. 154; Diaconescu, Lazarovici, Tincu 2013, p. 52–53; Hervella *et alii* 2015).

The initial field investigations began in 1972 with surface surveys, which led to the recovery of the funerary inventory from seven graves, labelled Gr. 3 to Gr. 9. Systematic archaeological research at the Iclod site began one year later, led by a team from the National Museum of Transylvanian History under the direction of Gh. Lazarovici, in what was defined later on as **Iclod C**. Further excavations, carried out in collaboration with Z. Kalmar-Maxim, focused on **Iclod A**, that was severely affected by riverbank erosion. After ten years of research, around 40 graves had been unearthed within this perimeter (Lazarovici, Bulbuc 1983; Lazarovici 1983, p. 50–54, 61; 1991, p. 5–7).

In the following years research was expanded to all sectors **Iclod A**, **B**, **C** and **D**, revealing a Neolithic settlement that kept developing and increasing over time, enclosed by three ditches and four palisades (**Iclod B** and **D**), with two burial areas (**Cemetery A** and **Cemetery B**, the latter in **Iclod B**) and additional settlement features in **Iclod C** (Lazarovici 1983, p. 50–54, fig. 1–4; 1991, p. 5–9; Lazarovici, Lazarovici 2006, p. 625–626; Maxim 1999, p. 81–91) (**Pl. I/2–3**).

Iclod B encompassed the central habitation zone and funerary areas (designated as **Cemetery B**), consisting of burials dispersed within dwellings, ditches, and palisade corridors. By the year of 1981, 25 graves had been excavated from here. **Iclod C**, identified in 1976, revealed Neolithic habitation structures, but no burials (Lazarovici 1991, p. 7–8; Maxim 1999, p. 82; Simalcsik 2023a, p. 256–257).

Excavations between 1982–1989 progressively uncovered more graves – Gr. 26 to Gr. 43, while also documenting habitation features and fortification elements (Dumitru-Kogălniceanu 2009, p. 16; Lazarovici, Kalmar 1986, p. 25–39; 1987; 1988; 1989; Lazarovici, Kalmar-Maxim 1990–1993; Lazarovici, Maxim 1989–1993). Between 1993 and 1996, three more graves were unearthed, Gr. 51 to Gr. 53 (Lazarovici 1996a; 1996b; Lazarovici *et alii* 1995; 1997a; 1997b).

Research resumed in 2002 in the north-western part of the site, yielding 15 additional graves (Gr. 54 to Gr. 68) along with domestic features (Maxim *et alii* 2003, p. 146). The final documented campaign in 2005 focused at the point of the *Western Gate*, where two more graves were recovered (Gr. 69 and Gr. 70) (Maxim, Bindea, Lazarovici 2006).

In 2008 and 2010, C. Mischka performed geomagnetic surveys at the site, covering over 11 ha and revealed significant Neolithic structures. The largest features identified are three concentric ditches, with diameters between 140 and 240 meters, enclosing areas from 1.7 to 4.7 ha. Two outer ditches connect in the south, suggesting the presence of a gate and indicating their contemporaneity. The settlement's layout is marked by numerous round anomalies corresponding to settlement pits, and by rectangular ones interpreted as house structures. At least 33 habitation structures are visible, arranged in three concentric rings in the northwest and two parallel rows in the northeast, hinting at dynamic settlement processes, including expansion and contraction phases. Surrounding the entire site is a triple ring of small linear anomalies, possibly remains of palisades, although their existence remains hypothetical due to weak magnetogram evidence. If confirmed, the palisade system would enclose an area of about 10.6 ha (Mischka 2012, p. 155–158, 162, fig. 5–6, 11).

Between 2015 and 2017, a research team from the "1 Decembrie 1918" University of Alba Iulia, led by M. Gligor, conducted rescue excavations in the previously unexplored southeastern sector of the site. During these campaigns, amongst other features, a total of 24 Neolithic inhumation graves were identified, all culturally attributed to the Iclod group (Fetcu 2018; 2021; Gligor, Fetcu, Bogdan 2018; Gligor *et alii* 2018) (**Pl. I/2–3**).

In 2021, a team coordinated by P. Pupeză, undertook a new series of preventive excavations in the north-eastern part of the site, extending into the area of the ditches and palisade structures previously identified through geomagnetic surveys by C. Mischka, also revealing eight additional graves (Pupeză 2022, Pl. I/2–4, II, III/1–5).

Cemetery A and Cemetery B

Cemetery A was used during the early phases of Neolithic occupation. This area suffered extensive damage as a result of the river's shifting course, but despite this, around 40 burials were researched. Beginning with 1982, the funerary space identified within or adjacent to various phases of the settlement's fortification system was designated as **Cemetery B** (Lazarovici 1983, p. 50, 52, 60–61; 1991, p. 5–8; Lazarovici, Bulbuc 1983; Lazarovici, Kalmar 1987, p. 9–39; Lazarovici, Kalmar-Maxim 1990–1993; Lazarovici *et alii* 1994; 1995; 1996a; Maxim 1999, p. 88, 90; Diaconescu, Lazarovici, Tincu 2013, p. 49). However, **Cemetery B** does not represent a conventional cemetery but rather a cluster of graves found within domestic structures or positioned between palisades and defensive ditches, as the settlement continued to change and expand (Simalcsik 2023a, p. 257, Pl. I, II/1). Depending on the source consulted, excavations in this area carried out over

several decades, investigated a total of 69 (Diaconescu, Lazarovici, Tincu 2013, p. 49) or 74 graves (Maxim, Bindea, Lazarovici 2006, p. 177)[6].

Funerary practices

The majority of the deceased were laid in a supine position in simple rectangular pits (Dumitru-Kogălniceanu 2009, p. 482, 484–488, 491–494, 496, 500–510, 513–524, 525, 528, 534–535). Other burial positions were less frequent: right lateral decubitus (4.39%) (Dumitru-Kogălniceanu 2009, p. 497, 512, 533–534), left lateral flexed (2.63%) (Dumitru-Kogălniceanu 2009, p. 498, 514, 525), lying on the left lateral decubitus (1.75%), and flexed on the right side (0.88%) (Dumitru-Kogălniceanu, 2009, p. 489)[7]. Among the burials with skeletons placed in a supine position, the analysis of arm placement indicates a preference for positioning the arms bent at the elbow, with the hands resting on or near the pelvis in 23.44% of cases. Arms extended along the sides of the body are represented in 9.38% of cases. Other combinations are present such as one hand placed on the chest, shoulder, or face (Dumitru-Kogălniceanu 2009, p. 78–88, 480–535, fig. 32, 34, 36, tab. 11).

Grave orientation at Iclod has previously been studied by researchers from the Cluj-Napoca Astronomical Observatory. They concluded that most graves fall within the solar arc, defined by the sun's position on the horizon between solstices (Maxim *et alii* 2002, p. 19–30). Graves that fall outside this arc generally contain fewer ceramic vessels and have been attributed to a later phase of the settlement, which may indicate a shift in funerary practices, correlated with economic transformations that suggest a transition to the Bronze Age. A notable concentration of graves is oriented toward the W (14.91%) and W-NW (8.77%), while other directions are only weakly represented. It is worth noting that some graves with extreme orientations correspond to atypical cases: burials in flexed or lateral positions in **Cemetery A** (Gr. 37 oriented toward the SSW, Gr. 11 to the NW), or cenotaphs (Gr. 13 to NW). In **Cemetery B**, the most aberrant orientations are those of Gr. 18 (NNV-SSV) and Gr. 51 (oriented S-N), associated with individuals presumed to have been hunters within the community (Dumitru-Kogălniceanu 2009, p. 94–97, fig. 41–42; Maxim *et alii* 2002, p. 20, 25–28, fig. 7–9, table 2; Simalcsik 2023a, p. 266–267, Pl. II, V).

[6] Given the extent of the research, some discrepancies and interpretative variations are to be expected, as the necropolis has been investigated over multiple years, by different teams, and under varying methodological frameworks. These factors contribute to occasional inconsistencies in documentation, contextual assessments, or typological attributions.

[7] Lateral decubitus referes to the sketelal remains being found lying on the side (right or left), with the limbs extended; lateral flexed refers to an individuals' skeletal remains being found with the upper, lower limbs flexed at the arms, hips, knees, a posture resembling a crouched position.

Grave goods include ceramic vessels, flint, obsidian, opal, and shale tools, stone axes, bone and antler implements – mostly placed at the head and feet area, as well as jewellery made of *Spondylus* beads placed at the neck and chest, wrists, and feet. Meat offerings were likely part of the burial ritual, as faunal remains were discovered in association with the deceased (Lichter 2001, Abb. 97, 102; Lazarovici 1991, p. 8–9; Maxim 1999, p. 88–91; Lazarovici *et alii* 1996, p. 272, fig. 4, Pl. I–V). Additionally, red ochre was found in some graves, either as concentrated lumps placed beside the deceased or as deposits inside ceramic vessels located nearby (Lazarovici, Kalmar-Maxim 1987–1988, p. 1007).

Anthropological profiles

Several anthropologists analysed the human remains, at different times. E. M. Georgescu and L. Georgescu analysed the skeletal remains found until 1977 (81 individuals, 40 from **Cemetery A** and 41 from **Cemetery B**) (Georgescu, Georgescu 1999). Z. Vincze determined the biological profile of individual Gr. 42 found in 1988 (Vincze 1993), and G. Miu examined the remains from the 1990 to 1993 campaigns (25 skeletons) (Miu 2004, apud Dumitru-Kogălniceanu 2009, p. 18). A. Simalcsik reanalysed the skeletal remains of the two presumed hunters from Gr. 18 and Gr. 51 – **Cemetery B** (Simalcsik 2023a, p. 259–265, Pl. I–V; 2023b, p. 186–187, 190, 192, Tab. 1–2).

Detailed data concerning the Iclod Neolithic population comes from the lot analysed by E. M. Georgescu and L. Georgescu. Mortality patterns indicate a higher proportion of male deaths in both cemeteries (51.22% in **Cemetery A** and 40.97% in **Cemetery B**), while child mortality (ages 0–14) was relatively low (12.14% and 7.3%, respectively). Life expectancy was estimated at approximately 28.4 years in **Cemetery A** and 26.8 years in **Cemetery B** for the youngest age group (0–14), and around 20–22 years for individuals aged 20–30. No individual was recorded as living past the age of 60, although a few reached around 55 years of age. The dominant anthropological type was gracile Mediterranean, with attenuated proto-Europoid and occasional Alpinoid traits, and cranial forms ranging from mesocranial and meso-dolichocranial to meso-brachycranial. Morphofunctional observations revealed robust muscular insertions (triceps, deltoid, pectoral), marked femoral and tibial modifications (platimeria, platycnemia, torsion), and skeletal features associated with intense physical activity, likely related to agriculture and possibly nomadic behaviours. Estimated stature ranged from 161.1 to 177.3 cm for males and 148.2 to 169.4 cm for females, with one female reaching a height of 169.78 cm (Georgescu, Georgescu 1999, p. 358–360).

An in-depth study concerning the skeletal material from Iclod was published by A. Simalcsik, who synthesised what is anthropologically known up to the present

time, about the human remains discovered at the site and argued for a systematic, modern, context integrated reevaluation of the osteological collection (Simalcsik 2023b, p. 182, 185–96, Tab. 1–2). The same author provided a renewed assessment of the skeletal remains belonging to male individuals (Gr. 18 and Gr. 51) from **Cemetery B** – unearthed during archaeological research campaigns from 1977, respectively 1994, who stand out due to the rich and diverse funerary inventories, but also through the orientation of their graves – NNE-SSV for Gr. 18, and S-N for Gr. 51 (Simalcsik 2023a, p. 266–267, Pl. I–V; 2023b, p. 186–187, 190, 192, Tab. 1–2); Lazarovici 1983, p. 52; 1991, p. 8–9; Lazarovici, Kalmar 1986, p. 25, 41; Lazarovici *et alii* 1995, p. 508–509, 519; Maxim *et alii* 2002, p. 20, 28; Dumitru-Kogălniceanu 2009, p. 94–97, fig. 41–42).

Gr. 18's remains belong to a robust middle-aged adult male (40–45 years), over 180 cm tall, with pronounced muscular attachments, a gracilized proto-Europoid phenotype, excellent dental health, and signs of past physiological stress (cribra cranii and healed tibial periostitis). Skeletal indicators point to intense physical activity: early-stage hip osteoarthritis, multiple enthesopathies, features linked to habitual squatting and dorsiflexion, and lower-limb stress injuries like "jumper's knee". These suggest high terrestrial mobility, probably consistent with a hunter's lifestyle (Simalcsik 2023a, p. 259–267, Pl. III–IV; 2023b, p. 186, Tab. 1). Gr. 51's skeletal remains belong also to a robust male individual, aged between 20–25 years old at death. The individual had a long, thick, dolichocranial skull and gracilized proto-Europoid traits. The dentition had supragingival calculus deposits but no other pathological conditions were observed. Anthropological and archaeological evidence from Iclod supports that these two men likely engaged in hunting activities. However, the physical stress markers observed on their skeletons may also result from other labor-intensive activities. These are consistent with life in a fortified Neolithic settlement, where constructing and maintaining enclosures would have required substantial physical effort using basic tools (Simalcsik 2023a, p. 262–267; 2023b, p. 190, 192, Tab. 1–2).

As part of an extensive study analysing mitochondrial DNA from 59 ancient individuals from present-day Romania, spanning the Neolithic to Bronze Age, three samples were obtained from skeletal remains excavated at the Iclod necropolis (from Cemetery B – I6/Gr. 20, I8/Gr. 68, I9/Gr. 67), in order to assess their genetic contribution to modern European populations. Individual I6 (G. 20) was a male aged 30–35 years, with an estimated stature of 164 cm. Despite the poor preservation of the skeleton, which included the complete destruction of the facial bones, Mediterranean-type features were identified. Individual I8 (G. 68) was an adult, oriented along N-S axis, with numerous incised and painted ceramic vessels placed on the left side of the body. Individual I9 (G. 67), a robust adult, oriented

N-S, with the hands resting on the pelvis. The associated grave inventory included a cylindrical cup near the head, an amphibolite axe and an opal scraper, a tall-footed cup near the hip, and a large cylindrical vessel at the feet. The research showed that their genetic profiles belonged to haplogroups J and T1a, which are commonly linked to Neolithic populations that came from the Near East. These individuals were grouped with others from nearby Neolithic sites (Vărăști and Sultana) in what the authors of the study defined as the M-NEO group. This group had a high frequency of haplogroup H (the most common in today's Europeans) and also included U haplogroups, linked to earlier European hunter-gatherers. Overall, the Iclod individuals shared many genetic traits with populations inhabiting the territory of what is now southeastern Romania during that period. Also, the DNA from Iclod and the other Middle Neolithic sites is genetically closer to modern Europeans than the DNA from earlier Neolithic groups. This supports the idea that a second wave of migration from northwest Anatolia, through the Balkans, had a bigger impact on the genetics of European populations than the first wave of farmers. So, the Iclod population offers strong evidence that the people living there were part of a larger movement that helped shape the genetic makeup of today's Europe (Hervella *et alii* 2015, p. 3, 5–6, 12–13, table 1–2; Rotea *et alii* 2014, p. 25).

New excavations (2015–2017)

Rescue excavations conducted between 2015 and 2017 were prompted by an investment project for a fish breeding facility, covering a sector of 2.91 ha in the northeastern part of the nowadays Iclod village. The newly investigated sector is situated southeast of the previously researched site and overlaps it for approximately 0.8 ha. These recent excavations have led to the discovery of 24 new burial graves (**Pl. I/2–3**).

The deceased were placed in oval pits, with relatively shallow depths, ranging between 0.40 to 0.80 m (**Pl. II–XIII**; **Table 2**). Exceptions include graves **SK 132**, **147**, **152**, **153**, **157**, and **SK 159**, which were placed into rectangular with rounded corners pits (**Pl. VI /1**; **VII /3**; **VIII/1**; **IX/1**; **Table 2**). Most individuals were placed in dorsal decubitus, predominantly with their arms positioned over the pelvic area, as observed in eight burials (**SK 119**, **SK 125**, **SK 132**, **SK 147**, **SK 152**, **SK 195**, **SK 197**, and **SK 201**) (**Pl. IV/1**; **V/3**; **VI/1**; **VII/3**; **VIII/1**; **XI/3**; **XII/1**; **XIII/1**; **Table 2**).

Variations in arm positioning were recorded for several other individuals: **SK 105** and **SK 122** had both arms extended alongside the body (**Pl. II; IV /3**); **SK 116** had the left arm flexed over the thoracic sector and the right arm flexed across the pelvic sector (**Pl. III/3**); **SK 153** had the right arm extended along the body and the left arm placed over the pelvic region (**Pl. VIII/3**); **SK 159** had the right arm over the pelvic area and the left arm extended alongside the body (**Pl. IX/3**). **SK**

190 was positioned in lateral decubitus, oriented toward the right side (**Pl. XI/1**). **SK 109** had both arms placed over the pelvic sector, with legs slightly flexed to the left (**Pl. III/1**). For nine burials, specific information about limb placement is missing from the archaeological record, although they are mentioned as being placed in dorsal decubitus (**Table 2**).

The orientation of the graves is predominantly along the W-E geographical axis (16 burials). Six graves (**SK 107**, **SK 109**, **SK 116**, **SK 119**, **SK 152**, and **SK 153**) are oriented along the SW-NE axis (**Pl. II /3; III/1**, **3**; **IV/1**; **VIII/1**, **3**; **Table 2**), while two graves (**SK 105** and **SK 233**) follow a NW-SE orientation (**Pl. II/1; XIII/3**; **Table 2**).

Anthropological data

Twenty-four human skeletons were examined using established osteological methodologies. These assessments aimed to reconstruct key demographic parameters such as sex, age-at-death, and general health status. Biological profiles constitute a fundamental component of palaeodemographic analysis, offering essential insights into the composition, structure, and health of past populations. When integrated with palaeopathological observations, these profiles can inform broader interpretations of social organisation, subsistence strategies, and environmental stressors experienced by prehistoric communities. Sex determination of adult individuals was primarily based on the macroscopic evaluation of discrete morphological features, following standard criteria. Age-at-death estimation employed a combination of techniques tailored to the developmental stage of each individual. For non-adult remains, age was estimated based on dental development (formation and eruption sequences), epiphyseal fusion of long bones, and diaphyseal length. In adult individuals, degenerative changes were assessed, including pubic symphysis morphology, auricular surface characteristics of the ilium, cranial suture closure, and dental wear. Age classifications adhered to the standards proposed by J. E. Buikstra and D. H. Ubelaker, which distinguish the following categories: infant (0–3 years), child (3–12 years), adolescent (12–20 years), young adult (20–35 years), middle adult (35–50 years), and old adult (50+ years) (Buikstra, Ubelaker 1994; Schaefer, Black, Scheuer 2009; AlQahtani, Hector, Liversidge 2010; White, Folkens 2005).

All the analysed skeletons are highly fragmented and in a poor state of preservation, which prevented the estimation of the individuals' stature.

Archaeological and anthropological assessment

SK 105. The inhumation grave was an oval-shaped pit, oriented NW-SE and tapering toward the individual's lower limbs. The skeletal remains were found in dorsal decubitus, with the arms extended alongside the torso, and lower limbs

fully extended. The grave goods are represented by ceramic vessels (placed at the feet, right knee, and right upper limb), perforated animal-tooth beads and seashell beads around the neck and head. Approximately 70% of the skeleton is preserved; the bones are showing damage from erosion and root activity. Parts from the thoracic cage and the distal diaphyses of the lower limbs are missing. Osteological assessment indicates an individual aged 14.5–15.5 years (adolescent). Cribrotic lesions are visible on the orbital roofs. The maxillary incisors are shovel-shaped (**Pl. II/1–2**; **XIV/5**).

SK 107. The grave was a broad-oval pit. The skeleton is highly fragmented and is poorly represented (30% preserved). The individual was placed in dorsal decubitus, oriented SW-NE. Grave goods consist of ceramic vessels and a fragment of a curved flint blade. The skeletal remains belong to a probably female individual, aged between 25 to 29 years old at death (young adult) (**Pl. II/3–4**). Dental pathology is extensive – heavy calculus deposits, caries, abscesses, periodontal disease (**Pl. XV/4–5**). Craniosynostosis is suspected, the lambdoid suture showing extensive closure (**Pl. XVIII/1**). The right maxillary third molar bears an enamel pearl.

SK 109. The inhumation grave was oval in shape and the skeleton was oriented SW-NE, in a dorsal decubitus position with its hands resting on the pelvis, left forearm flexed at the elbow and the lower limbs slightly flexed at the knees toward the left. Grave goods comprise faunal remains placed above the body, three miniature ceramic vessels, two medium-sized vessels beneath the left lower limb, and one vessel to the right of the skull. Osteological analysis indicates an individual of 13 years old age at death (adolescent) (**Pl. III/1–2**). The maxillary incisors are shovel-shaped.

SK 116. The grave had an oval-shaped pit, wider towards the feet. The individual was placed in a dorsal decubitus position and had a SW-NE orientation. His left arm was flexed across the thorax and the right arm was flexed toward the pelvis. Grave goods consist of three ceramic vessels to the right of the left leg, four ceramic vessels at the feet and two perforated animal bone plaques in the upper part of the thoracic cage. The skeletal remains belong to a probably male individual, with the age at death spanning from 23 to 25 years old (young adult) (**Pl. III/3–4**). Noted pathologies are heavy supragingival calculus deposits and periostitis on the diaphysis of lower limbs in form of lamellar bone formation; woven bone formation at the inferior side of the mid-shaft of both tibiae. At the superior side of the mid-shaft of the tibiae there is a mixture of woven and lamellar bone formation (**Pl. XX/2**).

SK 119. The inhumation grave was oval-shaped. The individual was placed in a dorsal decubitus position, oriented SW-NE, with both arms extended alongside the pelvis. Grave goods consist of bone bracelets that encircled each forearm, and a

cluster of five ceramic vessels had been placed to the left of the body. Approximately 45% of the bones are preserved. Osteological analysis indicates an adolescent of 13.5–15.5 years old (**Pl. IV/1–2**). Pathological observations include cribra orbitalia on the left orbit, linear enamel hypoplasia on the mandibular incisors and canines, and osteophytosis on the odontoid process of the second cervical vertebra (**Pl. XIX/1**).

SK 122. The inhumation grave was oval and oriented W-E. The skeleton was found in dorsal decubitus, arms extended besides the trunk and lower limbs straight. Grave goods consist of one ceramic vessel that was placed at the head, four other vessels and a stone axe deposited at the feet. The individual was a male, with the age at death estimated to be 50 years old (borderline old adult) (**Pl. IV/3–4**). In terms of non-metric traits, we note a persistent metopic suture, lambdoid ossicles (**Pl. XIV/1, 4**), and bilateral supraorbital notches. Pathological conditions observed on the skeleton are: cribra orbitalia visible on the present right orbit, linear enamel hypoplasia, supragingival calculus deposits, multiple carious lesions, and extensive endocranial impressions following vascular grooves on the left parietal (**Pl. XX/3**).

SK 124. The inhumation grave was oval and elongated in shape, oriented W-E. The individual was placed in dorsal decubitus. Due to the high degree of fragmentation and the absence of key anatomical elements necessary for more precise age estimation, the skeleton was assigned to an adult category based on the complete fusion of long bone epiphyses to the diaphyses. The degree of preservation, below 30%, did not allow for sex determination. Grave goods consisted of five ceramic vessels, two placed near the left hand and three at the feet, and a stone axe deposited at the pelvis region (**Pl. V/1–2**).

SK 125. The inhumation grave was elongated and oval in shape, oriented W-E. The skeleton was found in dorsal decubitus, with the hands positioned over the abdominal area. Grave goods included ceramic vessels placed to the right of the body, near the pelvis, as well as an animal-tooth necklace found in the upper thoracic region. The skeletal remains belong to a male individual. The age at death was estimated at around 20 years (young adult) (**Pl. V/3–4**).

SK 132. This skeleton originated from a rectangular grave with rounded corners, oriented along a W-E axis. The individual was placed in dorsal decubitus, with arms flexed toward the thorax and abdomen and the legs extended. Grave goods consisted of one ceramic vessel at each lower limb and an additional vessel at the right hand. The skeletal remains are approximately 60% preserved and highly fragmented. The individual was assessed as female, aged between 35 to 55 years old at death (middle adult) (**Pl. VI/1–2**). Palaeopathological observations revealed extensive dental pathology, including carious lesions affecting both maxillary and mandibular dentition (left maxillary second premolar, left mandibular third molar,

and right mandibular premolars and molars), abscesses (right maxillary second and third molar and left maxillary first molar), supragingival calculus deposits and periodontitis, impaction of the left mandibular canine, tooth rotation – the right mandibular canine rotated mesio-lingually towards the first premolar (**Pl. XV/1**, **3**; **XVI/1–4**).

SK 133. The grave was oval-shaped. Funerary goods consisted of ceramic vessels deposited near the skull. The skeletal remains belong to a non-adult individual, aged approximately 3.5–4 years (child) (**Pl. VI /3–4**). Linear enamel hypoplasia is present on the maxillary first deciduous molars and endocranial alterations are visible on the inner surface of the frontal bone (**Pl. XX/4**).

SK 142. The inhumation grave was oval-shaped. The skeletal remains belong to a non-adult individual aged around ten years at death (child) (**Pl. VII/1–2**). Two zygomaticofacial foramina were observed on the left zygomatic bone (**Pl. XI /2**). The superior portion of the labial crown surface of the left lateral mandibular incisor is chipped (**Pl. XV/2**).

SK 147. The inhumation grave, a rectangular pit with rounded corners, was located near SK 152. The individual was placed in dorsal decubitus, with the arms flexed over the abdomen and the lower limbs fully extended. Grave goods include – two ceramic vessels at the feet, two additional vessels in the northern and western corners of the grave, a string of beads on the right arm, a beaded necklace with a shell pendant at the neck, and a bone awl deposited in the vessel near the right foot. The remains belong to a non-adult, estimated to have been approximately 13 years old at the time of death (adolescent) (**Pl. VII/3–4**). Pathological indicators include enamel hypoplasia on the maxillary canines and mandibular incisors, as well as supragingival calculus deposits.

SK 152. The inhumation grave was approximately rectangular with rounded corners, located near SK 147. The individual was placed in dorsal decubitus, with the hands on the pelvis and the legs nearly extended. The orientation was on the SW-NE axis. The grave goods consist of a ceramic vessel at the head and another one at the left lower limb. The skeleton was determined to belong to a male individual aged between 45–50 years old (middle adult). Palaeopathological observations include: osteoarthritis at the left pedal phalanges, eburnation on the trapezoid with second metacarpal articulation (left side) (**Pl. XIX/2**), and osteophytes of the vertebrae (**Pl. XIX/3**). Other conditions observed are antemortem trauma on the central ribs (left side) (**Pl. XIX/4–5**), and at the fourth proximal phalanx of the right foot. Enthesophytes are visible on both patellae. Dental pathologies include supragingival calculus accumulation leading to periodontitis, caries on both the maxillary and mandibular dentition, and a periapical abscess on the left first maxillary molar.

SK 153. The burial pit was rectangular with rounded corners. The individual was placed in dorsal decubitus, with the right arm extended alongside the body and the left arm resting over the pelvis. The legs were extended. Its orientation was on the SW-NE axis. Grave goods consist of two nested groups of ceramic vessels placed between the feet and one additional vessel near the right leg. Sex was determined as female and the age at death was estimated at 25 to 29 years (young adult) (**Pl. VIII/3–4**). Pathologically we note periosteal changes on fragmented ribs.

SK 157. The inhumation grave was rectangular shaped. The individual was placed in dorsal decubitus, with the right hand resting on the pelvis, oriented on the W-E axis. Grave goods consist of ceramic vessels placed in the lower limb area. Approximately 50% of the skeleton is preserved and it belongs to a female individual, with the age at death estimated between 35 and 50 years (middle adult) (**Pl. IX/1–2**). Palaeopathological observations include entheses on the anterior iliac spine (**Pl. XVIII/2**), signs of an active healing infection on the tibia (mixture of woven and lamellar bone) (**Pl. XX/1**), and multiple dental conditions (caries, periapical abscesses, supragingival calculus deposits, antemortem tooth loss, and periodontitis). Both dental arches exhibit atypical occlusal wear patterns, likely due to the use of teeth in non-masticatory activities such as material processing (**Pl. XVII/1–2**). Ossification of the ligamentum flavum was noted on thoracic vertebrae (**Pl. XVIII/3**). The long bones and clavicles are robust, showing strong muscular insertions.

SK 159. The inhumation grave was rectangular with rounded corners. The individual was placed in dorsal decubitus, with the right forearm placed across the pelvis and the left arm along the body, oriented W-E. Grave goods include a stone axe near the pelvis, an obsidian piece near the right arm, and ceramic vessels near the cranium. Age at death was estimated between 20 and 35 years (young adult) (**Pl. IX/3–4**).

SK 180. The inhumation grave was approximately oval in shape. The individual was placed in dorsal decubitus, with the legs straight, orientated on the W-E axis. Grave goods include seven ceramic vessels deposited in the area of the lower limbs. Approximately 30% of the skeleton is preserved and it belongs to an adult individual, probably male (**Pl. X/1–2**).

SK 181. The inhumation grave was roughly oval. The individual was deposited in dorsal decubitus, oriented W-E. Grave goods include four ceramic vessels placed at the feet. Approximately 30% of the skeleton is preserved. Dental eruption patterns indicate an age at death of approximately six years (child) (**Pl. X/3–4**). Cribrotic lesions are visible on the surface of the left orbit.

SK 190. The inhumation grave was oval in shape. The individual was laid on the right side and oriented on the W-E axis. One ceramic vessel was found at the

feet area. Anthropological assessment identified the individual as female, aged between 20 and 35 years at death (young adult) (**Pl. XI/1–2**). Palaeopathological findings include several dental pathologies, supragingival calculus, periodontitis, diastema (noted between the second incisor, canine, and first premolar on the right maxilla), impacted mandibular left canine, retained deciduous teeth (first molar), and agenesis of the second premolar (**Pl. XVII/4–6**).

SK 195. The inhumation grave was oval in shape. The individual was deposited in dorsal decubitus with the hands resting on the pelvis and oriented on W-E axis. One ceramic vessel was found in the area of the lower limbs. The individual was identified as male, aged between 35–45 years at death (middle adult) (**Pl. XI/3–4**).

SK 197. The inhumation grave was oval-shaped. The individual was placed in dorsal decubitus, with the hands resting on the pelvis, oriented W-E. One ceramic vessel was found at the feet. Approximately 80% of the skeleton is preserved. The remains belong to a female individual, aged between 40 and 44 years at death (middle adult) (**Pl. XII/1–2**). Marginal osteophytes are visible on the thoracic vertebrae.

SK 200. The inhumation grave was oval in shape. The individual was placed in dorsal decubitus and oriented on the W-E axis. Grave goods consist of five ceramic vessels: one placed near the head and four others near the feet. Approximately 50% of the skeleton is preserved and it belongs to a female individual, aged approximately 42.5 years at death (middle adult) (**Pl. XII/1–2**). Palaeopathological observations include dental conditions such as abscesses and caries on the mandibular second premolar and first molar on the left side (**Pl. XVI/5–6**).

SK 201. The inhumation grave was oval in shape. The individual was deposited in dorsal decubitus with arms on the pelvis, oriented W-E. Grave goods consist of two ceramic vessels – one placed at the feet, one near the head. The skeletal remains belong to a male, aged between 25 and 35 years at death (young adult) (**Pl. XIII/1–2**). Non-metric traits include bilateral supraorbital notches. Palaeopathological findings include cribrotic lesions and various dental conditions: caries on the right and left second maxillary premolars, enamel hypoplasia lines on the incisors, malocclusion of the right mandibular canine and maxillary first premolar, and antemortem tooth loss of the right mandibular first and second molar (**Pl. XVII/3**).

SK 233. The inhumation grave was oval and elongated, oriented NW-SE. The individual was placed in dorsal decubitus. The skeletal remains belong to a female, aged between 17 and 25 years (young adult) (**Pl. XIII/3–4**). Epigenetic traits include bilateral supraorbital notches (**Pl. XXI/1**). Cribrotic lesions are present on both orbits (**Pl. XXI/1**). The dentition is affected by supragingival calculus and periodontitis.

Non-Metric Traits

Epigenetic or non-metric traits are heritable features that may indicate genetic relationships among individuals. A number of traits falling into this category were observed in the analysed skeletal sample and recorded according to the primary descriptive non-metric traits outlined in standardised reference works (Berry, Berry 1967, p. 361).

Individual SK 122 exhibits a persistent metopic suture visible along the frontal bone, extending from the nasion to the bregma, as well as lambdoid ossicles at the junction of the parietal and occipital bones (**Pl. XIV/1**, **4**). Generally, the interfrontal suture fuses completely by the age of two to three years. In some cases, its retention may be pathological, as in craniosynostosis, a condition characterised by premiddle closure of cranial sutures. However, the case observed here is considered non-pathological and likely of genetic origin. Metopism exhibits variable prevalence across populations, with higher frequencies generally observed in temperate regions. Reported rates include approximately 9% in European Caucasians, 5% in Asians, and 1% in individuals of African descent. Some studies note significantly higher values, such as 38.17% in Indian skulls (Agarwal, Malhotra, Tewari 1979, p. 470–474), while R. A. Bergman places the overall range between 1–12% (Bergman 1988). These variations suggest a possible climatic influence on the persistence of the metopic suture (Agarwal, Malhotra, Tewari 1979, p. 470–474; Berry, Berry 1967, p. 367, fig. 6; Gardner 2016, p. 1, fig. 1).

Sutural bones, also known as Wormian bones or ossa suturalia, are small, irregular ossicles that form within cranial sutures due to accessory ossification centers in the skull's mesenchyme. Their presence is associated with conditions such as osteogenesis imperfecta, rickets, Menkes syndrome, otopalatodigital syndrome, cleidocranial dysostosis, pycnodysostosis, hypoparathyroidism, hypophosphatasia, primary acro-osteolysis, and Down syndrome. However, they can also appear in healthy individuals as a normal anatomical variation (Berry, Berry 1967, fig. 1–2, p. 365; Kumar *et alii* 2016, p. 2331–2332).

Individuals SK 142 and SK 157 exhibit double zygomaticofacial foramina (**Pl. XIV/2–3**). Typically, the anterosuperior portion of the zygomatic bone houses a single passage for the zygomaticofacial nerve (Berry, Berry 1967, p. 365, fig. 3). The zygomaticofacial nerve, a branch of the maxillary division of the trigeminal nerve, innervates the skin of the cheek and passes through the orbicularis oculi muscle. Its associated foramen may be single, multiple, or absent, a variability likely linked to the number of ossification centres in the zygomatic bone, which typically form by the eight weeks of gestation and fuse by the 22nd week (Nteli Chatzioglou *et alii* 2024, p. 2, 5–6).

Skeletal remains of SK 105 and SK 109 are characterised by shovel-shaped upper incisors (**Pl. XIV/5**), a trait commonly found in East Asian and Native American populations. Recent genetic studies have showed that this dental trait is closely associated with the EDAR gene variant T1540C (rs3827760). In two Japanese populations, the presence of the 1540C allele accounted for 18.9% of the variation in shovelling grade, indicating a strong additive genetic effect. This allele also influences overall tooth size and the mesiodistal-to-buccolingual diameter ratio. Although the variant is a major factor, the authors conclude that other genetic elements contribute to dental morphology. The high frequency of this variant in Asia suggests it may have undergone positive selection during human evolution (Kimura *et alii* 2009, p. 528–529, 533, fig. 2).

Supraorbital notches are passage ways for the supraorbital vessels and nerves (Berry, Berry 1967, p. 369, fig. 3, 6). Three individuals present with this trait, namely SK 122, SK 201 and SK 233 (**Pl. XXI/1**).

Bone pathologies

Craniosynostosis, the early fusion of cranial sutures, results in abnormal skull morphology due to inhibited growth perpendicular to the fused suture and compensatory expansion at unfused sutures. It is a congenital and often hereditary condition. It could result from intrauterine infections or trauma sustained during birth. Besides the visible cranial deformities, early suture closure can restrict brain development, can create the increased intracranial pressure leading to visual and/or mental impairment (Roberts, Manchester 2010, p. 54–55; Johnson, Wilkie 2011, p. 369–370, fig. 1/e–f; Gault et *alii* 1992, p. 377). A possible case of craniosynostosis is observed in the cranial fragments of individual SK 107 (young adult), whose lambdoid cranial sutures appear to be fully fused (**Pl. XVIII/1**).

Cribra orbitalia is a common pathological marker observed in osteological collections. It is considered a skeletal manifestation of underlying systemic stress, not a disease per se. The general consensus has been that anaemia is the main factor responsible for the development of porotic lesions, whether due to acquired causes (parasitic infections, nutritional deficiencies) or genetic blood conditions (thalassaemia or sickle-cell anaemia). Anaemia often leads to hypertrophy or hyperplasia of the bone marrow, resulting in the expansion of trabecular or cranial diploic bone due to increased haematopoiesis. This expansion, coupled with disrupted remodelling of the outer cortical bone, can produce visible porotic lesions (Ortner 2003, p. 89–106; Stuart-Macadam 1989, p. 187–192; Aufderheide, Rodríguez-Martin 1998, p. 478; Mensforth *et alii* 1978; Roberts, Manchester 2010, p. 225–234).

However, recent literature has challenged these scenarios, suggesting that cribra orbitalia is primarily a vascular phenomenon, unrelated to marrow hyperplasia

or anemia. Instead, the alterations likely result from vascular disturbances such as venous malformations, hemorrhages, or possibly lacrimal gland infections with *Chlamydia* or *Trichomonas*. These observations are emphasising that cribra orbitalia should no longer be considered an indicator of anemia or generalised skeletal stress, but rather as a distinct condition with a fundamentally vascular etiology (Rothschild *et alii* 2020, p. 1711–1714, fig. 1, 2).

Porotic hyperostosis or cribra cranii is characterised by a porous, thinned appearance of the parietal and occipital bones. It is frequently associated with cribra orbitalia, with some authors conflating the two conditions and proposing a shared etiology. Suggested origins include multifactorial anaemia, malaria, nutritional deficiencies, vitamin C deficiency, bacteraemia, or the presence of parasites (Aufderheide, Rodríguez-Martin 1998, p. 350; Stuart-Macadam 1989, p. 187; Roberts, Manchester 2005, p. 230–231; Walker *et alii* 2009, p. 114–115).

Genetic research has provided new evidence supporting the hypothesis that porotic hyperostosis in ancient populations is linked not only to environmental factors, but also to inherited biological traits. Ancient DNA samples taken from 80 individuals spanning the Palaeolithic to the Iron Age and found that those exhibiting porotic hyperostosis had significantly lower genetic scores for haemoglobin levels and bone mineral density. In contrast, no statistically significant associations were identified with genes related to iron or vitamin B_{12} metabolism, malaria resistance, or low vitamin D. The results indicate a genetic predisposition to both anaemia and reduced bone density in individuals with porotic hyperostosis. The study also noted that the genetic scores for bone density were lowest during the Neolithic, suggesting that it may be linked to a genetic decline in bone mineral density due to an adaptation to low UV radiation and reduced vitamin D synthesis in early, dark-skinned Europeans. As lighter skin evolved post-Neolithic, the density increased, potentially lowering the porotic hyperostosis rates. Overall, the condition appears to result from a combination of genetic predisposition and environmental pressures, not merely dietary or infectious factors (Ferrando-Bernal 2023, p. 2–6, table 1–2, fig. 2–6).

Recent studies challenge the traditional view that cribra orbitalia and porotic hyperostosis share a common aetiology as manifestations of anaemia-induced marrow hyperplasia. The study analysed 98 skulls and found that cribra can occur independently of diploic bone expansion and without the presence of porotic hyperostosis. In some individuals, the condition was accompanied by cranial thinning rather than thickening, suggesting hypoplastic rather than hyperplastic processes. While porotic hyperostosis remains closely associated with diploic bone hypertrophy caused by compensatory hematopoiesis (typically seen in iron-deficiency anaemia, thalassaemia, or sickle cell disease), cribra orbitalia could

result from conditions that suppress marrow activity – chronic disease anaemia, renal failure, protein deficiency, endocrine disorders, or scurvy. The absence of cranial vault involvement in many cribra orbitalia cases further supports the notion of distinct underlying mechanisms. Therefore, these two manifestations should be regarded as separate pathological entities rather than interchangeable indicators of systemic stress or anaemia (Rivera, Mirazon Lahr 2017, p. 2, 4–5, 9–17).

In the Iclod sample, lesions consistent with cribrotic changes were identified in six individuals (SK 105, SK 119, SK 122, SK 181, and SK 201), affecting the orbital roofs (**Pl. XXI/1–2**). The parietal bone of SK 133 has modifications consistent with cribra cranii.

Endocranial lesions were noted in individuals SK 122, SK 133 (**Pl. XX/3–4**), and SK 200. Such lesions have been documented in both adult and non-adult skeletal samples, with differing underlying causes. They may manifest as abnormal bone growth, enlargement, structural alterations, or vascular impressions on the endocranial surface. Possible explanations include trauma, bacterial or viral infections (like tuberculosis and syphilis), tumours, or nutritional deficiencies (vitamins A, C, and D), might be secondary to systemic disease like scurvy or the result of trauma, including child abuse (Lewis 2017, p. 82–83, 94–96).

In the case of individual SK 133 (aged 3.5 years at death), the "hair-on-end" pattern (grade IV) observed on the inner surface of the frontal bone may reflect either normal growth or pathological causes such as meningitis, trauma, tumours, or hypervascularization (**Pl. XX/4**).

In adults, these endocranial abnormalities often present as bone accretions, new bone formations, or pronounced vascular impressions. For instance, a well-defined vascular groove following a blood vessel path is visible on the left parietal bone of individual SK 122 (**Pl. XX/3**). The pattern of endocranial thickening suggests a possible case of hyperostosis frontalis interna, a condition predominantly observed in females and frequently associated with endocrine disorders, including postmenopausal hormonal shifts, pituitary dysfunction, or breast cancer. However, the condition may also occur in males, especially after the age of 50, and is linked also to hormonal imbalances or obesity (Hershkovitz *et alii* 1999, p. 303, 307–309, 311–312, 317, 323, fig. 1–5, 8).

Individual SK 200 (female, middle adult) also presents a localised endocranial bony growth on the right parietal bone, also possibly hyperostosis frontalis interna.

Degenerative Diseases – Osteoarthritis. Degenerative and dystrophic conditions are commonly encountered in osteoarchaeological analyses (Ortner 2003, p. 545). Osteoarthritis is a degenerative joint disease affecting articular cartilage and is typically observed in synovial joints. It has a multifactorial etiology including age-related degeneration, trauma, infection, obesity,

mechanical overuse, congenital anomalies, genetic predisposition, endocrine and metabolic disorders. As individuals age, articular cartilage undergoes progressive degeneration through four stages. The initial stage involves enzymatic degradation of the cartilage matrix, disrupting the function of chondrocytes and altering the synthesis of extracellular matrix proteins. In the second stage, subchondral bone synthesis increases, resulting in joint stiffening. This is followed by metaplasia of peripheral synovial cells, leading to the formation of osteochondrophytes, bony overgrowths that compensate for tissue loss. The last stage includes subchondral microcyst formation, microfractures, and eburnation of the articular surface (Waldron 2009, p. 26–28; Ortner 2003, p. 545–560, Roberts, Manchester 2010, p. 138–143).

According to T. Waldron, a diagnosis of osteoarthritis should be based on the presence of eburnation or at least two of the following: marginal osteophytes, new bone formation on the joint surface, articular surface porosity, or changes in joint morphology (Waldron 2009, p. 33–34).

In the Iclod sample, individuals SK 119, SK 152, SK 153, and SK 197 exhibited significant degenerative changes consistent with osteoarthritis. In SK 152, eburnation is evident on the trapezoid-metacarpal II articulation (left side) (**Pl. XIX/2**). New bone formation and porosity are also visible on the lower limb elements (left fifth metatarsal and bilateral distal phalanges of the hallux). Additional degenerative changes are present on the vertebral bodies, particularly the thoracic vertebrae that display marginal osteophytes (**Pl. XIX/3**).

SK 153 presents deformed margins of the femoral head near the fovea capitis, articular margin irregularities, and advanced porosity at the right coxofemoral articulation.

SK 197 displays structural changes on thoracic vertebrae, including marginal osteophytes. A Schmorl's node, typical of disc herniation, is also present. Schmorl's nodes, or intervertebral disc herniations, occur when the nucleus pulposus breaches the vertebral body due to degeneration of cartilaginous joints (Waldron 2009, p. 45).

A notable case is SK 119, a non-adult, presenting osteophytes and structural anomalies on the odontoid process of the second cervical vertebra (eburnation is evident on the trapezoid-metacarpal II articulation (left side) (**Pl. XIX/1**). Since such degenerative changes are rare in individuals under 40 years old and this case may result from mechanical stress or trauma to the cervical spine (Waldron 2009, p. 31).

Vertebral osteophytes can compress adjacent anatomical structures, leading to diverse complications. In the cervical region, they may affect the pharynx and esophagus, causing dysphagia, aspiration, vocal fold paralysis, and sleep apnea.

Posterior osteophytes may compress the spinal cord, while those on the uncinate process can impair vertebral artery flow. Thoracic vertebrae bone growth may damage the esophagus or lacerate the aorta, resulting in pseudoaneurysms or aspiration pneumonia due to bronchial compression. Lumbar ones may affect the inferior vena cava and abdominal aorta. Their etiology is multifactorial, with obesity as the primary contributor due to increased mechanical stress on the spine. Other factors include hypervitaminosis A and abnormal stimulation of bone growth factors. Age-related degeneration of the nucleus pulposus and annulus fibrosus plays a central role in their development, leading to compensatory bony outgrowths at the zygapophyseal joints. From an anthropological perspective, osteophyte formation has been linked to both mechanical stress and postural demands, though some studies suggest a stronger connection to erect bipedal locomotion than to occupational strain (Klaassen *et alii* 2011, p. 1–5, table 1, fig. 3–5).

All the individuals exhibiting osteoarthritic changes fall into the middle adult category, two males SK 152 and SK 153 and SK 197 determined anthropologically as female.

Enthesopathies. In some cases, entheses, the sites where tendons, ligaments, and joint capsules attach to bone, may become inflamed and react through new bone formation. These changes can result from repeated mechanical stress, systemic disease, genetic predisposition, or ageing (Mariotti, Facchini, Belcastro 2007, p. 291). The high degree of fragmentation and erosion of the skeletal remains has significantly hindered the observation of muscular attachment sites, limiting the ability to assess biomechanical stress markers that could otherwise offer valuable insights into physical activity levels and occupational patterns within the population. However, where it was possible identification and classification followed the scoring system proposed by Mariotti, Facchini, Belcastro (2007).

SK 157 has enthesophytes present at the anterior superior iliac spine (where *sartorius* muscle originates – involved in hip flexion) (Papilian 2014, p. 230; Netter 2019, pl. 305–306). The clavicle also shows grade 1b rugosity at the trapezoid ligament attachment (connects the coracoid process of the scapula to the trapezoid line on the inferior surface of the clavicle and contributes to the overall range of motion of the shoulder during arm elevation) (Papilian 2014, p. 108–110, 193, fig. 132/3, 227/10; Netter 2019, pl. 408–412, 415; Mariotti, Facchini, Belcastro 2007, p. 292, 303, table 1, fig. 5).

SK 152 presents grade 3 enthesophytes at the quadriceps femoris tendon on both patellae (Papilian 2014, p. 133–134, fig. 172/4; Netter 2019, pl. 497, 498). Overuse involving this articulation are frequently amongst ageing individuals or the ones who are highly engaged in different physical activities and are particularly

affecting the proximal region of the patella, a condition known as "jumper's knee" (Mariotti, Facchini, Belcastro 2007, p. 310, fig. 21; Toumi *et alii* 2006, p. 47–48).

Infections – Periostitis. In bone, infections may result in destructive changes, bone remodelling, or a combination of both. It is the result of infection or trauma and it is described as the inflammation of the periosteum. The pathogens involved are typically staphylococci, streptococci, pneumococci, or more rarely, *Salmonella typhi.* When the periosteum is inflamed, vertical striations of new woven bone are formed over the outer cortical bone. It is most frequently observed on tibiae, as the skin is thinner on the anterior part of the bone (Roberts, Manchester 2010, 167–168). Non-specific infectious changes consistent with periostitis were identified in individuals SK 116, SK 153, and SK 157.

Periostitic markings are present at the shafts of lower long bones of SK 116, in the form of longitudinally striated markings. More specifically, lamellar bone formation is observed at the shafts of the femora, tibiae and fibulae (lesions healed at the time of death). At the inferior side of the mid-shaft of both tibiae woven bone formation is observed (lesions active at the time of death), while at the superior side of the mid-shaft there is a mixture of woven and lamellar bone formation (lesions in the process of healing at the time of death) (**Pl. XX/2**).

In SK 157, lamellar bone formations are present on the left tibial diaphysis, healing at the time of death (**Pl. XX/1**).

In SK 153, periosteal changes are observed on fragmented ribs. Due to fragmentation, lateralisation and anatomical identification could not be determined. The ribs display caudal margin porosity and narrowed diaphyses that might be the result of trauma followed by infection or possibly infectious pulmonary disease (Roberts, Manchester 2010, p. 167–168).

Trauma – Antemortem Fractures

Evidence of trauma on the skeleton provides important information about the lifestyle, health, and social context of past populations. Trauma refers to any disruption in the continuity of the bone (Roberts, Manchester 2010, p. 84).

Antemortem traumatic injuries were observed in individual SK 152. This includes a healed fracture of the central ribs on the left side, marked by callus formation (**Pl. XIX/4–5**), and a fracture of the fourth proximal phalanx of the left foot. Rib fractures can occur after blunt force trauma – impact from a fall, accident or violence-related activities (Dhaniwala *et alii* 2022, p. 54).

Most fractures typically result from axial loading, such as stubbing the toe, or from compressive trauma, like being struck by a falling object. Less commonly, hyperextension of the joint can lead to spiral or avulsion-type fractures (Hatch, Hacking 2003, p. 2413).

Additional conditions observed

Individual SK 157 (middle adult) exhibits ossification of the ligamentum flavum, visible on the thoracic vertebrae, located cranially and caudally along the vertebral arches (**Pl. XVIII/3**). Clinically, this condition is most often documented in East Asian populations and is rarely referenced in palaeopathological literature. Ossification of the ligamentum flavum is considered a predisposing factor for the development of myelopathies and may result from biomechanical stress, genetic predisposition, or advanced age. It frequently co-occurs with osteoarthritic changes in the vertebral column (Geber, Hammer 2018, p. 1–2).

Dental Pathologies

Dental diseases represent the most frequent pathological conditions observed in osteological collections. These conditions are interrelated and often develop due to poor oral hygiene, local trauma, or genetic predispositions. The primary mechanism involves the accumulation of bacterial plaque, acid production, and carbohydrate fermentation, which degrade dental enamel. Periodontitis and its precursor, gingivitis are the leading causes of tooth loss. They result from the presence of fungi and bacteria in the oral cavity, which lead to calculus accumulation. It is characterised by the progressive destruction of the alveolar bone and periodontal ligament, leading to tooth mobility and eventual tooth loss. Supragingival and subgingival calculus, act as persistent irritants, exacerbating inflammation. Over time, this contributes to alveolar bone resorption, identifiable in osteoarchaeological material by recession of the alveolar border and porosity at the tooth socket. In advanced cases, periapical abscesses may form when infection spreads to the root apex, often following untreated caries or pulp exposure. These infections can cause bone destruction around the tooth root. Caries originates from acid-producing bacteria metabolising dietary carbohydrates. The demineralisation process first affects enamel, progressing to dentine and sometimes reaching the pulp cavity. In skeletal remains, caries appears as well-defined cavitations, typically on occlusal surfaces, interproximal contact points, or near the cementoenamel junction. These processes are influenced not only by diet and hygiene but also by the morphological and chemical structure of teeth, salivary flow, and genetic predisposition (Waldron 2009, p. 237; Roberts, Manchester 2010, p. 65; Ogden 2007, p. 286–287; 288–289; Hillson 2005, p. 286–291, 304).

Eleven individuals in the Iclod sample – SK 107, SK 119, SK 122, SK 132, SK 133, SK 147, SK 152, SK 157, SK 190, SK 200, and SK 201 – present various combinations of dental pathologies, including periodontitis, calculus deposits, caries, periapical abscesses, malocclusion, impaction, retention of deciduous teeth, and enamel formation defects (hypoplasia and hyperplasia) (**Pl. XIV–XVIII**).

Retention of deciduous teeth. SK 190 has a retained mandibular deciduous second molar (**Pl. XVII/6**). Retained deciduous teeth refer to primary teeth that remain in the oral cavity beyond their expected exfoliation period. Unlike impacted teeth, retained teeth persist despite the eruption of permanent successors, leading to a myriad of connected dental issues – malocclusion, caries, periodontal complications. Recent observations suggest dietary shifts toward softer foods may contribute to increased retention prevalence, however genetic disorders, decreased oral health and other associated dental pathological conditions – caries, periodontal disease, impaction, or geographical variations are also causes (Ruiyi, Ruijie 2025, p. 51–52, 54–55).

Calculus deposits are present on the dentition of all the adult individuals SK 122, SK 132, SK 147, SK 152 and SK 157 (**Pl. XV–XVII**).

Various typologies of carious lesions were identified in six of the adult individuals (coronal and surface contact) – SK 107, SK 122, SK 132, SK 152, SK 157, and SK 201. SK 107 has caries at the mesial side (at the cemento-enamel junction) of the right maxillary third molar and on the mandibular second and first molars, right side (**Pl. XV/4**). SK 122 has a caries lesion on right maxillary canine, labially. SK 132 has extensive dental pathology, including carious lesions affecting both maxillary and mandibular dentition (left maxillary second premolar, left mandibular third molar, right mandibular premolars and molars) (**Pl. XV/3**; **XVI/2**). SK 152 has developed carious lesions on the right maxilla, affecting the canine and first premolar; on the left maxilla – the second molar; on the mandible, the left first premolar and the right first molar. SK 157 has carious lesions were identified on the following elements: on right maxilla – second premolar (distally), on the second (distally) and third molar (the cemento-enamel junction, lingually); on left maxilla – second premolar – caries on the lingual and buccal side; left sided-mandible – first premolar (caries occlusal); right sided mandible first and second premolars – caries distally (**Pl. XVII/1**). Additionally, white-chalky enamel mottling was visible on most of the dentition. SK 201 has a carious lesion on the right-sided maxillary premolar and on the left-sided second incisor.

Antemortem tooth loss and bone remodelling were observed in the mandibles of individuals SK 132, SK 157 and SK 201 (**Pl. XV–XVII**).

Periapical lesions. Inflammation of a dental pulp increases the internal pressure and leads to the death of the pulp. A necrotic pulp is very likely to be infected and bone cavities are formed for the drainage of the pus. The cavity could be a granuloma, a cyst or an abscess. The rounded margins of the cavity that are surrounded by woven bone represent a chronic abscess (Ogden 2007, p. 293–298, fi. 13.8, 13.10–13.11). These were observed in individuals SK 107, SK 132, SK 152, SK 157 and SK 200). SK 107 has an abscess of medium size (>3 mm) on the external

side of the alveolar bone, above the tip of the root of the right maxillary second incisor, and one more of medium to large size (6.8 mm) at the buccal side of the alveolar bone of the right mandibular molars. This second abscess is surrounded by woven bone formation (halo) (**Pl. XV/4**). SK 132 has abscesses affecting the right maxillary second and third molars, as well as the left maxillary first molar (**Pl. XV/1**). The right left molar of SK 200 also displays a periapical abscess (**Pl. XVI/5–6**). Both SK 152 and SK 157 have abscesses at the site of the left maxillary first, respectively second molar.

Two individuals have been noted with impacted teeth within the sample – SK 132 and SK 190. A particularly noteworthy case is SK 132 who displays a mandibular canine impacted within the body of the left mandible, near the mental protuberance. This is accompanied by irregular bone formation suggestive of an active infection at the time of death. The individual exhibits numerous co-occurring dental pathologies: crowding, periodontitis, advanced dental wear, caries, and abscesses, all likely exacerbated by poor oral hygiene and dental misalignment (**Pl. XV/3**; **XVI/1–4**). SK 190 presents also with impaction of the left mandibular canine, but the tooth is preserved in its original alveoli (**Pl. XVII/4–5**). Contributing factors to dental impaction include trauma during tooth development, infections, endocrine imbalances, and malocclusion (Ruiyi, Ruijie 2025, p. 51; Rajic, Muretic, Percac 1996, p. 477).

Individual SK 190 displays a pronounced diastema at the maxillary frontal teeth. The midline diastema, defined as a space between the maxillary central incisors, is a common feature in early dentition and typically closes with the eruption of lateral incisors and canines. It is more frequent in individuals of African and Mediterranean descent and displays age- and sex-related differences. While once attributed primarily to an enlarged labial frenum, current understanding acknowledges a multifactorial etiology: pernicious habits such as thumb sucking or lip biting; muscular imbalances like tongue thrust or macroglossia, and physical impediments such as mesiodens, retained primary teeth, or cysts or abnormalities in maxillary arch structure and dental anomalies (Huang, Creath 1995, p. 171).

SK 190 also has a retained a deciduous second molar and an impacted canine, as previously noted, with agenesis of the second premolar (**Pl. XVII/6**). Dental agenesis, especially of the third molars, is common and more frequently observed in females (Rakhshan 2015, p. 1–2). In this particular case, the several interrelated dental anomalies were probably caused by the congenital absence of the second premolar, that prevented normal tooth replacement and led to severe crowding within the dental arcade, causing the impaction of the canine. Such a sequence of anomalies illustrates how a single agenesis can trigger a cascade of secondary dental pathologies.

Malocclusion is present in individuals SK 132 and SK 201. In SK 132, the right mandibular canine is rotated toward the first premolar (**Pl. XV/3**). In SK 201, the right mandibular canine and the left maxillary first premolar are both misaligned. Malocclusion is defined as the misalignment of the upper and lower teeth during jaw closure. It has been associated with a higher risk of periodontal disease due to increased plaque accumulation. Various genetic and environmental factors contribute to its high prevalence and include hereditary traits, congenital conditions, endocrine or metabolic disturbances, oral habits (thumb sucking, tongue thrust), and anomalies in tooth size, shape, eruption, or number (Alqahtan *et alii* 2020, p. 62–63, table 1).

Enamel hypoplasia. Enamel morphogenesis is a continuous and intricate process that begins with the secretion of enamel matrix proteins, followed by their mineralisation and maturation. This developmental sequence starts at the cusps or incisal edges of the teeth and gradually advances toward the cervical regions. Disruptions occurring at various stages of this process can result in developmental defects of enamel, such as enamel hypoplasia. This condition is characterised by a reduction in enamel thickness, which may be presented as linear grooves, pits, or even areas of completely missing enamel. It is typically the result of multiple contributing factors rather than a single cause, such as trauma or infection, nutritional deficiencies, illnesses, or genetic conditions, such as amelogenesis imperfecta or other inherited syndromes (Anthonappa, King 2015, p. 16, 18–20; Waldron 2009, p. 243–245). Enamel hypoplasia, the linear type, was recorded in SK 119, SK 122, SK 133, SK 147, and SK 201.

Enameloma, an enamel pearl, was noted on the third maxillary molar (right side) of individual SK 107. Enamel pearls are rare developmental anomalies characterised by small ectopic globules of enamel, usually found on the root surface of teeth, most often molars. Macroscopically, they present as smooth, white, rounded nodules ranging from 0.3 to 4 mm in diameter. Located distally near the cervical margin at the furcation, enamel pearls are asymptomatic but may trap food debris, contributing to dental complications (Rathva 2012; Hillson 2005, p. 316).

Non-masticatory activities

Dental wear naturally results from chewing but also from using teeth for non-masticatory purposes. These two types of wear differ: masticatory wear is generally uniformly distributed and affects primarily the crowns, whereas non-masticatory wear leads to regular facets, chipping, and depressions on various teeth, depending on use (Walsh 2022, p. 1264–1265).

Common features include enamel chipping, interproximal grooves or notches, and depressions, which vary in location and morphology according to function.

Using the dentition as a tool is documented as early as the Palaeolithic and continues into modern times. Ethnographic parallels suggest this practice was used in basketry, reed or tendon processing for bowstrings, fishing nets, rope, or mats (Bonfiglioli *et alii* 2004, p. 449–454, fig. 1–5; Walsh 2022, 1264–1265; Molnar 1971, 185–188; 2011, p. 682–684, 686, fig. 1–2, 5; Molnar *et alii* 1972, p. 515).

Most of the analysed individuals show enamel chipping and microfractures, likely due to dietary habits. SK 157, a male individual aged between 35 to 50 years old at death shows intense polishing of the occlusal surfaces of maxillary and mandibular teeth, displaying a pattern of labial rounding (**Pl. XVII/1–2**). SK 142 has the superior portion of the labial crown surface of the left lateral mandibular incisor chipped (**Pl. XV/2**).

Radiocarbon data

Four human bone samples taken from the skeletal remains of non-adult and adult individuals were selected as being suitable for radiocarbon analysis – SK 105, SK 116, SK 119, and SK 147.

Calibration of radiocarbon data from ICL 2015–2017 in OxCal 4.4 (Bronk Ramsey 2009) using the IntCal20 (Reimer *et alii* 2020) curve at 1-year resolution provides the following data:

ICL#1 (Poz-118958) was sampled from the inhumation grave of **SK 105** at a depth of 0.40 m. The sample consisted of a fragment of the left ischium from a non-adult individual aged between 14.5–15.5 years old at death, and yielded the radiocarbon age 5950 ± 35 BP. When calibrated, the computed chronospan[8] is with 68.3% probability: 4897 BC (17.0%) 4865.9 BC and 4849.8 BC (51.3%) 4784.2 BC and with 95.4% probability: 4933.5 BC (3.2%) 4918.2 BC and 4907.5 BC (92.3%) 4723.6 BC.

ICL#2 (Poz-118960) was sampled from the inhumation grave of **SK 116** at a depth of 0.36 m. The sample consisted of a fragment of the left ilium from an adult individual aged between 17 to 29 years old at death. It yielded the radiocarbon age 5930 ± 40 BP. When calibrated, the computed chronospan is with 68.3% probability: 4843.5 BC (49.0%) 4774.2 BC and 4759.2 BC (19.3%) 4725.5 BC and with 95.4% probability: 4930.9 BC (1.1%) 4922.3 BC and 4904.4 BC (94.4%) 4713.6 BC.

[8] ChronoSpan – similar to the chronological life span (CLS) used in biology, which measures the viability of a population of non-dividing cells over time – is a new term we used for the calibrated and modelled probability distribution function in radiocarbon dating. It best synthesises the scatter, amplitude and timeline position of the temporal probability spectrum used in archaeology, especially when it is reduced through Exploratory Chronology (Condurățeanu, Gligor 2022, p. 39) to the σ 1 and σ 2 intervals.

ICL#3 (Poz-118961) was sampled from the inhumation grave of **SK 119** at a depth of 0.39 m. The sample consisted of a fragment of the humeral diaphysis of a non-adult individual, aged between 13.5–15.5 years old at death, and yielded the radiocarbon age 5975 ± 35 BP. When calibrated, the computed chronospan is with 68.3% probability: 4903.2 BC (30.1%) 4860.7 BC and 4854.7 BC (38.1%) 4795.9 BC and with 95.4% probability: 4984.6 BC (1.2%) 4972.2 BC, 4951.5 BC (91.6%) 4779.4 BC and 4752.4 BC (2.7%) 4728.4 BC.

ICL#4 (Poz-118962) was sampled from the inhumation grave of **SK 147** at a depth of 0.40 m. The sample consisted of a fragment of the right ilium of a non-adult individual, aged 13 years old at death, and yielded the radiocarbon age 5940 ± 40 BP. When calibrated, the computed chronospan is with 68.3% probability: 4889.5 BC (9.4%) 4869.5 BC, 4847 BC (48.3%) 4780.2 BC and 4749.9 BC (10.6%) 4728.4 BC and with 95.4% probability: 4933.5 BC (2.6%) 4918.3 BC and 4907.5 BC (92.8%) 4717.9 BC.

The radiocarbon data from ICL 2015–2017 was also modelled on the OxCal4.4 platform using the IntCal20 curve at 1-year resolution in CQL language using Phase () and provided the following values for the modelled ChronoSpans:

ICL#1 (5950 ± 35 BP): 68.3% probability: 4845.3 BC (68.3%) 4791.4 BC; 95.4% probability: 4901.5 BC (93.1%) 4769.5 BC and 4752.5 BC (2.4%) 4733.4 BC; Agreement 121.7%.

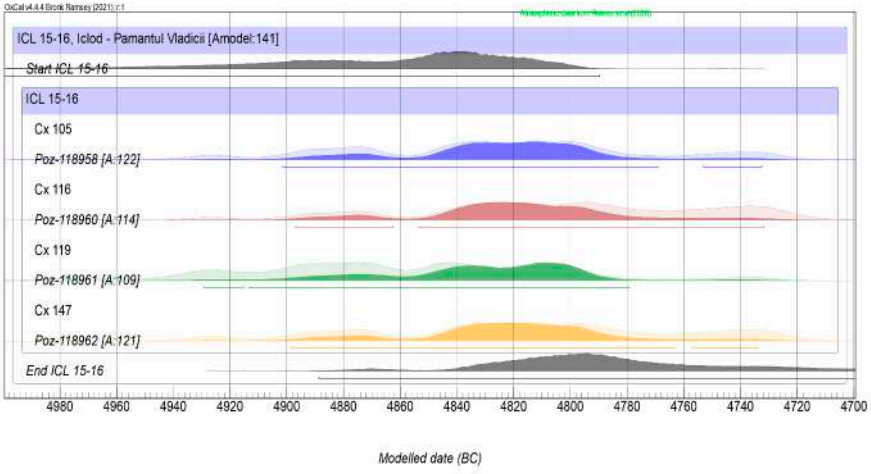


Fig. 1. Calibrated and modelled ^{14}C data from ICL 15–17 Iclod–*Pământul Vlădicii*. OxCal 4.4, IntCal20, 1 yr. resolution.
Fig. 1. Datele radiocarbon (^{14}C) calibrate și modelate de la ICL 15-17 Iclod–*Pământul Vlădicii*. OxCal 4.4, IntCal20, rezoluție de 1 an.

ICL#2 (5930 ± 40 BP): 68.3% probability: 4844.5BC (68.3%) 4787.5BC; 95.4% probability: 4896.7 BC (10.5%) 4862.4 BC and 4853.5 BC (84.9%) 4732.4 BC. Agreement 114.4%.

ICL#3 (5975 ± 35 BP): 68.3% probability: 4850.7 BC (68.3%) 4792.2 BC; 95.4% probability: 4927.4 BC (95.4%) 4779.2 BC. Agreement 108.5%.

ICL#4 (5940 ± 40 BP): 68.3% probability: 4845.6 BC (68.3%) 4789 BC; 95.4% probability: 4898.1 BC (92.1%) 4760.2 BC and 4756.9 BC (3.4%) 4734.7 BC. Agreement 120.6%.

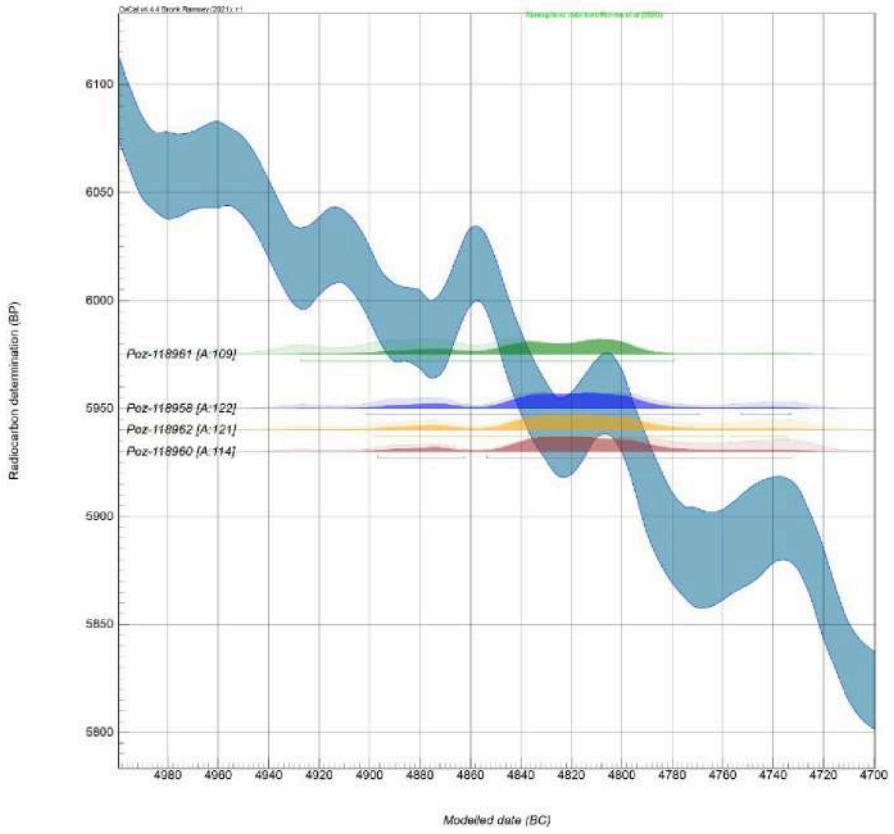


Fig. 2. Calibrated and modelled ^{14}C data from ICL 15–17 Iclod–*Pământul Vlădicii*. OxCal 4.4, IntCal20, 1 yr. resolution against IntCal20 calibration curve background.
Fig. 2. Datele radiocarbon (^{14}C) calibrate și modelate de la ICL 15–17 Iclod–*Pământul Vlădicii*. OxCal 4.4, IntCal20, rezoluție de 1 an, comparativ cu curba de calibrare IntCal20 în fundal.

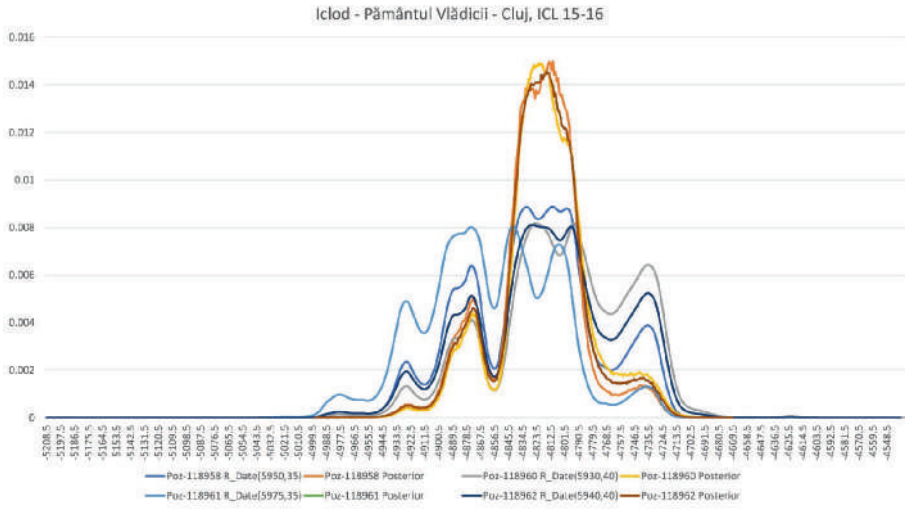


Fig. 3. Raw data analysis of the calibrated and modelled ^{14}C data from ICL 15–17 Iclod–*Pământul Vlădicii*. OxCal 4.4, IntCal20, 1 yr. resolution.
Fig. 3. Analiza datelor brute radiocarbon (14C) calibrate și modelate din ICL 15–17 Iclod–*Pământul Vlădicii*. OxCal 4.4, IntCal20, rezoluție de 1 an.

Thus, the data presented in **Table 1** were completed, displaying very good individual agreements with the applied model, while the overall model achieved an agreement of 141% (**Fig. 1–2**). The raw data coming from the calibrated and modelled (posterior values) data is presented in **Fig. 3**.

The new data from ICL 2015–2017 were subsequently integrated and cross-checked for consistency with previously published ^{14}C data (Diaconescu, Lazarovici, Tincu 2013, Tab. 1, p. 50–51), also sampled from human remains.

The resulted model for the Iclod necropolis yielded high agreements for all ^{14}C samples, with a notable exception of the oldest ^{14}C date from **M 67**, **Iclod B**, Poz 53762, 6015 ± 35 BBP, with an agreement of only 75% and the youngest ^{14}C date from **M 31**, **Iclod B**, Poz 53758, 5735 ± 30 BP, with an even lower agreement of 62.2%. But, taking into consideration that the accepted threshold of 60% was met in both cases, both ^{14}C dates were kept as part of the overall model (**Fig. 4–5**) of the Late Neolithic Iclod necropolis. The human remains from ICL 2015–2017 cluster together (see central portion of **Fig. 3**) within a time span barely exceeding half a century and, based on the radiocarbon data (**Fig. 5**), can therefore be attributed to the first phase of habitation at the Iclod–*Pământul Vlădicii* site.

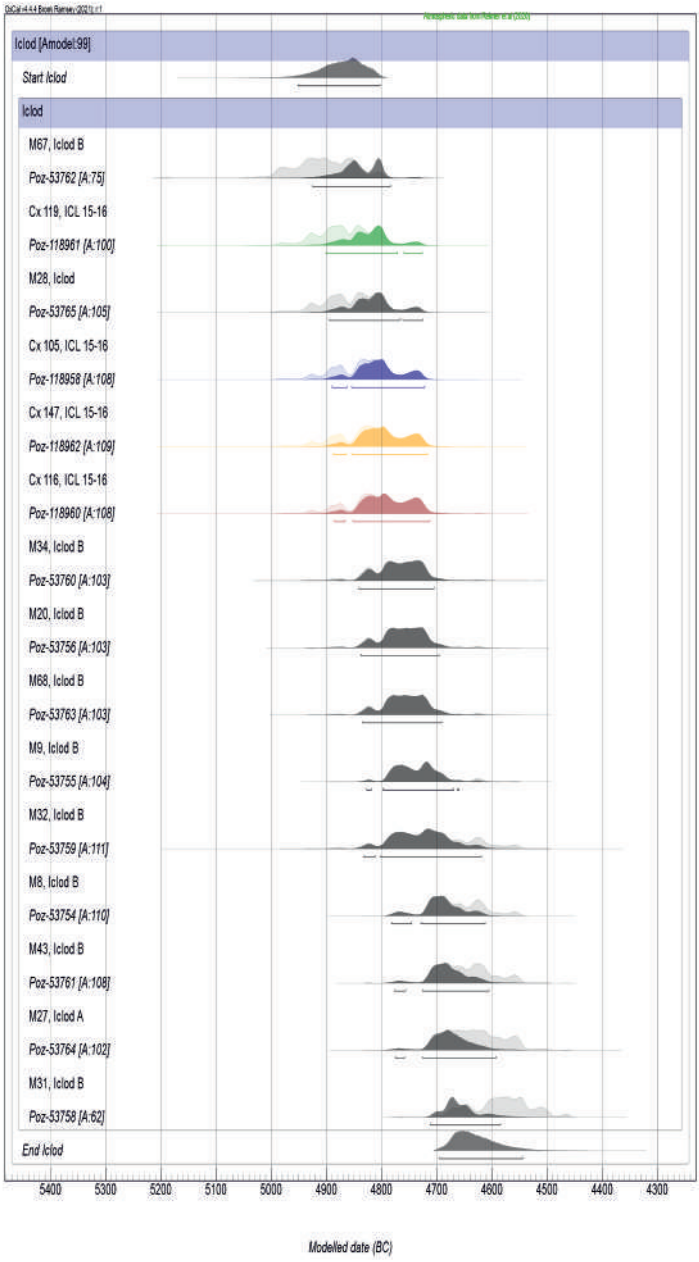


Fig. 4. Calibrated and modelled ^{14}C data from the Late Neolithic necropolis from Iclod. OxCal 4.4, IntCal20, 1 yr. resolution.
Fig. 4. Datele radiocarbon (^{14}C) calibrate și modelate din necropola neolitică târzie de la Iclod. OxCal 4.4, IntCal20, rezoluție de 1 an.

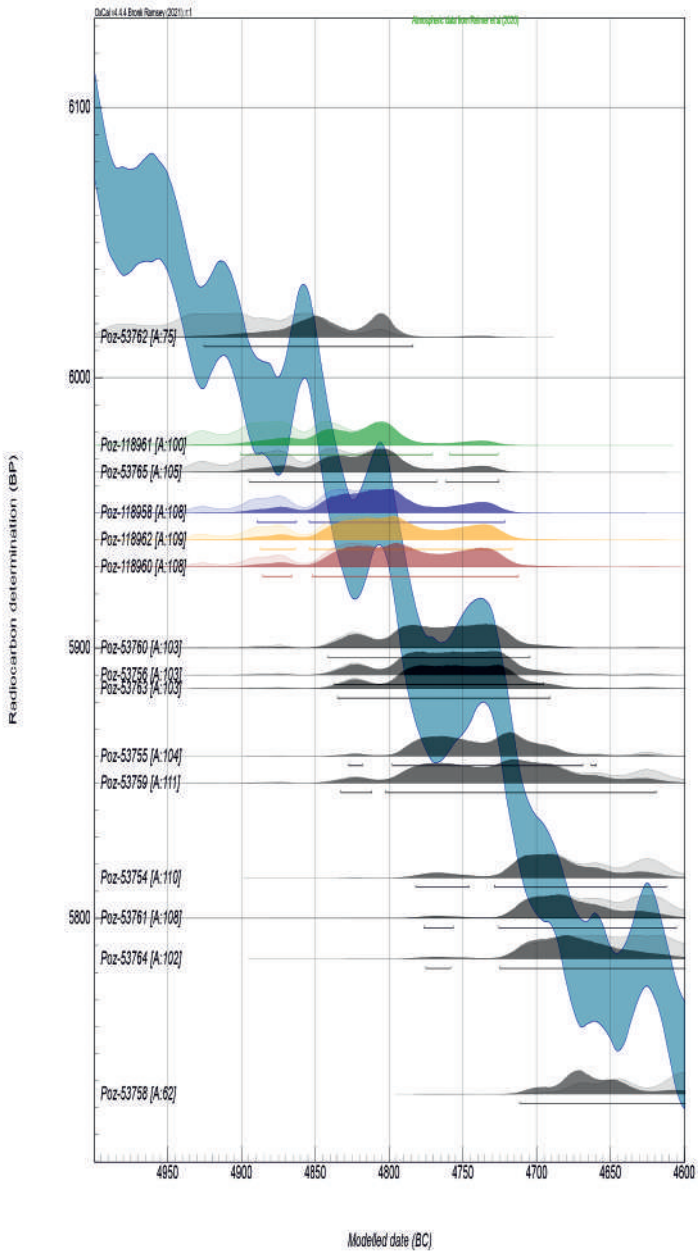


Fig. 5. Calibrated and modelled ^{14}C data from the Late Neolithic necropolis from Iclod. OxCal 4.4, IntCal20, 1 yr. resolution against IntCal20 calibration curve background.
Fig. 5. Date radiocarbon (^{14}C) calibrate și modelate din necropola neolitică târzie de la Iclod. OxCal 4.4, IntCal20, rezoluție de 1 an, comparativ cu curba de calibrare IntCal20 în fundal.

Discussion

For the Neolithic and Eneolithic periods of Transylvania and Crișana historical regions, necropolises have been identified at: Decea Mureșului (Alba County) (Dodd-Oprițescu 1978), Cămin–*Podul Crasnei* (Németi 1988, p. 123–126), Moftinu Mare–*Hamiliz* (Satu Mare County) (Marta *et alii* 2017), Zalău–*Aeroport* (Sălaj County) (Lazăr, Băcueț-Crișan 2011, p. 5, 11, 25, 39–40, 63–64; Gligor, Băcueț-Crișan 2014, p. 53; Băcueț-Crișan, Constantinescu 2019, p. 13), Urziceni–*Vade Ret-Vamă* (Satu Mare County) (Virag 2004; Szűcs-Csillik, Virag 2016; Virag, Astaloș 2017; Virag *et alii* 2018; Virag, Astaloș, Orsolya 2019; 2020; Sommer, Virag 2024), Pecica–*Est* (Arad County) (Sava, Mărginean, Ursuțiu 2017; Sava *et alii* 2023). Other significant funerary discoveries include the burials from Gura Baciului (Cluj County) (Lazarovici 1995, p. 321–434), Orăștie–*Dealul Pemilor* (Hunedoara County) (Luca 2000), Porț–*Corău* (Sălaj County) (Lazăr, Băcueț-Crișan 2011, p. 5, 11–12, 24, 36, 39, 41, 63; Gligor, Băcueț-Crișan 2014, p. 66–67; Băcueț-Crișan, Constantinescu 2019, p. 10–12, 14).

The Decea Mureșului necropolis, first excavated in 1912 by István Kovács, yielded 19 graves, of which four of them had no skeletal remains preserved and were identified through red ochre stains. The individuals were placed in a supine position, with the legs flexed at the knees and placed either to their left or right. There is a possibility that the knees were initially raised, later collapsing either to the right or to the left. The orientation of the graves was mostly SW-NE. Grave goods included ceramic vessels, lithic tools, copper objects (double-edged knives, needles, beads, necklaces, and a torque), belts made of discoidal beads cut from *Unio* shells, granite maces. In each burial, the presence of red ochre was recorded, either as clumps spread in the fill soil or as small deposits placed near the lower limbs or the head of the deceased (Dodd-Oprițescu 1978, p. 87–88).

The necropolis of Cămin–*Podul Crasnei*, documented primarily between 1981 and 1983, yielded a series of nine disturbed and intact inhumation graves, many discovered accidentally during infrastructure projects. The burial tradition involved crouched inhumations, generally oriented E-W and placed in oval shaped pits. Grave goods consist of a typologically uniform ceramic assemblage, including grey or reddish "milk jug" pots with small handles, flowerpot-shaped vessels decorated with rounded protrusions, shallow bowls, and pedestal cups, some perforated with rhomboidal holes. Miniature vessels and fine-ware bowls occasionally accompany these sets, and faunal remains, particularly pig bones, suggest food offerings. Notably, a gold foil ornament decorated with incised lines was recovered from Grave 6, while lithic artefacts such as obsidian arrowheads and flint blades appear sporadically (Németi 1988, p. 123–126, 138–146, fig. 7–13).

Archaeological context	Sample /Anthrop. Inf.	Photo	$_{14}$C uncalib.	Lab.	Cal BC (1σ) (68.3%)	Cal BC (2σ)
ICL#1 Cx. 105/SK 105 Depth 0.40m Inhumation grave	Human bone – left ischium. Non-adult individual, age at death 14.5–15.5		5950 ± 35 BP	Poz-118958 3.2%N, 9.5%C, 9.3% collagen	4845.3–4791.4 BC	4901.5–4769.5BC (93.1%) 4752.5–4733.4BC (2.4%) Agreement 121.7%
ICL#2 Cx. 116/SK 116 Depth 0.36m Inhumation grave	Human bone – left part of ilium Young adult individual, age at death 23–25		5930 ± 40 BP	Poz-118960 1.8%N, 6.6%C, 1.8% collagen	4844.5–4787.5 BC	4896.7–4862.4 BC (10.5%) 4853.5–4732.4 BC (84.9%) Agreement 114.4%
ICL#3 Cx. 119/SK 119 Depth 0.39m Inhumation grave	Human bone – humeral diaphysis Non-adult individual, age at death 13.5–15.5		5975 ± 35 BP	Poz-118961 3.5%N, 10.5%C, 9.2% collagen	4850.7–4792.2 BC	4927.4–4779.2 BC (95.4%) Agreement 108.5%
ICL#4 Cx. 147/SK 147 Depth 0.40m Inhumation grave	Human bone – right ilium Non-adult individual, age at death 13		5940 ± 40 BP	Poz-118962 3.8%N, 10.7%C, 6.1% collagen	4845.6–4789 BC	4898.1–4760.2 BC (92.1%) 4756.9–4734.7 BC (3.4%) Agreement 120.6%

Table 1. Summary of the radiocarbon date sampled from deceased pertaining to ICL 15–16 Iclod–*Pământul Vlădicii*.
Tab. 1. Sinteza datelor radiocarbon (^{14}C) prelevate de la scheletele din cadrul ICL 15–16 Iclod–*Pământul Vlădicii*.

The Late Neolithic necropolis recent identified at Moftinu Mare–*Hamiliz* contain 11 graves arranged in clusters of two or three. All the burial pits, rectangular-shaped, are oriented along an E-W axis, with the deceased placed in a crouched position, with the head to the east. With a single exception, all graves contained funerary inventory: ceramic vessels, polished stone axes, and chipped lithic tools (made of flint and obsidian). The clustering of graves may suggest that the burials followed rules which likely reflected certain group identities (Marta *et alii* 2017, p. 190).

At the cremation necropolis discovered at Zalău–*Aeroport*, the graves were consistently represented by urn burials, with the burned human remains deposited after the burning in special vessels, forming a distinct cemetery, located approximately 500 m away from the main settlement. The human remains were often found in association with burnt non-human remains (*Ovis aries*/*Capra hircus*), most likely reflecting the practice of funerary feasting. The grave pits were also circular-shaped (0.20–0.30 m). Anthropological analyses were conducted on the cremains of three individuals namely C3, C5 and C9, although several of the graves were heavily disturbed or partially destroyed by agricultural activities. The individuals analysed were two adults – C3 and C9, with C5 being determined as a non-adult aged between 5–14 years old at death (Lazăr, Băcueț-Crișan 2011, p. 5, 11, 25, 39–40, 63–64, fig. 1, 6–7; Gligor, Băcueț-Crișan 2014, p. 53; Băcueț-Crișan, Constantinescu 2019, p. 13).

Archaeological investigations carried out at Urziceni–*Vade Ret-Vamă* uncovered 132 inhumation graves and represents the largest Bodrogkeresztúr cemetery ever excavated in what is nowadays Romania and is particularly renowned for its numerous gold ornaments and other scientifically valuable artefacts. The necropolis was discovered in 2003 during rescue excavations. The individuals were placed in crouched most containing crouched skeletons, oriented W-E, placed in rectangular pits with slightly rounded corners (Virag 2004, p. 41–45; Szűcs-Csillik, Virag 2016, fig. 1–6; Virag, Astaloș 2017; Virag *et alii* 2018; Virag, Astaloș, Orsolya 2019; Virag, Astaloș, Orsolya 2020; Sommer, Virag 2024, p. 188–197, fig. 1–2, 6–7).

The rescue excavations carried out in 2015 and 2016 at Pecica–*Est* (Arad County) revealed the largest Eneolithic necropolis documented to date in the Lower Mureș Basin, with 143 inhumation graves excavated. The cemetery is attributed to the Tiszapolgár cultural horizon, with evidence also suggesting Bodrogkeresztúr influences. Crouching position dominates the burial posture (118 individuals), with a smaller number in dorsal decubitus with flexed limbs (one case), and 24 burials where the position could not be determined. Lateral body placement follows previously noted patterns: 49 individuals lay on their

right side and 45 on the left. Orientation was predominantly SE-NW, with some deviations (E-W, NE-SW, N-S). The majority of burials were single interments, but at least five double graves, and one triple burial, were identified. A number of 114 out of the 143 graves uncovered had grave goods. Most graves contained ceramic vessels (337 in total), often accompanied by items made of gold (seven pieces) and copper (45 items including beads, rings, and tools). Lithic artefacts were particularly numerous (1479 items), mainly beads, along with blades and arrowheads. Bone tools and ornaments, animal bones, shells, ochre, and adobe fragments were also present. The richest inventories, such as in graves Cx. 97 and Cx. 142, indicate possible social differentiation within the community (Sava, Mărginean, Ursuțiu 2017, p. 56–67, fig. 1–3, 7–20; Sava *et alii* 2023, p. 245–246, 249, 253–254, fig. 1–2, 8–9).

At Gura Baciului, the Early Neolithic community practiced both inhumation (Gr. 1 to Gr. 6 and Gr. 8 to Gr. 10) and cremation (Gr. 7). Archaeological excavations recovered 10 burials, eight of them in surface dwelling features. The orientation of the graves varies, with Gr. 3, Gr. 4, and Gr. 6 aligned NW-SE, the others consistently facing E. The deceased were placed in crouched positions, either to the right or left side. Some graves, such as M 1, were covered with pottery fragments and bones, while others, like Gr. 6, contained fragments of large storage vessels. The funerary inventory includes pottery fragments, lithic objects, a fragment of an *Equus hydruntinus* maxilla (M 3), a grinding tool and pestle (M 4), flint, bone awls (Lazarovici 1995, p. 321–322, 396, 400, pl. I–II, Va, d, VIc, d, XI, XIIIb, XVIa, XVII–XXI, fig. 4–5).

At Orăștie–*Dealul Pemilor*, five graves were discovered, two of which were cenotaphs (Turdaș culture/Late Neolithic). The fill of all graves contains charcoal, red ochre, particularly concentrated in the head, torso, and feet regions, burnt animal bones, and ceramic fragments. The latter likely originate from vessels intentionally broken during funerary feasts, as many fragments can be partially reconstructed. All skeletons are oriented E-W. The bodies were laid on their right side in a crouched position. Each burial included a meat offering, typically placed near the head (Luca 2000, p. 59–62, plan 1, fig. 1–3).

The Late Neolithic funerary discoveries from Porț–*Corău* are represented by both cremation and inhumation graves. The inhumations are mostly scattered within the settlement, with a small cluster located in the southern area, while a peripheral sector included two rows of 17 cremation burials. The cremation graves often consisted of small circular pits (0.50×0.70 m), often accompanied by grave goods such as cups, bowls, or painted vessels and lithic artefacts. In some of the cases, the cremains bore the traces of red ochre. Burnt non-human remains (*Ovis aries*/*Capra hircus*) were found in association with the cremains, notably in Gr. 3/

C180/2010 (adult individual) and Gr. 6/C180/2–12 (a non-adult). Analysis of eight cremation graves shows a predominance of adults, mostly male, with only one female and one non-adult represented (Lazăr, Băcueț-Crișan 2011, p. 5, 11–12, 24, 36, 39, 41, 63, fig. 1, 6; Gligor, Băcueț-Crișan 2014, p. 50, 66–67, pl. IV–V; Băcueț-Crișan, Constantinescu 2019, p. 10–12, 14).

The funerary context researched between 2015–2017 at Iclod comprises 24 new inhumation graves (**Pl. I**). The majority of the burial pits were oval-shaped followed by rectangular ones with rounded corners. A total of 18 graves (SK 105, SK 107, SK 109, SK 116, SK 119, SK 122, SK 124, SK 125, SK 133, SK 142, SK 180, SK 181, SK 190, SK 195, SK 197, SK 200, SK 201, and SK 233) were excavated with oval/elongated profiles, often tapering toward the feet or exhibiting slight irregularities. Six graves (SK 132, SK 147, SK 152, SK 153, SK 157, and SK 159) were rectangular with rounded corners. There is no clear correlation between grave shape and the sex or age of the deceased, as both oval and rectangular pits contain male and female individuals of various age groups (**Table 2**).

Sixteen graves exhibit a W-E orientation, while six (SK 107, SK 109, SK 116, SK 119, SK 152, and SK 153) follow a SW-NE alignment, and two (SK 105 and SK 233) are oriented NW-SE. Most individuals (22 out of 24) were deposited in dorsal decubitus, often with the upper limbs extended alongside the body – SK 105, SK 119, and SK 122 or resting over the pelvic area – SK 125, SK 132, SK 195, SK 197, and SK 201. Variations in arm positioning were observed in SK 116 and SK 153, while SK 109 displays slight flexion of the lower limbs. SK 190 represents the only individual interred in lateral decubitus. The recurrence of dorsal decubitus and consistent grave orientations reflect shared mortuary norms within the community, while isolated deviations such as SK 190 or the limb flexion in SK 109 may indicate specific practices, social aspects, or individualised ritual treatment (**Table 2**; **Fig. 6**).

Prior excavations at the two Iclod cemeteries yielded around 109 individuals. Anthropological analyses, though fragmented and conducted by various researchers across institutions and timeframes, some only partially published or lacking archaeological context, provided insights into the dominant anthropological types, demographic patterns, and burial practices of the community.

Our anthropological analysis of the Neolithic skeletal assemblage from Iclod consisting of 24 individuals, brings new data that could complement previous research conducted at the site. These new discoveries have the potential of enhancing the demographic structure, health conditions, and social dynamics of the Iclod community, contributing to a more comprehensive reconstruction of this prehistoric population.

Burial	Depth	Shape	Position	Orientation
SK 105	0.40	oval	DD; arms placed along the body	NW-SE
SK 107	0.40	oval	DD	SW-NE
SK 109	0.36	oval	DD; arms placed on the pelvic area; legs flexed towards the left	SW-NE
SK 116	0.36	oval	DD; left arm flexed, placed on thoracic area; right arm flexed and placed on the pelvic area	SW-NE
SK 119	0.39	oval	DD; arms placed on the pelvic area	SW-NE
SK 122	0.36	oval	DD; arms placed along the body	W-E
SK 124	0.36	oval	DD	W-E
SK 125	0.40	oval	DD; arms placed on the pelvic area	W-E
SK 132	0.40	rectangular with rounded corners	DD; arms placed on the pelvic area	W-E
SK 133	0.40	oval	DD	W-E
SK 142	0.40	oval	DD	W-E
SK147	0.40	rectangular with rounded corners	DD; arms placed on the pelvic area	W-E
SK 152	0.40	rectangular with rounded corners	DD; arms placed on the pelvic area	SW-NE
SK 153	0.40	rectangular with rounded corners	DD; right arm along the body; left arm placed on the pelvic area	SW-NE
SK 157	0.40	rectangular with rounded corners	DD	W-E
SK 159	0.40	rectangular with rounded corners	DD; right arm placed on the pelvic area; left arm placed along the body	W-E
SK 180	0.40	oval	DD	W-E
SK 181	0.40	oval	DD	W-E
SK 190	0.40	oval	LD; right side	W-E
SK 195	0.40	oval	DD; arms placed on the pelvic area	W-E
SK 197	0.40	oval	DD; arms placed on the pelvic area	W-E
SK 200	0.40	oval	DD	W-E
SK 201	0.40	oval	DD; arms placed on the pelvic area	W-E
SK 233	0.40	oval	DD	NW-SE

Table 2. Summary of archaeological data ICL 2015–2017
(individual, depth, grave-shape variation, position of the skeletal remains and orientation;
DD – dorsal decubitus; LD – lateral decubitus).
Tab. 2. Sinteza datelor arheologice pentru situl ICL 2015–2017
(individ, adâncime, forma mormântului, poziția resturilor scheletice și orientarea;
DD – decubit dorsal; LD – decubit lateral).

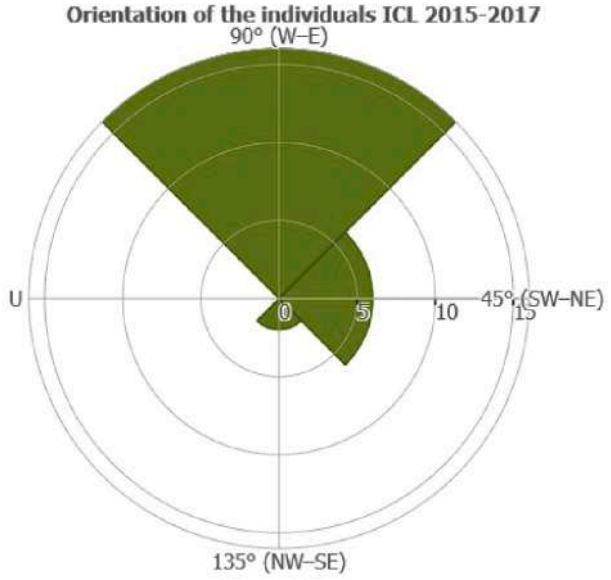


Fig. 6. Orientation of graves in the ICL 2015–2017 research. W-E (90°) – graves aligned along a W-E axis; SW-NE (45°) – graves aligned along a SW-NE axis; NW-SE (135°) – graves aligned along a NW-SE axis; Rose diagram created with https://geographyfieldwork.com/RoseDiagramCreator.html, accessed 20.06.2025; degrees indicate the azimuthal orientation on a 360° compass, where 0° = North, 90° = East, 180° = South, and 270° = West. The length of each sector in the diagram represents the number of graves with that orientation.

Fig. 6. Orientarea mormintelor cercetate în campania ICL 2015–2017. W-E (90°) – morminte aliniate de-a lungul axului W-E; SW-NE (45°) – morminte aliniate de-a lungul axului SW-NE; NW-SE (135°) – morminte aliniate de-a lungul axului NW-SE; Diagramă creată cu https://geographyfieldwork.com/RoseDiagramCreator.html, accesată la 20.06.2025; gradele indică orientarea azimutală pe o busolă de 360°, unde 0° = Nord, 90° = Est, 180° = Sud și 270° = Vest. Lungimea fiecărui sector din diagramă reprezintă numărul de morminte cu respectiva orientare.

Sex determination was possible for 15 of the adult individuals (62.5% of the total sample of 24). Of these, eight were female – SK 107, SK 132, SK 153, SK 157, SK 190, SK 197, SK 200, and SK 233 (53.3% of the sexed adults, 33.3% of the total sample), and seven were male, namely SK 116, SK 122, SK 125, SK 152, SK 180, SK 195, and SK 201 (46.7% of the sexed adults, 29.2% of the total sample). Two additional adults (SK 124 and SK 159 – 8.3% of the total) could not be sexed due to poor preservation. The remaining seven individuals (29.2% of the total – SK 105, SK 109, SK 119, SK 133, SK 142, SK 147, and SK 181) are non-adults (children and adolescents) (**Fig**. **7**; **9**).

Age-at-death estimation reveals that young adults (20–25 years) form the largest group, comprising eight individuals (33.3% of the total sample): SK 107♀, SK 116♂, SK 125♂, SK 153♀, SK 159?, SK 190♀, SK 201♂, and SK 233♀; SK 159 could not be properly aged due to poor preservation) (**Fig. 8**).

Middle adults (35- to 50-year-olds) are represented by six individuals (25%): SK 132♀, SK 152♂, SK 157♀, SK 195♂, SK 197♀, and SK 200♀. Adolescents (12 to 20 years) account for four individuals (16.7%): SK 105, SK 109, SK 119, and SK 147, while the child category (3 to 12-year-olds) includes three individuals (12.5%): SK 133, SK 142, and SK 181. One individual, SK 122♂, is classified as a borderline old adult, aged 50 years old at death (4.2%). Two other adult individuals (8.3%), SK 124 (undetermined) and SK 180 (male), could not be determined precisely due to poor preservation. Two additional adults (8.3%), SK 124? and SK 180♂, could not be aged more precisely due to poor preservation (**Fig. 8**). This distribution reflects a relatively balanced presence of males and females among the sexed adult population, with a slight predominance of women in the young and middle adult age groups (**Table 3**; **Fig. 8–9**).

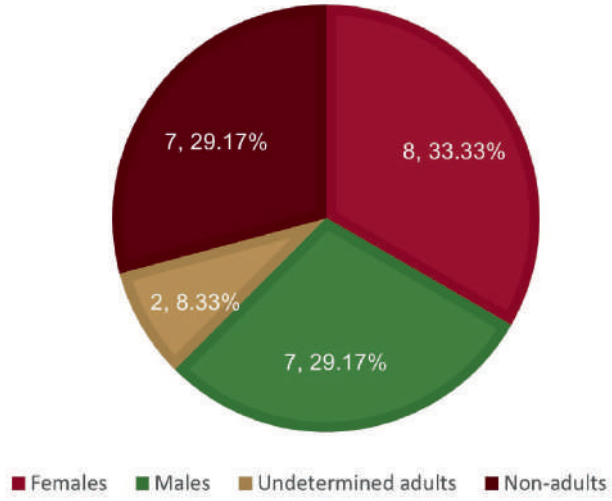


Fig. 7. Distribution of individuals by sex and age category in the ICL 2015–2017 research, indicating eight females, seven males, two undetermined adults, and seven non-adults.
Fig. 7. Distribuția indivizilor în funcție de sex și categoriile de vârstă în seria ICL 2015–2017, indicând opt femei, șapte bărbați, doi adulți nedeterminați și șapte non-adulți.

Taken together, young and middle adults constitute 58.3% of the total sample (14 individuals), underscoring significant mortality during the prime reproductive and productive stages of life. There is a slight overrepresentation of females (33.3%)

compared to males (29.2%). Non-adults (children and adolescents) account for 29.2% of the individuals (seven cases), reflecting the elevated juvenile mortality typical of prehistoric populations. The minimal presence of old adults (4.2%) likely reflects both actual demographic trends and the difficulty of confidently identifying advanced age due to taphonomic and diagnostic limitations (**Table 3**; **Fig**. **10**).

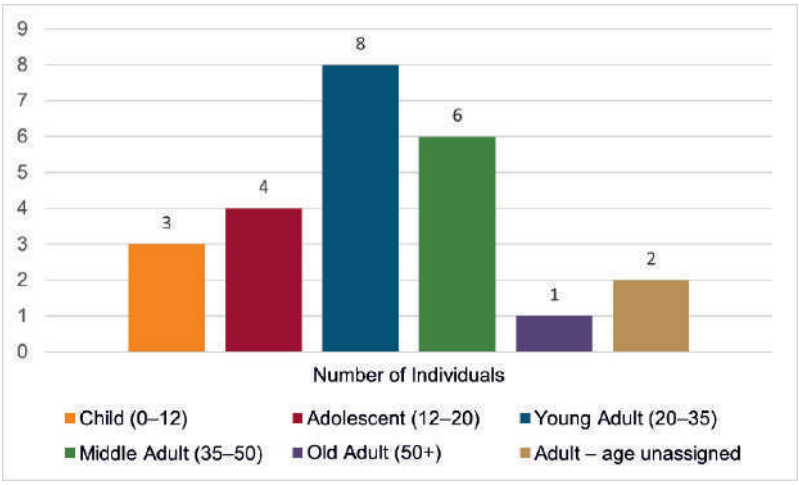
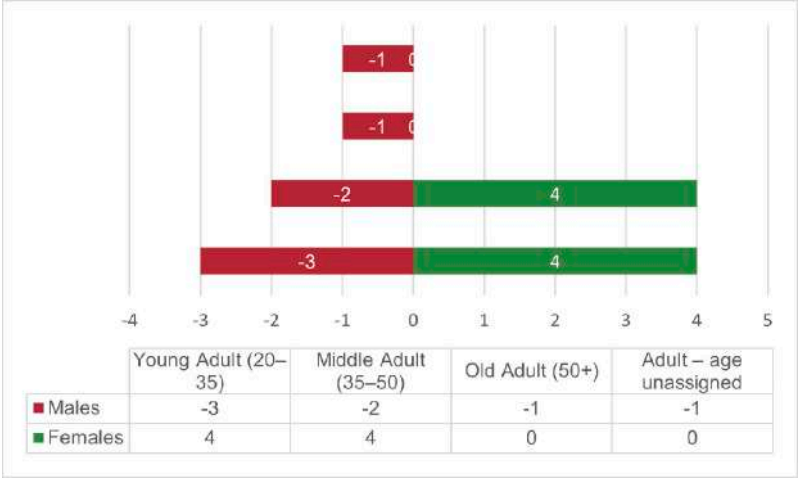


Fig. 8. Distribution of individuals by age groups in the ICL 2015–2017 research.
Fig. 8. Distribuția indivizilor pe grupe de vârstă în seria ICL 2015–2017.



	Young Adult (20–35)	Middle Adult (35–50)	Old Adult (50+)	Adult – age unassigned
Males	-3	-2	-1	-1
Females	4	4	0	0

Fig. 9. Age and sex distribution in the ICL 2015–2017 adult sample (negative numbers are male individuals; positive numbers are females individuals).
Fig. 9. Distribuția pe sexe și categorii de vârste în eșantionul de adulți ICL 2015–2017 (numerele negative reprezintă indivizi de sex masculin, iar cele pozitive, indivizi de sex feminin).

Non-metric traits contribute to the biological characterization of the group and may suggest intragroup genetic relatedness. Nine individuals display six non-metric traits within this sample: SK 122 has a persistent metopic suture, lambdoid ossicles and bilateral supraorbital notches (**Pl. XIV/1, 3**); SK 142 and SK 157 display double zygomaticofacial foramina (**Pl. XIV/2–3**); SK 105 (**Pl. XIV/5**) and SK 109 have shovel-shaped upper incisors and SK 201 and SK 233 (**Pl. XXI/1**) have bilateral supraorbital notches (**Table 4**).

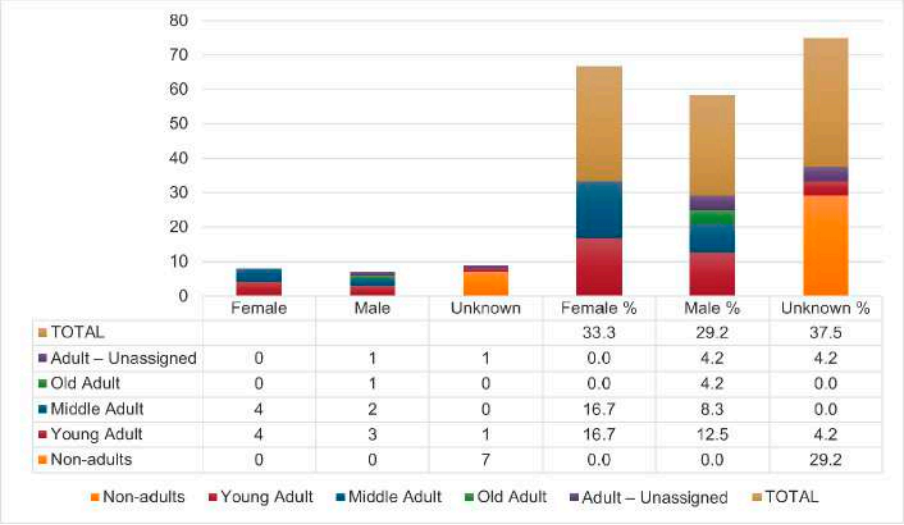
Burial no.	Biological Sex	Age (years old)	Age group
105	I	14.5–15.5	AD
107	F	25–29	YA
109	I	13.5	AD
116	M	23–25	YA
119	I	13.5–15.5	AD
122	M	50	OA
124	I		A
125	M	20	YA
132	F	35–55	MA
133	I	3.5–4	C
142	I	10	C
147	I	13	AD
152	M	45–50	MA
153	F	25–35	YA
157	F	35–50	MA
159	I	25–35	YA
180	M		A
181	I	6	C
190	F	20–35	YA
195		35–45	MA
197	F	40–44	MA
200	F	35–40	MA
201	M	25–35	YA
233	F	17–25	YA

Table 3. Summary data of the sample (burial number, sex determination, age intervals and age groups; C – child; AD – adolescent; YA – young adult; MA – middle adult; OA – old adult; A – indeterminate adult individual).
Tab. 3. Sinteza datelor eșantionului (numărul mormântului, determinarea sexului, intervalele și grupele de vârstă; C – copil; AD – adolescent; YA –adult tânăr; MA – adult de vârstă mijlocie; OA – adult bătrân; A – individ adult cu vârsta nedeterminată).

Palaeopathological evidence in our sample reveals a broad spectrum of conditions (**Table 4**). A probable case of craniosynostosis was identified in SK 107 (**Pl. XVIII/1**). Cribra orbitalia, potentially reflecting either haematopoietic stress

or vascular aetiology, was documented in six individuals (SK 105, SK 119, SK 122, SK 181, SK 201, and SK 233) (**Pl. XXI/1–2**), while cribra cranii was recorded in SK 133. A rarely recorded pathological encounter is present on the thoracic vertebrae of SK 157, a middle adult female individual, namely the ossification of ligamentum flavum (**Pl. XVIII/3; Table 4**).

Endocranial alterations were present in SK 122, SK 133, and SK 200, including vascular grooves and focal bone growths, the latter possibly attributable to hyperostosis frontalis interna (**Pl. XX/3-4; Table 4**).



	Female	Male	Unknown	Female %	Male %	Unknown %
TOTAL				33.3	29.2	37.5
Adult – Unassigned	0	1	1	0.0	4.2	4.2
Old Adult	0	1	0	0.0	4.2	0.0
Middle Adult	4	2	0	16.7	8.3	0.0
Young Adult	4	3	1	16.7	12.5	4.2
Non-adults	0	0	7	0.0	0.0	29.2

Fig. 10. The distribution of the 24 individuals from ICL 2015–2017 by age group and biological sex (The largest proportion is represented by young adults, followed by middle adults and non-adults; sex was undetermined for the entire non-adult group and for a small number of adults due to poor preservation).

Fig. 10. Distribuția celor 24 de indivizi din seria ICL 2015–2017 după grupe de vârstă și sexul biologic (Proporția maximă este reprezentată de tinerii adulți, urmați de adulții de vârstă mijlocie și de non-adulți; sexul a fost nedeterminat pentru întreg grupul de non-adulți și pentru un număr mic de adulți, din cauza conservării precare a resturilor scheletice).

Osteoarthritic changes were noted in SK 119, SK 152 (**Pl. XIX/2–3**), SK 153, and SK 197, predominantly involving vertebrae and lower limb joints. These degenerative features, including eburnation and osteophyte formation, affected mostly middle adults, but one adolescent (SK 119) also displayed incipient spinal degeneration, likely activity-related (**Pl. XIX/1**). Enthesopathic modification, including enthesophytes and muscular attachment remodelling, were evident in SK 152 and SK 157 (**Table 4**).

SK	Sex /age	Non-metric traits	Palaeopathological observations
105	14.5–15.5	Shovel-shaped upper incisors	CO
107	F25–29	•	Craniosynostosis; dental pathology
109	13.5	Shovel-shaped upper incisors	•
116	M23–25	•	Periostitis on lower limbs; calculus deposits
119	15.5–16	•	Osteophyte formation on C_2; DEH; CO
122	M50	Persistent metopic suture; lambdoid ossicles; bilateral supraorbital notches	Endocranial lesions; CO; DEH; dental pathologies
124	Adult	•	•
125	M20	•	•
132	F35–55	•	Dental pathology – impacted L-mandibular canine; caries; supragingival calculus, periodontitis, abscesses on maxillary dentition
133	3.5–4	•	Porotic hyperostosis; endocranial lesions; DEH
142	10	Double zygomaticofacial foramina	Chipping of lateral mandibular incisor
147	13	•	DEH.
152	M45–50	•	Dental pathology; healed fracture of the central ribs – L side; fracture of the 4th proximal phalanx of the L foot; OA – trapezoid-2nd metacarpal; L 5th metatarsal and bilateral distal phalanges of the 1st metatarsal; marginal vertebral osteophyte; enthesophytes – patellae
153	F24–45	•	Signs of possible respiratory infection-porous aspect of the caudal part of the ribs; lipping at the femoral head, porosities at the R coxo-femoral articulation
157	F35–50	Double zygomaticofacial foramina	Periostitis on L tibia; osteophyte formation – L iliac crest; dental pathology; enthesophytes on the iliac crest; ossification of the ligamentum flavum.
159	25–35	•	•
180	M Adult	•	•
181	6.5–7.5	•	CO
190	F20–35	•	Dental pathologies, impacted L mandibular canine
195	M35–45	•	•
197	F40–44	•	Faint osteophyte formation on thoracic vertebrae; Schmorl's node – thoracic
200	F25–40	•	Endocranial lesions; dental pathology
201	M25–35	Bilateral supraorbital notches	CO; dental pathology
233	F17–25	Bilateral supraorbital notches	CO; dental pathology

Table 4. Summary of anthropological data (burial context number, sex determination, age estimation and age groups, palaeopathology and non-metric variations; F – female; M – male; Not possible to determine; • Not observed; CO – cribra orbitalia; DEH – dental enamel hypoplasia; OA – osteoarthritis; R – Right; L – Left).

Tab. 4. Sinteza datelor antropologice (numărul mormântului, determinarea sexului, estimarea vârstei și grupele de vârstă, datele paleopatologice și variațiile non-metrice; F – femeie; M – bărbat; Nedeterminabil; • Neobservabil; CO – *cribra orbitalia*; DEH – hipoplazia smalțului dentar; OA – osteoartrită; R – drept; L – stâng).

Evidence of periostitis, with lamellar subperiosteal bone formation, was noted in SK 116, SK 153, and SK 157, indicative of chronic low-grade infection. SK 152 also showed signs of antemortem trauma, including rib and phalangeal fractures (**Pl. XIX/4; Table 4**).

Dental pathologies were extensive, with 11 individuals presenting combined lesions such as caries, periodontitis, calculus, abscesses, enamel hypoplasia, malocclusion, and impaction. Notably, SK 132 and SK 190 exhibited impacted canine (**Pl. XV–XVII**), and SK 107 presented an enamel pearl. Enamel hypoplasia was recorded in five individuals – SK 119, SK 122, SK 133, SK 147, and SK 201 and likely reflects systemic stress during the amelogenesis process (**Table 4**).

Conclusions

Although our dataset is limited in both size and preservation, with many individuals lacking complete anatomical elements and, in some cases, contextual information, taphonomic alterations (such as erosion, root activity) and post-depositional processes further restrict our ability to fully reconstruct the mortuary sequence. Similarly, sex estimation and age determination remain uncertain in several instances due to skeletal fragmentation.

Despite these challenges, the findings from the 2015–2017 excavations at Iclod offer valuable insights into Neolithic funerary practices in Transylvania. The data suggest a broadly consistent mortuary tradition, reflected in repeated patterns of body positioning, grave architecture, and associated material culture. Nevertheless, within this overall coherence, there is also evidence of ritual and social variability, expressed through differences in age and sex distributions as well as the diversity of grave goods, the latter category being discussed in a second part of this study.

Critically, the integration of this recent evidence with findings from earlier campaigns is essential for a clear understanding of the Iclod community. Only by correlating all archaeological, anthropological, and palaeopathological data from both old and new research phases can a more accurate and dynamic model of Neolithic life and death at Iclod be articulated.

It is therefore imperative that all burial data sets, past and recent, be systematically synthesised, allowing for the identification of long-term patterns, changes in funerary practice, and shifts in health and social structure across the entire occupational span of the necropolis.

Future research should pursue stratigraphic and spatial analyses to refine intra-cemetery organisation, explore potential kinship or household clustering, and apply biomolecular techniques aDNA, stable isotopes, to test hypotheses of mobility, diet, and relatedness in this prehistoric community.

Bibliography

Agarwal, Malhotra, Tewari 1979: S. K. Agarwal, V. K. Malhotra, S. P. Tewari, *Incidence of the metopic suture in adult Indian crania*, Acta Anatomica (Basel) 105, 4, 1979, p. 469–474.

Alqahtan *et alii* 2020: I. M. Alqahtan, R. A. Azizkhan, L. T. Alyawer, S. S. Alanazi, R. A. Alzahrani, L. S. Alhazmi, F. F. Bsher, L. M. Zahran, R. A. Aljahdali, R. R. Alqwizany, R. K. Tayeb, A. M. Kashghari, *An overview of diagnosis and management of malocclusion: literature review*, Annals of Dental Speciality 8, 4, 2020, p. 62–65.

AlQahtani, Hector, Liversidge 2010: S. J. AlQahtani, M. P. Hector, H. M. Liversidge, *Brief communication: The London atlas of human tooth development and eruption*, American Journal of Physical Anthropology 142, 3, 2010, p. 481–490.

Anthonappa, King 2015: R. P. Anthonappa, N. M. King, *Enamel defects in the permanent dentition: Prevalence and etiology*. In: B. K. Drummond, N. Kilpatrick (Eds.), *Planning and care for children and adolescents with dental enamel defects: Etiology, research and contemporary management*, Berlin, 2015, p. 15–30.

Aufderheide, Rodríguez-Martin 1998: A. C. Aufderheide, C. Rodríguez-Martin, *The Cambridge encyclopedia of human paleopathology*, Cambridge, Cambridge University Press, 1998.

Băcueț-Crișan, Constantinescu 2019: S. Băcueț-Crișan, M. Constantinescu, *Oameni și cioburi. Mormintele neo-eneolitice descoperite în Sălaj. Rezultatele analizelor antropologice*, Acta Musei Porolissensis 41, 2019, p. 9–16.

Bergman 1988: R. A. Bergman, *Compendium of human anatomical variation: Text, atlas and world literature*, Baltimore, 1988, p. 282–288.

Berry, Berry 1967: A. C. Berry, R. J. Berry, *Epigenetic variation in the human cranium*, Journal of Anatomy 101, 2, 1967, p. 361–379.

Bonfiglioli *et alii* 2004: B. Bonfiglioli, V. Mariotti, F. Facchini, M. G. Belcastro, S. Condemi, *Masticatory and non-masticatory dental modifications in the Epipalaeolithic necropolis of Taforalt (Morocco)*, International Journal of Osteoarchaeology 14, 2004, p. 448–456.

Bronk Ramsey 2009: C. Bronk Ramsey, *Bayesian analysis of radiocarbon dates*, Radiocarbon 51, 1, 2009, p. 337–360.

Buikstra, Ubelaker 1994: J. E. Buikstra, D. H. Ubelaker, *Standards for data collection from human skeletal remains*, Arkansas Archaeological Survey Research Series 44, Fayetteville, 1994.

Condurățeanu, Gligor 2022: M.-B. Condurățeanu, M. Gligor, *Modelarea peisajelor temporale probabilistice ale contextelor funerare eneolitice de la Alba Iulia–Lumea Nouă*. In: M. Gligor, A. Soficaru (Eds.), *Studierea și interpretarea practicilor funerare din trecut. O perspectivă bioarheologică*, Cluj-Napoca, 2022, p. 11–43.

Dhaniwala *et alii* 2022: N. S. Dhaniwala, M. N. Dhaniwala, P. Shah, K.K Khan, V. Jadawala, S. Jadhav, *Traumatic first rib fracture: An indication of life-threatening injuries*, Journal of Orthopaedic Case Reports 12, 4, 2022, p. 54–57.

Diaconescu, Lazarovici, Tincu 2013: D. Diaconescu, Gh. Lazarovici, S. Tincu, *Considerații privind poziția cronologică absolută a cimitirelor preistorice de la Iclod,* Acta Musei Porolissensis 35, 2013, p. 47–63.

Dodd-Oprițescu 1978: A. Dodd-Oprițescu, *Les éléments steppiques dans l'énéolithique de Transylvanie*, Dacia N.S. 22, 1978, p. 87–97.

Dumitru-Kogălniceanu 2009: R. Dumitru-Kogălniceanu, *Primele necropole din neoliticul și eneoliticul României*, Ph.D. thesis, *mss*. Universitatea „Alexandru Ioan Cuza", Iași, 2009.

Ferrando-Bernal 2023: M. Ferrando-Bernal, *Ancient DNA suggests anaemia and low bone mineral density as the cause for porotic hyperostosis in ancient individuals*, Scientific Reports 13, 2023, 6968.

Fetcu 2018: A. Fetcu, *Date osteoarheologice privind trei non-adulți din necropola neolitică de la Iclod, județul Cluj*, Buletinul Cercurilor Științifice Studențești 24, 2018, p. 25–39.

Fetcu 2021: A. Fetcu, *Dental disease in the Neolithic assemblage from Iclod necropolis* (*Cluj County, Romania)*, The International Conference on Archaeology, Cultural Heritage and History, Doctoral School of History „1 Decembrie 1918" University of Alba Iulia, 2021, *On-line*.

Gardner 2016: S. Gardner, *A persistent metopic suture: A case report*, Austin Journal of Anatomy 3, 1, 1049, 2016, p. 1–2.

Gault *et alii* 1992: D. T. Gault, D. Renier, D. Marchac, B. M. Jones, *Intracranial pressure and intracranial volume in children with craniosynostosis*, Plastic and Reconstructive Surgery 90, 3, 1992, p. 377–381.

Geber, Hammer 2018: J. Geber, N. Hammer, *Ossification of the ligamentum flavum in a nineteenth-century skeletal population sample from Ireland: Using bioarchaeology to reveal a neglected spine pathology*, Scientific Reports 8, 9313, 2018, p. 1–10.

Georgescu, Georgescu 1999: L. Georgescu, E. M. Georgescu, *Considerații antropologice și demografice privind populația din necropolele "A" și "B" de la Iclod*, Acta Moldaviae Meridionalis 21, 1999, p. 357–363.

Gligor *et alii* 2018: M. Gligor, A. Fetcu, D. Bogdan, A. Bințințan, A. Bobînă, A. Brozou, *Cercetări preventive la Iclod, jud. Cluj (2015–2017). Studiu preliminar privind mormintele de inhumație aparținând neoliticului târziu*, Sesiunea națională de comunicări științifice a Institutului de Arheologie „Vasile Pârvan" „Metodă, teorie și practică în arheologia contemporană", Bucharest, 28–30 March 2018, p. 2.

Gligor, Fetcu, Bogdan 2018: M. Gligor, A. Fetcu, D. Bogdan, *New excavations in old sites. Late Neolithic necropolis from Iclod, Cluj County (Romania)*, The 24th Annual Meeting European Association of Archaeologists (EAA), Barcelona, 5–8 September 2018, Abstract Book, vol. I, p. 224.

Gligor, Băcueț-Crișan 2014: M. Gligor, S. Băcueț-Crișan, *Inhumation versus cremation in Transylvanian Neolithic and Eneolithic*, Studia Antiqua et Archaeologica 20, 2014, p. 37–67.

Hatch, Hacking 2003: R. L. Hatch, S. Hacking, *Evaluation and management of toe fractures*, American Family Physician 68, 12, 2003, p. 2413–2418.

Hershkovitz *et alii* 1999: I. Hershkovitz, C. Greenwald, B. M. Rothschild, B. Latimer, O. Dutour, L. M. Jellema, S. Wish-Baratz, *Hyperostosis frontalis Interna: An anthropological perspective*, American Journal of Physical Anthropology 109, 3, 1999, p. 303–325.

Hervella *et alii* 2015: M. Hervella, M. Rotea, N. Izagirre, M. Constantinescu, S. Alonso, M. Ioana, C. Lazăr, F. Ridiche, A. D. Soficaru, M. G. Netea, *Ancient DNA from South-East Europe reveals different events during Early and Middle Neolithic influencing the European genetic heritage*, PLOS ONE 10, 6, 2015, e0128810.

Hillson 2005: S. Hillson, *Teeth*, Cambridge, 2005.

Huang, Creath 1995: W.-J. Huang, C. J. Creath, *The midline diastema: a review of its etiology and treatment,* Pediatric Dentistry 17, 3, 1995, p. 171–179.

Johnson, Wilkie 2011: D. Johnson, A. O. M. Wilkie, *Craniosynostosis*, European Journal of Human Genetics 19, 4, 2011, p. 369–376.

Kimura *et alii* 2009: R. Kimura, T. Yamaguchi, M. Takeda, O. Kondo, T. Toma, K. Haneji, T. Hanihara, H. Matsukusa, S. Kawamura, K. Maki, M. Osawa, H. Ishida, H. Oota, *A common variation in EDAR is a genetic determinant of shovel-shaped incisors*, American Journal of Human Genetics 85, 4, 2009, p. 528–535.

Klaassen *et alii* 2011: Z. Klaassen, R. S. Tubbs, N. Apaydin, R. Hage, R. Jordan, M. Loukas, *Vertebral spinal osteophytes*, Anatomical Science International 86, 1, 2011, p. 1–9.

Kumar *et alii* 2016: A. A. Kumar, B. Rajesh, K. Arumugam, V. Tamilalagan, *Sutural bones associated with lambdoid suture of human skull: presence, variations and clinical importance*, International Journal of Anatomy and Research 4, 2, 2016, p. 2331–2336.

Lazarovici 1977: Gh. Lazarovici, *Sfârșitul culturii Vinča-Turdaș în Câmpia Transilvaniei*, Studii și Comunicări Caransebeș 2, 1977, p. 211–230.

Lazarovici 1983: Gh. Lazarovici, *Șantierul arheologic Iclod (1977–1981)*, Materiale și Cercetări Arheologice 15, 1983, p. 50–61.

Lazarovici 1991: Gh. Lazarovici, *Grupul și stațiunea Iclod*, Cluj-Napoca, 1991.

Lazarovici 1995: Gh. Lazarovici, *Gura Baciului, Monografie arheologică*, Cluj-Napoca, 1995.

Lazarovici *et alii* 1994: Gh. Lazarovici, Z. Maxim, R. Pintea, M. Meșter, *Șantierul arheologic Iclod (jud. Cluj). Campania din 1993*, Acta Musei Napocensis 31, 1, 1994, p. 325–339.

Lazarovici *et alii* 1995: Gh. Lazarovici, Z. Maxim, C. Lazo, M. Meșter, *Șantierul arheologic Iclod. Campania 1994*, Acta Musei Napocensis 32, 1, 1995, p. 507–536.

Lazarovici, Maxim, Meșter 1996: Gh. Lazarovici, Z. Maxim, M. Meșter, *Iclod, jud. Cluj*, Cronica Cercetărilor Arheologice din România. Campania 1995, Brăila, p. 61–62.

Lazarovici *et alii* 1996: Gh. Lazarovici, Z. Maxim, M. Meșter, A. Bulbuc, S. Radu, *Șantierul arheologic Iclod. Campania din 1995*, Acta Musei Napocensis 33, 1, 1996, p. 267–307.

Lazarovici *et alii* 1997a: Gh. Lazarovici, Z. Maxim, M. Meșter, D. Bindea, S. Radu, M. Bodea, *Iclod, jud. Cluj*, Cronica Cercetărilor Arheologice din România. Campania 1996, Bucharest, 1997, p. 28–29.

Lazarovici *et alii* 1997b: Gh. Lazarovici, Z. Maxim, M. Meșter, D. Bindea, T. Piciu, S. Radu, M. Bodea, *Șantierul arheologic Iclod. Campania din 1996*, Acta Musei Napocensis 34, 1, 1997, p. 637–667.

Lazarovici, Bulbuc 1983: Gh. Lazarovici, A. Bulbuc, *Descoperiri arheologice în hotarul comunei Iclod*, Apulum 21, 1983, p. 161–166.

Lazarovici, Kalmar 1986: Gh. Lazarovici, Z. Kalmar, *Șantierul arheologic Iclod (1983–1984)*, Apulum 23, 1986, p. 25–41.

Lazarovici, Kalmar 1987: Gh. Lazarovici, Z. Kalmar, *Șantierul arheologic Iclod, Campania 1985*, Apulum 24, 1987, p. 9–39.

Lazarovici, Kalmar 1988: Gh. Lazarovici, Z. Kalmar, *Săpăturile arheologice de la Iclod. Campania din 1986*, Apulum 25, 1988, p. 9–47.

Lazarovici, Kalmar 1989: Gh. Lazarovici, Z. Kalmar, *Șantierul arheologic Iclod (Campania 1987)*, Apulum 26, 1989, p. 55–68.

Lazarovici, Kalmar-Maxim 1990–1993: Gh. Lazarovici, Z. Kalmar-Maxim, *Săpăturile arheologice de la Iclod (Campania 1988)*, Apulum 27–30, 1990–1993, p. 23–57.

Lazarovici, Maxim 1989–1993: Gh. Lazarovici, Z. Maxim, *Șantierul arheologic Iclod (Campania 1989)*, Acta Musei Napocensis 26–30, I/2, 1989–1993, p. 337–362.

Lazarovici, Kalmar-Maxim 1987–1988: Gh. Lazarovici, Z. Kalmar-Maxim, *Necropolele tumulare din Munții Perindului și Dealul Feleacului*, Acta Musei Napocensis 24–25, 1987–1988, p. 997–1009.

Lazarovici, Lazarovici 2006: C. M. Lazarovici, Gh. Lazarovici, *Arhitectura neoliticului și epocii cuprului din România*, I, Neoliticul, Iași, Editura Trinitas, Bibliotheca Archaeologica Moldaviae IV, 2006.

Lazăr, Băcueț-Crișan 2011: C. Lazăr, S. Băcueț-Crișan, *Mormintele de incinerație din perioada neolitică și eneolitică de pe teritoriul României. O analiză etnoarheologică*, Apulum 48, 2011, p. 1–68.

Lewis 2017: M. E. Lewis, *Paleopathology of children. Identification of pathological conditions in the human skeletal remains of non-adults*, Amsterdam, 2017.

Lichter 2001: C. Lichter, *Untersuchungen zu den Bauten des südosteuropäischen Neolithikums und Chalkolithikums*, Mainz am Rhein: Philipp von Zabern, 2001, p. 223–231.

Luca 2000: S. A. Luca, *Necropola turdășană de la Orăștie–Dealul Pemilor, Punct X2*, Banatica 15, 1, 2000, p. 59–66.

Mariotti, Facchini, Belcastro 2007: V. Mariotti, F. Facchini, M. G. Belcastro, *The study of entheses: proposal of a standardised scoring method for twenty-three entheses of the postcranial skeleton*, Collegium Antropologicum 31, 1, 2007, p. 291–313.

Marta *et alii* 2017: L. Marta, R. Gindele, C. Virag, C. Astaloș, *Moftinu Mare (com. Moftin, jud. Satu Mare), punct Moftinu Mare–Hamiliz*, Cronica Cercetărilor Arheologice din România. Campania 2016, Bucharest, 2017, p. 190–191.

Maxim 1999: Z. Maxim, *Neo-Eneoliticul din Transilvania Date arheologice și matematico-statistice*, Bibliotheca Musei Napocensis XIX, Cluj-Napoca, 1999.

Maxim *et alii* 2002: Z. Maxim, G. Chiș, T. Oproiu, I. Szücs-Csillik, *The astronomical aspects of the orientation of the graves in the burial site of Iclod*. In: K. Barlai, I. Bognár-Kutzián (Eds.), *Unwritten Messages from the Carpathian Basin*, Konkoly Observatory Monographs 4, Budapest, Konkoly Observatory of the Hungarian Academy of Sciences, 2002, p. 19–30.

Maxim *et alii* 2003: Z. Maxim, Gh. Lazarovici, M. Meșter, D. Bindea, L. Săsăran, *Iclod, com. Iclod, jud. Cluj, Punct: Pământul Vlădicii*, Cronica Cercetărilor Arheologice din România. Campania 2002, Bucharest, 2003, p. 146–147.

Maxim, Bindea, Lazarovici 2006: Z. Maxim, D. Bindea, Gh. Lazarovici, *Șantierul arheologic Iclod. Campania din anul 2005*, Acta Musei Napocensis 43, 1, 2006, p. 177–178.

Mensforth *et alii* 1978: R. P. Mensforth, C. O. Lovejoy, J. W. Lallo, G. J. Armellagos, *The role of constitutional factors, diet, and infectious disease in etiology of porotic hyperostosis and periosteal reactions in prehistoric infants and children*, Medical Anthropology 2, 1, 1978, p. 1–36.

Mischka 2012: C. Mischka, *Late Neolithic multiphased settlements in Central and southern Transylvania: a geophysical survey and test excavation*. In: R. Hofmann, F.-K. Moetz, J. Müller (Eds.), *Tells: Social and Environmental Space, Proceedings of the International Workshop Socio-Environmental Dynamics over the Last 12,000 Years: The Creation of Landscapes II*, Kiel, Bonn, 2012, p. 153–166.

Miu 2004: G. Miu, *Analiza individuală a materialului osteologic de la Iclod-Cluj*, Zilele Academice Ieșene, 23–30 September 2004, Sesiunea Secției de Cercetări Antropologice Iași, Academia Română – Filiala Iași.

Molnar 1971: S. Molnar, *Human tooth wear, tooth function and cultural variability*, American Journal of Physical Anthropology 34, 2, 1971, p. 175–189.

Molnar 2011: P. Molnar, *Extramasticatory dental wear reflecting habitual behavior and health in past populations*, Clinical Oral Investigations 15, 2011, p. 681–689.

Molnar *et alii* 1972: S. Molnar, M. J. Barrett, L. Brian, C. Loring Brace, D. S. Brose, J. R. Dewey, J. E. Frisch, P. Ganguly, N.-G. Gejvall, D. L. Greene, K. A. R. Kennedy, F. E. Poirier, M. J. Pourchet, S. Rhine, C. G. Turner II, L. Van Valen, G. H. R. Von Koenigswald, R. G. Wilkinson, M. H. Wolpoff, G. A. Wright, *Tooth wear and culture: A survey of tooth functions among some prehistoric populations*, Current Anthropology 13, 5, 1972, p. 511–526.

Németi 1988: I. Németi, *Noi descoperiri arheologice din eneoliticul târziu din nord-vestul României*, Acta Musei Porolissensis 12, 1988, p. 121–145.

Netter 2019: F. H. Netter, *Atlas of Human Anatomy*, Seventh Edition, Philadelphia, 2019.

Nteli Chatzioglou *et alii* 2024: G. Nteli Chatzioglou, L. Sağlam, B. N. Çandır, M. Yiğit, Ö. Gayretli, *Anatomical variations of the zygomaticofacial foramen and its related canal through the zygomatico-orbital and zygomaticotemporal foramina in dry human skulls*, Surgical and Radiologic Anatomy 46, 1, 2024, p. 33–40.

Ogden 2007: A. Ogden, *Advances in the palaeopathology of teeth and jaws*. In: R. Pinhasi, S. Mays (Eds.), *Advances in Human Palaeopathology*, Chichester, 2007, p. 283–308.

Ortner 2003: D. J. Ortner, *Identification of pathological conditions in human skeletal remain*s, Amsterdam, 2003.

Papilian 2014: V. Papilian, *Anatomia omului. Vol. I: Aparatul locomotor* 1, Bucharest, 2014.

Pupeză 2022: P. Pupeză, *Raportul de cercetare de la Iclod, jud. Cluj Punct: AFI-TRUCKS*, Cronica Cercetărilor Arheologice din România, Campania 2021, Bucharest, 2022, p. 542–546.

Rakhshan 2015: V. Rakhshan, *Congenitally missing teeth (hypodontia): A review of the literature concerning the etiology, prevalence, risk factors, patterns and treatment*, Dental Research Journal 12, 1, 2015, p. 1–13.

Rathva 2012: V. E. Rathva, *Ectopic enamel pearl*, Clinica Practica 2, 2012, 2: e46.

Reimer *et alii* 2020: P. J. Reimer, W. E. N. Austin, E. Bard, A. Bayliss, A. G. Blackwell, C. Bronk Ramsey, M. Butzin, H. Cheng, R. Lawrence Edwards, M. Friedrich, P. M. Grootes, T. P. Guilderson, I. Hajdas, T. J. Heaton, A. G. Hogg, K. A. Hughen, B. Kromer, S. W. Manning, R. Muscheler, J. G. Palmer, Ch. Pearson, J. van der Plicht, R. W. Reimer, D. A. Richards, E. M. Scott, J. R. Southon, C. S. M. Turney, L. Wacker, F. Adolphi, U. Büntgen, M. Capano, S. M. Fahrni, A. Fogtmann-Schulz, R. Friedrich, P. Köhler, S. Kudsk, F. Miyake, J. Olsen, F. Reinig, M. Sakamoto, A. Sookdeo, S. Talamo, *The IntCal20 northern hemisphere radiocarbon age calibration curve (0–55 cal kBP)*, Radiocarbon 62, 4, 2020, p. 725–757.

Rivera, Mirazon Lahr 2017: F. Rivera, M. Mirazon Lahr, *New evidence suggesting a dissociated etiology for cribra orbitalia and porotic hyperostosis*, American Journal of Physical Anthropology 164, 1, 2017, p. 1–21.

Roberts, Manchester 2010: C. Roberts, K. Manchester, *The Archaeology of Disease*, Stroud, 2010.

Roska 1942: M. Roska, *Erdély régészeti repertóriuma*, I, Őskor [Archaeological Repertoire of Transylvania I, Ancient], Thesaurus antiquitatum Transsilvanicarum I, Praehistorica, Cluj-Napoca, 1942.

Rotea *et alii* 2014: M. Rotea, M. G. Netea, C. De-la-Rua, T. Tecar, M. Hervella, S. Alonso, Z. Maxim, M. Răchită, *The archaeological contexts of DNA samples collected from prehistoric sites in Transylvania*, Acta Musei Napocensis 51, 2014, p. 21–60.

Rothschild *et alii* 2020: B. Rothschild, M. J. Zdilla, L. M. Jellema, H. W. Lambert, *Cribra orbitalia is a vascular phenomenon unrelated to marrow hyperplasia or anemia: Paradigm shift for cribra orbitalia*, Anatomical Record 304, 8, 2020, p. 1709–1716.

Ruiyi, Ruijie 2025: J. Ruiyi, H. Ruijie, *Retained deciduous teeth: the epidemiology, etiology and treatment plan*s, Journal of Clinical Pediatric Dentistry 49, 2, 2025, p. 51–58.

Rajic, Muretic, Percac 1996: S. Rajic, Z. Muretic, S. Percac, *Impacted canine in a prehistoric skull*, Angle Orthodontist 66, 6, 1996, p. 477–480.

Sava, Mărginean, Ursuțiu 2017: V. Sava, F. Mărginean, A. Ursuțiu, *The Eneolithic Cemetery in Pecica "Est" (Arad County)*, Ziridava 31, 2017, p. 55–69.

Sava *et alii* 2023: V. Sava, I. C. Cireap, F. Gogâltan, D. Diaconescu, A. Hegyi, D. Preda, C. Floca, A. C. Ardelean, A. Sărăsan, *ArheoPecica project. Preliminary results of the 2022 campaign*, Ziridava 37, 2023, p. 245–283.

Schaefer, Black, Scheuer 2009: M. Schaefer, S. Black, L. Scheuer, *Juvenile osteology. A laboratory and field manual*, Amsterdam, 2009.

Simalcsik 2023a: A. Simalcsik, *Morminte de vânători în cimitirul neolitic de la Iclod*, Arheologia Moldovei 46, 2023, p. 255–276.

Simalcsik 2023b: A. Simalcsik, *Colecția osteologică de la Iclod. Primele date antropologice și necesitatea unei reevaluări*, Studii de Preistorie 20, 2023, p. 181–200.

Sommer, Virag 2024: U. Sommer, C. Virag, *The Eneolithic necropolis at Urziceni–Vamă, Romania*: *excavations in 2023*, Archaeology International 27, 1, 2024, p. 188–199.

Stuart-Macadam 1989: P. Stuart-Macadam, *Porotic hyperostosis: relationship between orbital and vault lesions*, American Journal of Physical Anthropology 80, 1989, p. 187–193.

Szűcs-Csillik, Virag 2016: I. Szűcs-Csillik, C. Virag, *The orientation of the dead at Urziceni necropolis. An archaeoastronomical approach*, ArheoVest 4, 2016, p. 1–9.

Toumi *et alii* 2006: H. Toumi, I. Higashiyama, D. Suzuki, T. Kumai, G. Bydder, D. McGonagle, P. Emery, J. Fairclough, M. Benjamin, *Regional variations in human patellar trabecular architecture and the structure of the proximal patellar tendon enthesis*, Journal of Anatomy 208, 1, 2006, p. 47–57.

Vincze 1993: Z. Vincze, *Analiza antropologică a scheletului din M 42 de la Iclod*, Apulum 27–30, 1993, p. 59–63.

Virag 2004: C. Virag, *Cercetări arheologice la Urziceni*–Vamă, Acta Musei Porolissensis 26, 2004, p. 41–76.

Virag *et alii* 2018: C. Virag, C. T. Astaloș, G. Orsolya, D. M. Tentiș, L. Brânduşan, *Urziceni, com. Urziceni, jud. Satu Mare, Urziceni–Vade Ret, punct: Vamă*, Cronica Cercetărilor Arheologice din România. Campania 2017, Bucharest, 2018, p. 147–148.

Virag, Astaloș 2017: C. Virag, C. Astaloș, *Urziceni, com. Urziceni, jud. Satu Mare, punct Urziceni–Vade Ret (Vamă)*, Cronica Cercetărilor Arheologice din România. Campania 2016, Bucharest, 2017, p. 150–151.

Virag, Astaloș, Orsolya 2019: C. Virag, C. Astaloș, G. Orsolya, *Urziceni, com. Urziceni, jud. Satu Mare [Vade Ret], punct Vade Ret*, Cronica Cercetărilor Arheologice din România. Campania 2018, Bucharest, 2019, p. 239–241.

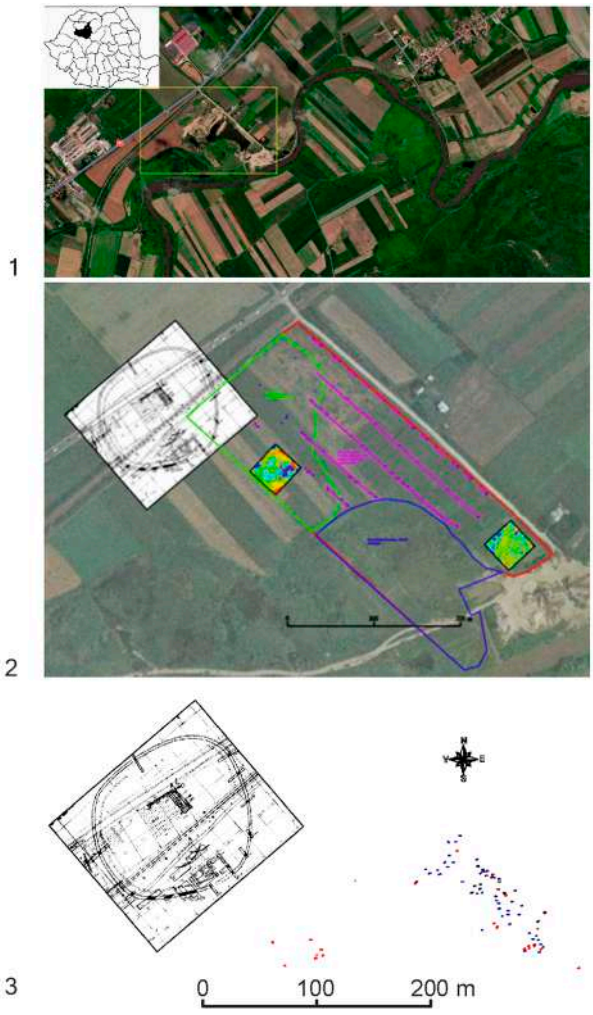
Virag, Astaloș, Orsolya 2020: C. Virag, C. Astaloș, G. Orsolya, *Urziceni, oraș Urziceni, jud. Satu Mare, punct Vade Ret (Vamă)*, Cronica Cercetărilor Arheologice din România. Campania 2019, Bucharest, 2020, p. 418–424.

Waldron 2009: T. Waldron, *Palaeopathology*, Cambridge, 2009.

Walker *et alii* 2009: P. L. Walker, R. Bathurst, R. Richman, V. A. Andrushko, *The causes of porotic hyperostosis and cribra orbitalia: a reappraisal of the iron-deficiency anemia hypothesis*, American Journal of Physical Anthropology 139, 2, 2009, p. 109–125.

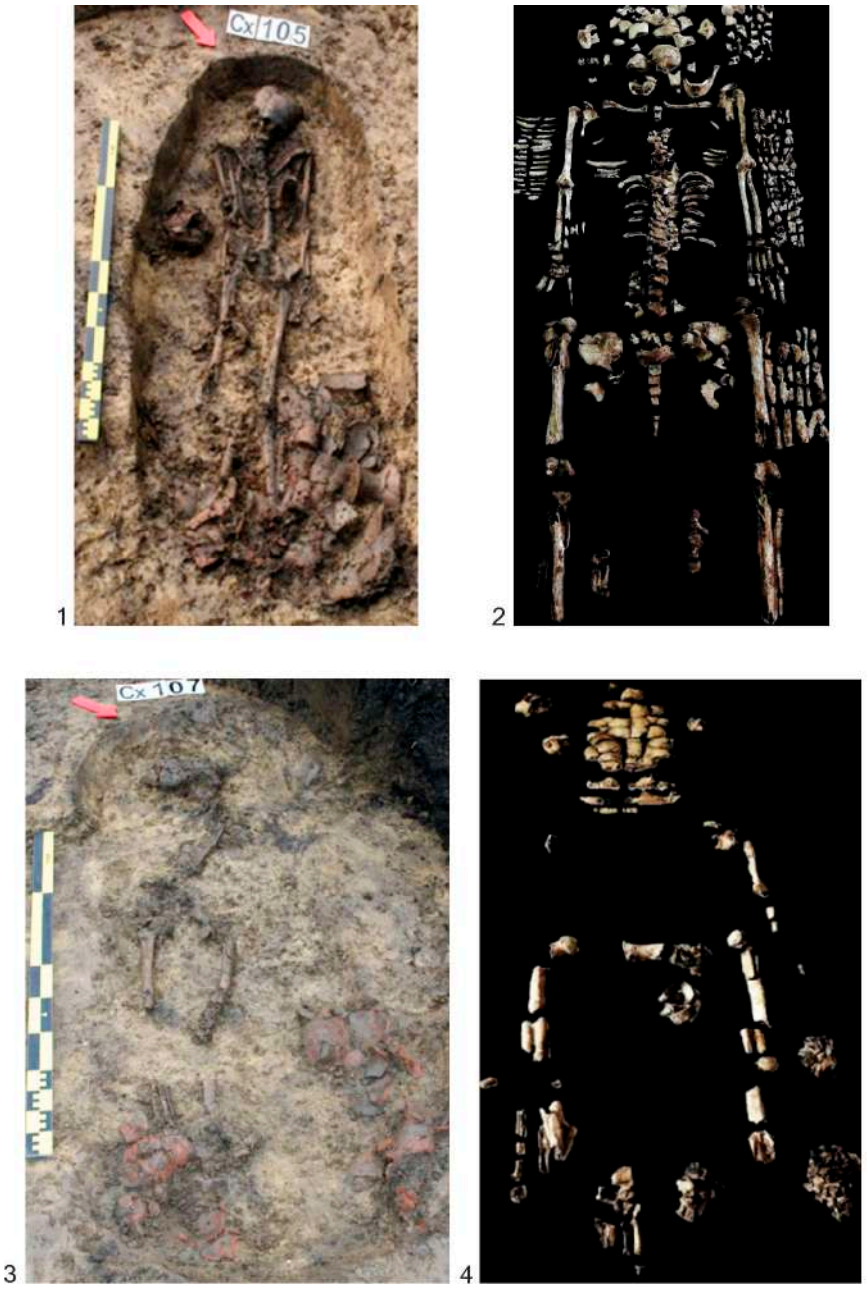
Walsh 2022: S. Walsh, *Early evidence of extra-masticatory dental wear in a Neolithic community at Bestansur, Iraqi Kurdistan*, International Journal of Osteoarchaeology 32, 6, 2022, p. 1264–1274.

White, Folkens 2005: T. D. White, P. A. Folkens, *The Human Bone Manual*, Amsterdam, 2005, p. 488.

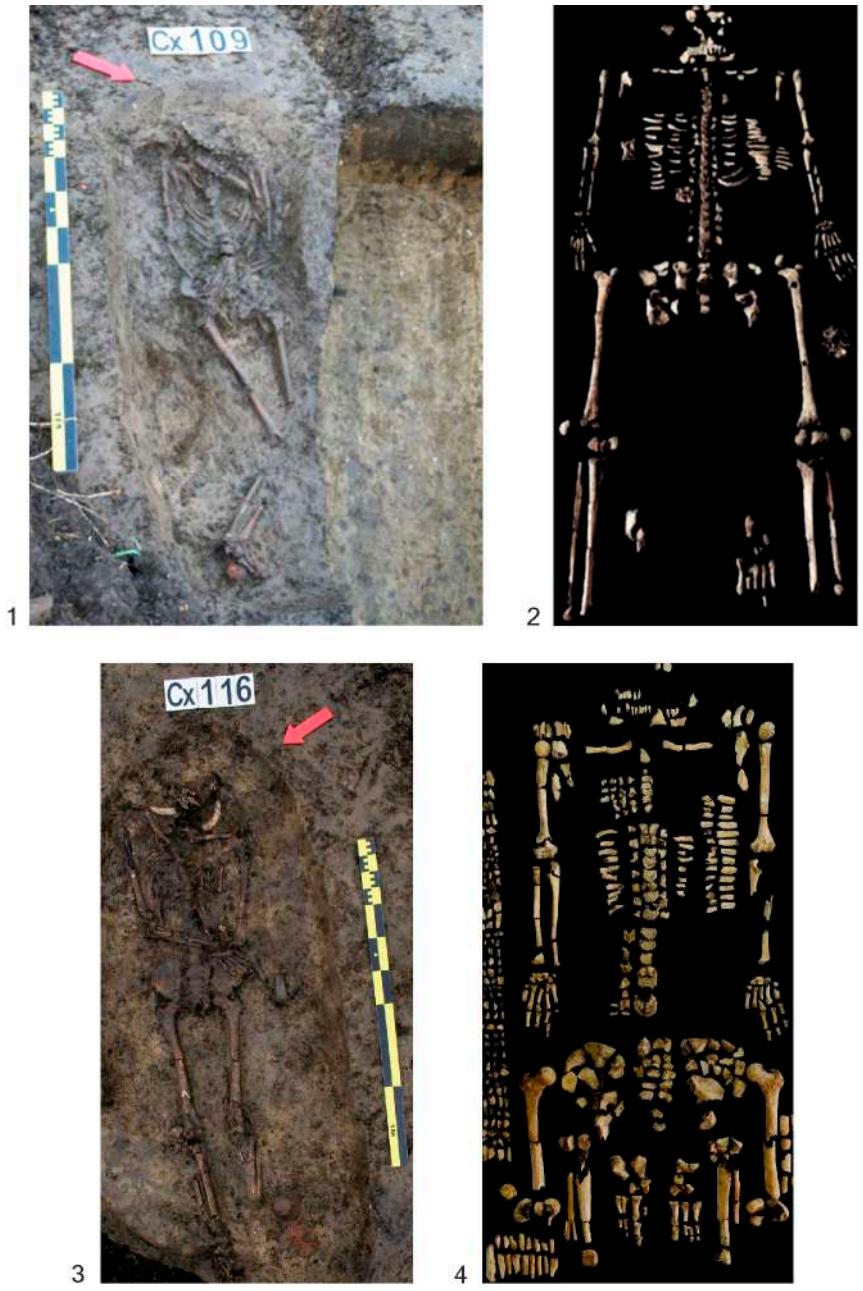


Pl. I. 1. Geographical location of Iclod–*Pământul Vlădicii* and the site location (image created with Satellite view pro, https://satellites.pro/Romania_map#46.967866,23.819733,14, accessed 18.05.2025); 2. Plan describing the settlement with the fortification layout and the researched area ICL 2015–2017; 3. Plan describing the settlement with the fortification layout and the researched area ICL 2015–2017, in red are displayed the Neolithic graves.

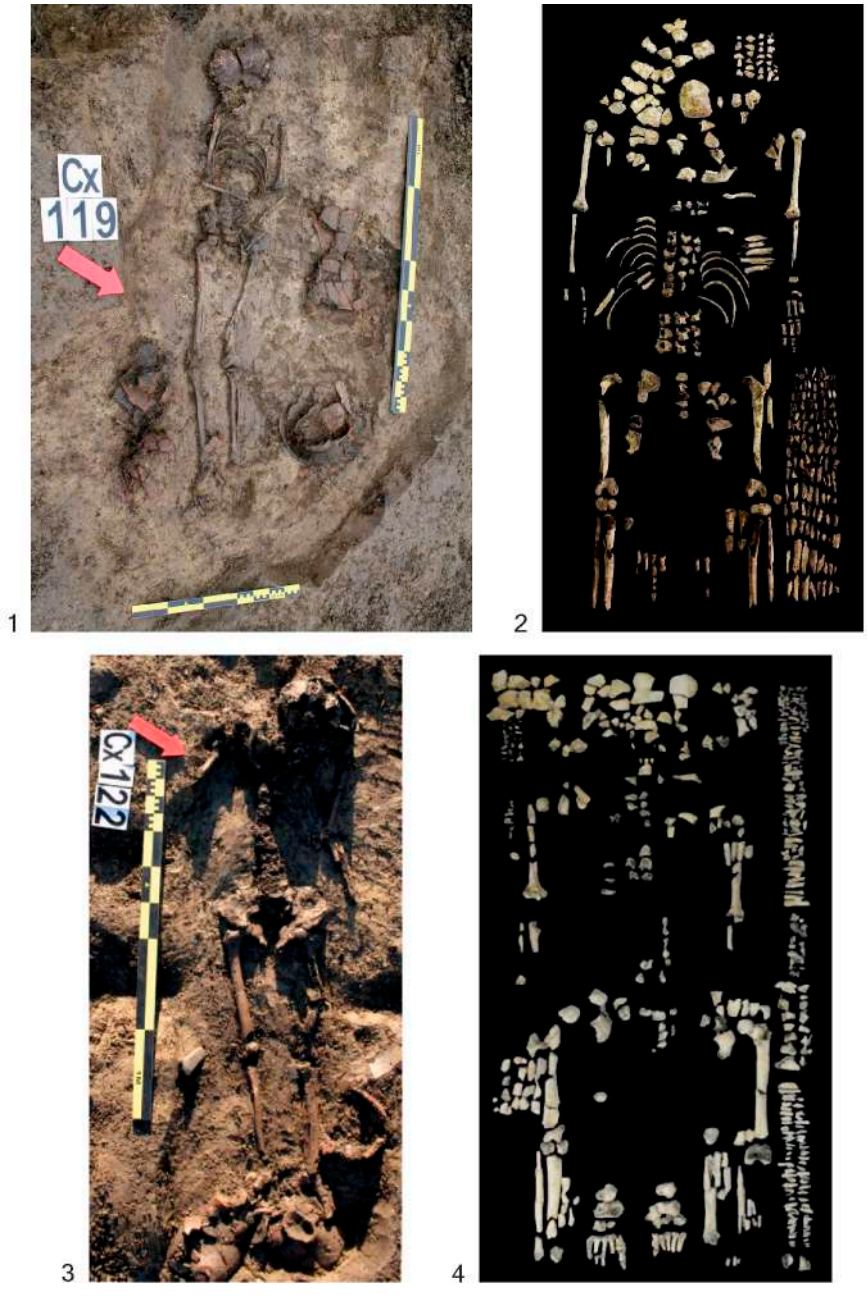
Pl. I. 1. Localizarea geografică a sitului Iclod–*Pământul Vlădicii* (imagine creată cu Satellite view pro, https://satellites.pro/Romania_map#46.967866,23.819733,14, accesată la 18.05.2025); 2. Planul așezării, cu structura fortificației și zona cercetată ICL 2015–2017; 3. Planul așezării, cu structura fortificației și zona cercetată ICL 2015–2017, cu roșu sunt evidențiate mormintele din perioada neolitică.



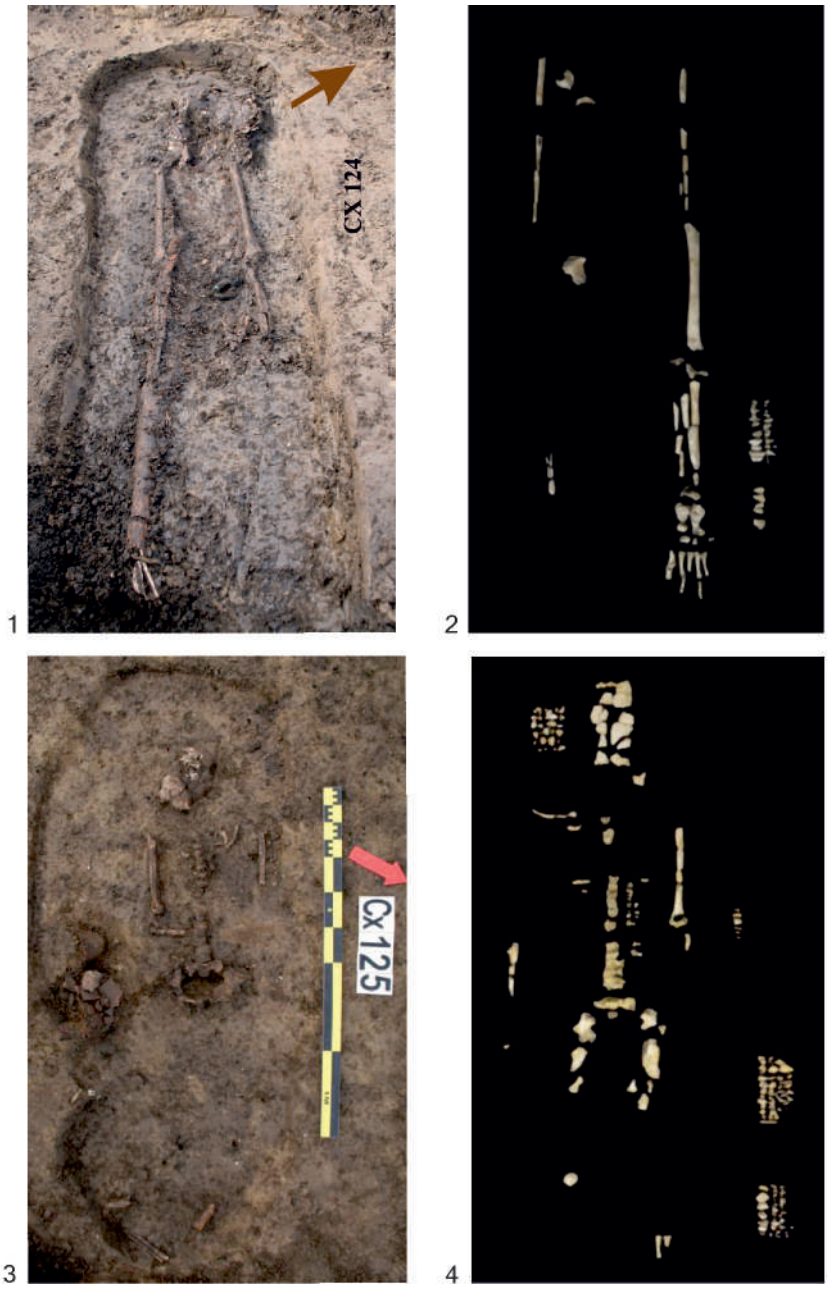
Pl. II. 1–2. SK 105, archaeological context and anatomical layout; 3–4. SK 107, archaeological context and anatomical layout.
Pl. II. 1–2. SK 105, contextul arheologic și reconstituirea anatomică; 3–4. SK 107, contextul arheologic și reconstituirea anatomică.



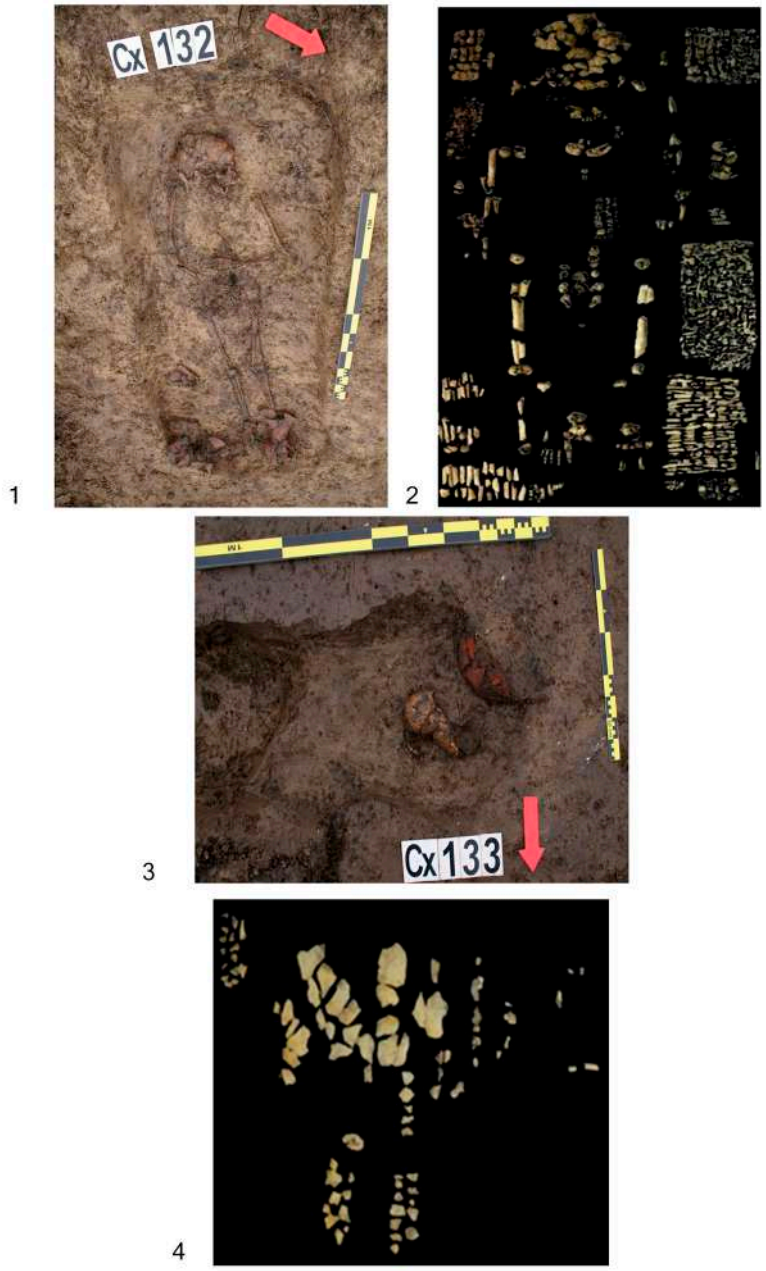
Pl. III. 1–2. SK 109, archaeological context and anatomical layout; 3–4. SK 116, archaeological context and anatomical layout.
Pl. III. 1–2. SK 109, contextul arheologic și reconstituirea anatomică; 3–4. SK 116, contextul arheologic și reconstituirea anatomică.



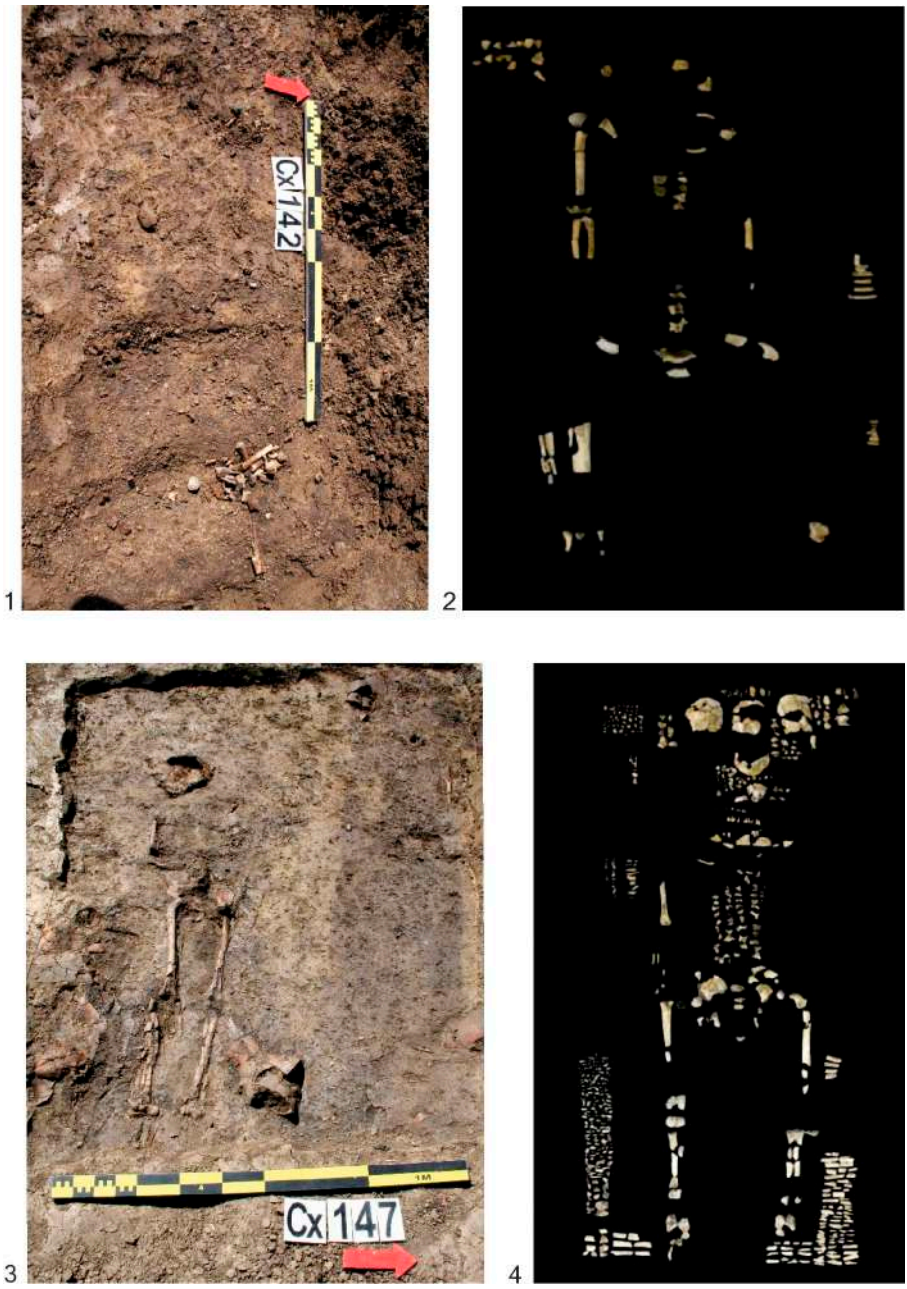
Pl. IV. 1–2. SK 119, archaeological context and anatomical layout; 3–4. SK 122, archaeological context and anatomical layout.
Pl. IV. 1–2. SK 119, contextul arheologic și reconstituirea anatomică; 3–4. SK 122, contextul arheologic și reconstituirea anatomică.



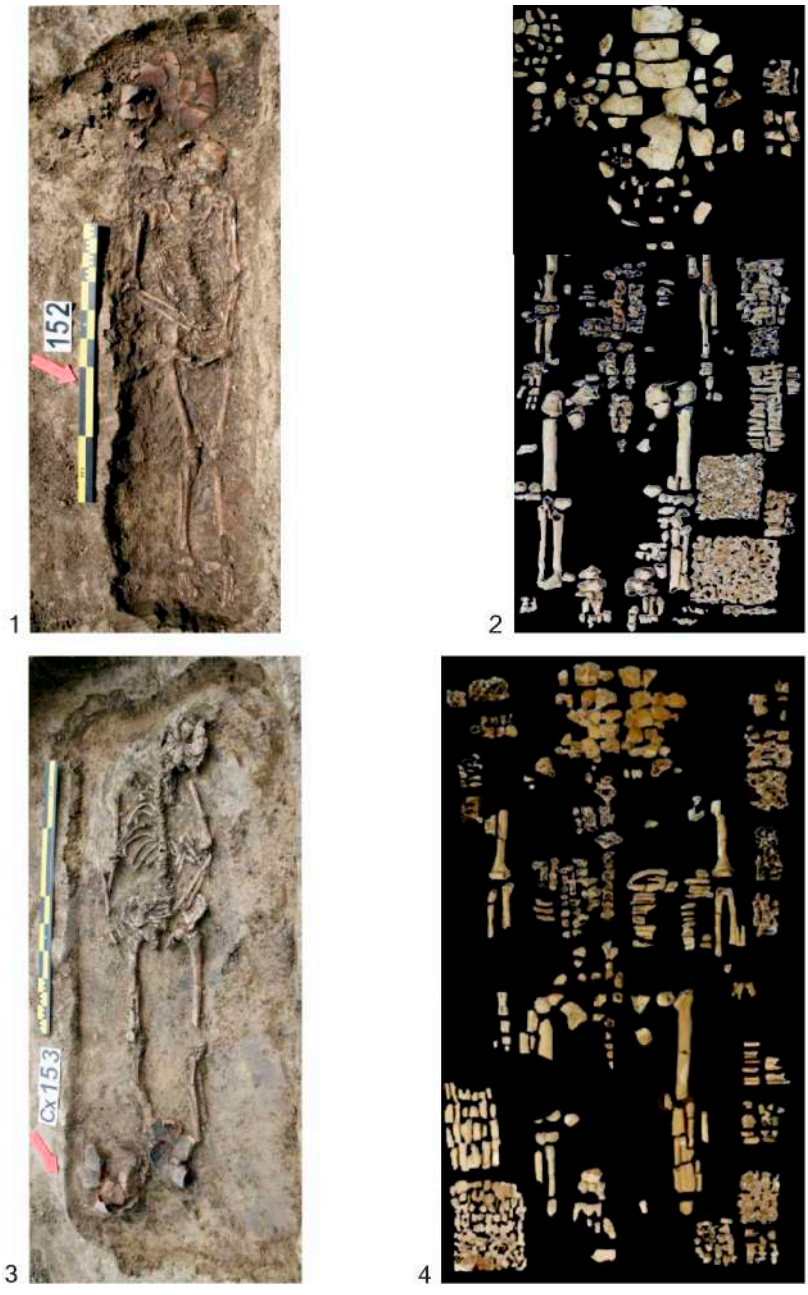
Pl. V. 1–2. SK 124, archaeological context and anatomical layout; 3–4. SK 125, archaeological context and anatomical layout.
Pl. V. 1–2. SK 124, contextul arheologic și reconstituirea anatomică; 3–4. SK 125, contextul arheologic și reconstituirea anatomică.



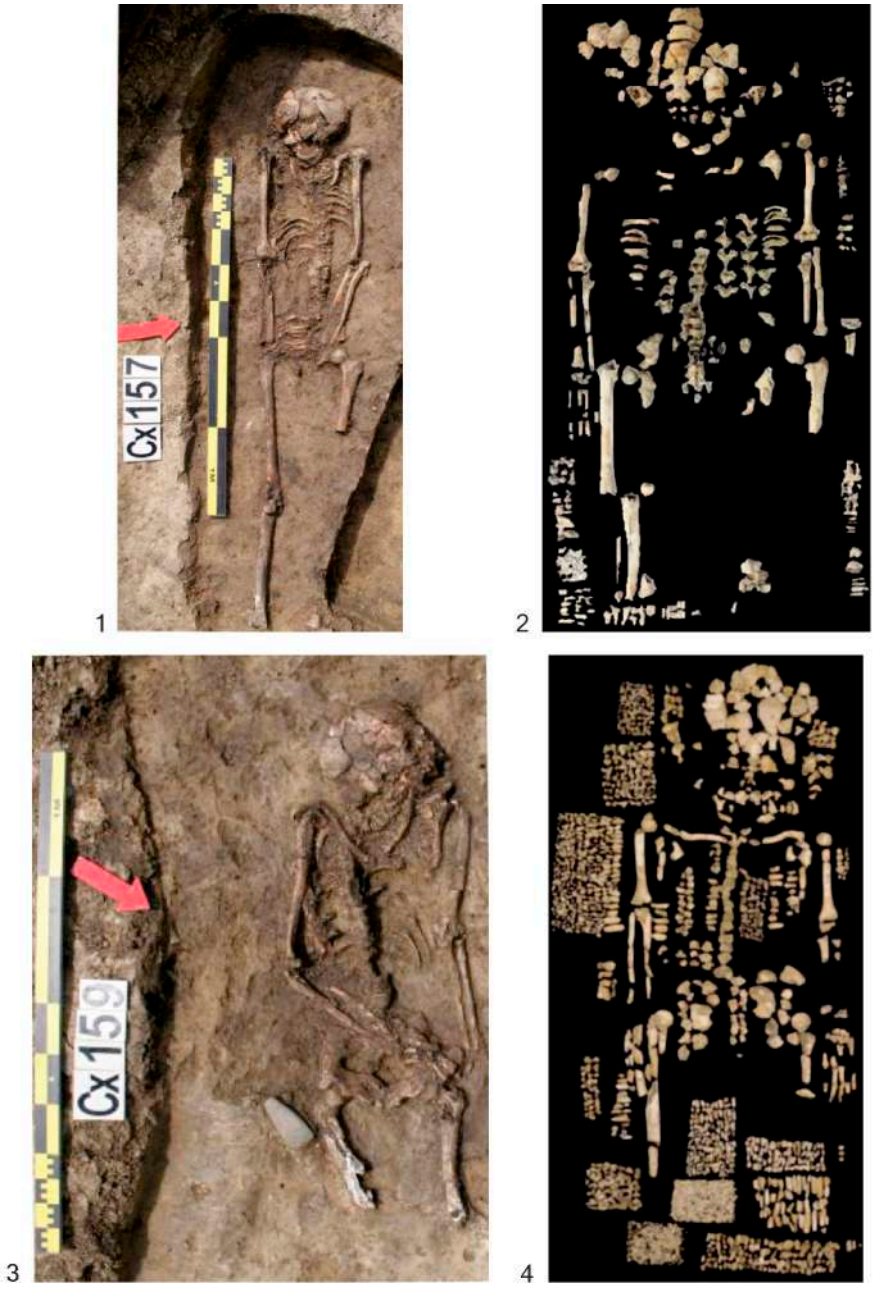
Pl. VI. 1–2. SK 132, archaeological context and anatomical layout; 3–4. SK 133, archaeological context and anatomical layout.
Pl. VI. 1–2. SK 132, contextul arheologic și reconstituirea anatomică; 3–4. SK 133, contextul arheologic și reconstituirea anatomică.



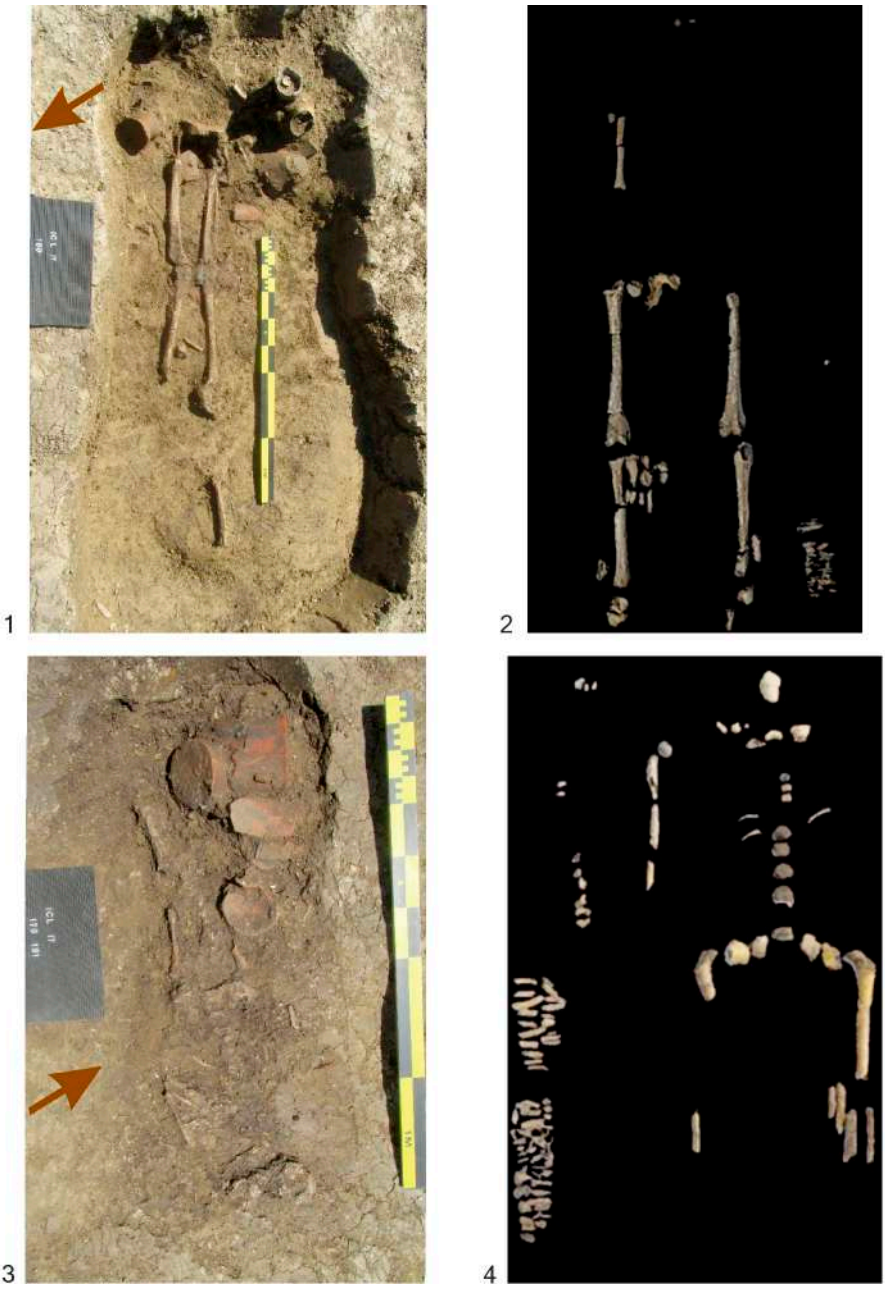
Pl. VII. 1–2. SK 142, archaeological context and anatomical layout; 3–4. SK 147, archaeological context and anatomical layout.
Pl. VII. 1–2. SK 142, contextul arheologic și reconstituirea anatomică; 3–4. SK 147, contextul arheologic și reconstituirea anatomică.



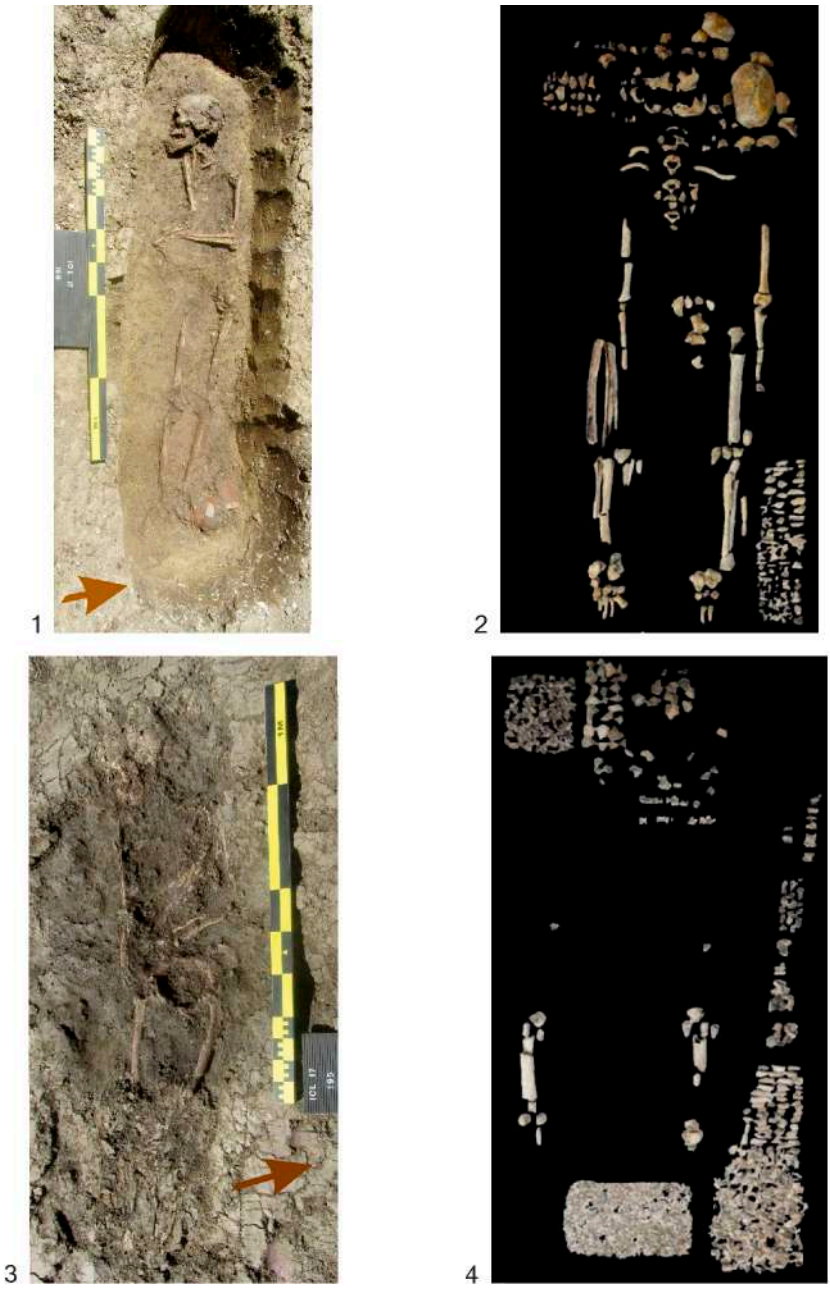
Pl. VIII. 1–2. SK 152, archaeological context and anatomical layout; 3–4. SK 153, archaeological context and anatomical layout.
Pl. VIII. 1–2. SK 152, contextul arheologic și reconstituirea anatomică; 3–4. SK 153, contextul arheologic și reconstituirea anatomică.



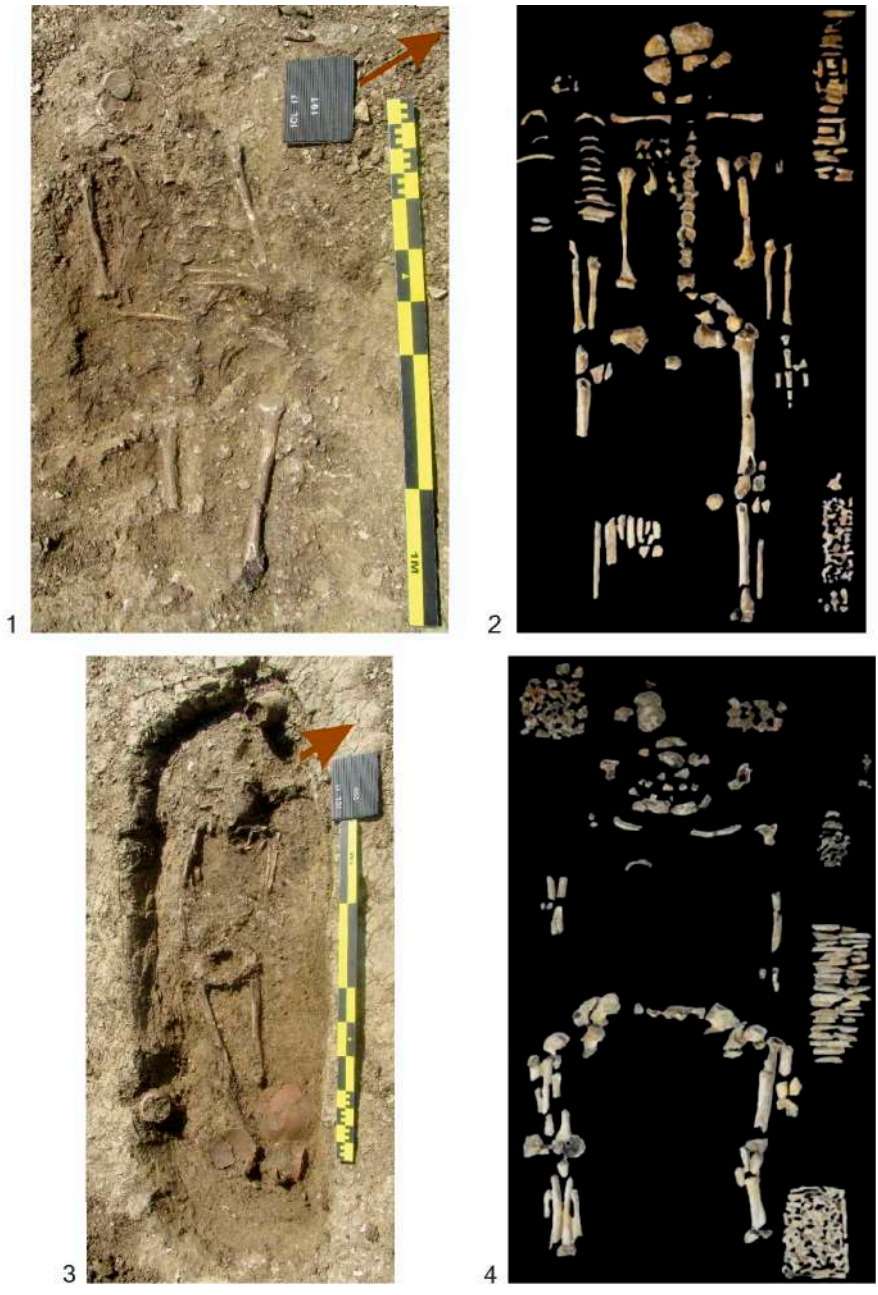
Pl. IX. 1–2. SK 157, archaeological context and anatomical layout; 3–4. SK 159, archaeological context and anatomical layout.
Pl. IX. 1–2. SK 157, contextul arheologic și reconstituirea anatomică; 3–4. SK 159, contextul arheologic și reconstituirea anatomică.



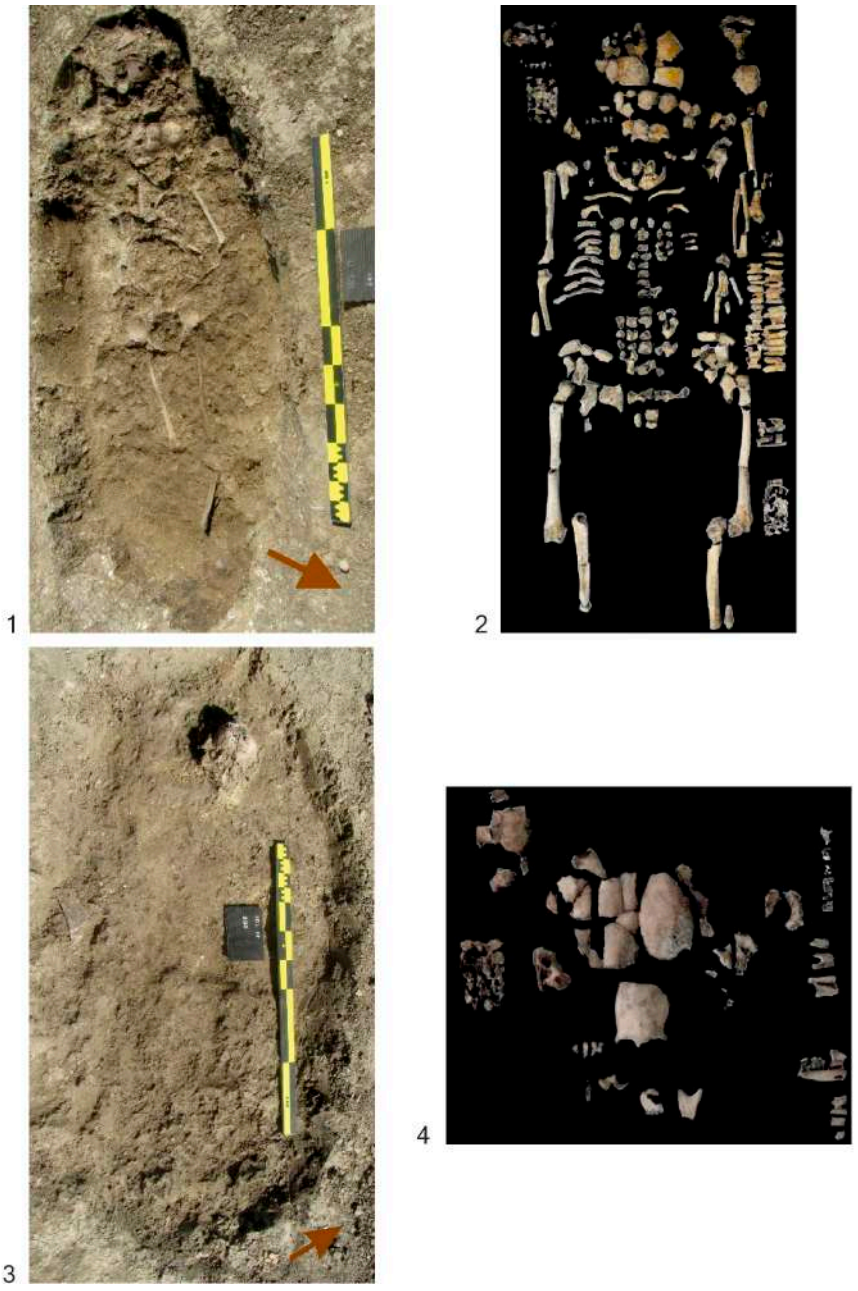
Pl. X. 1–2. SK 180, archaeological context and anatomical layout; 3–4. SK 181, archaeological context and anatomical layout.
Pl. X. 1–2. SK 180, contextul arheologic și reconstituirea anatomică; 3–4. SK 181, contextul arheologic și reconstituirea anatomică.



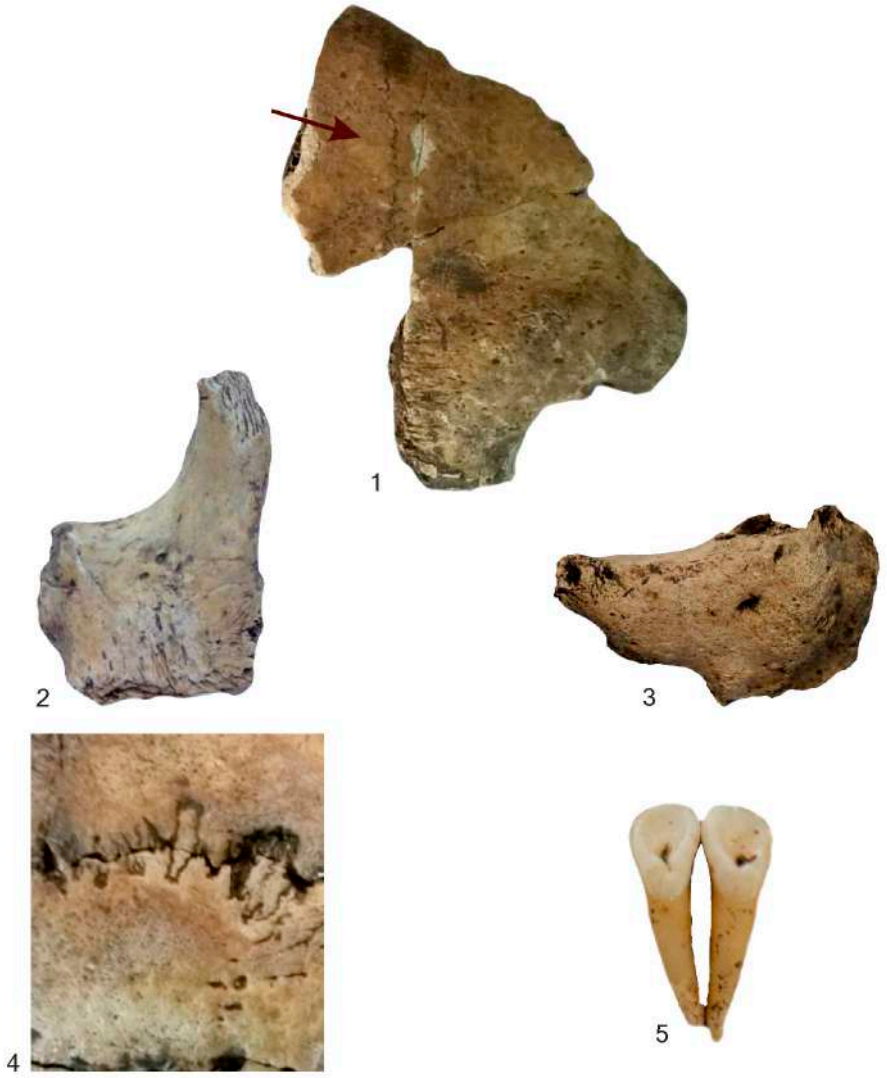
Pl. XI. 1–2. SK 190, archaeological context and anatomical layout; 3–4. SK 195, archaeological context and anatomical layout.
Pl. XI. 1–2. SK 190, contextul arheologic și reconstituirea anatomică; 3–4. SK 195, contextul arheologic și reconstituirea anatomică.



Pl. XII. 1–2. SK 197, archaeological context and anatomical layout; 3–4. SK 200, archaeological context and anatomical layout.
Pl. XII. 1–2. SK 197, contextul arheologic și reconstituirea anatomică; 3–4. SK 200, contextul arheologic și reconstituirea anatomică.

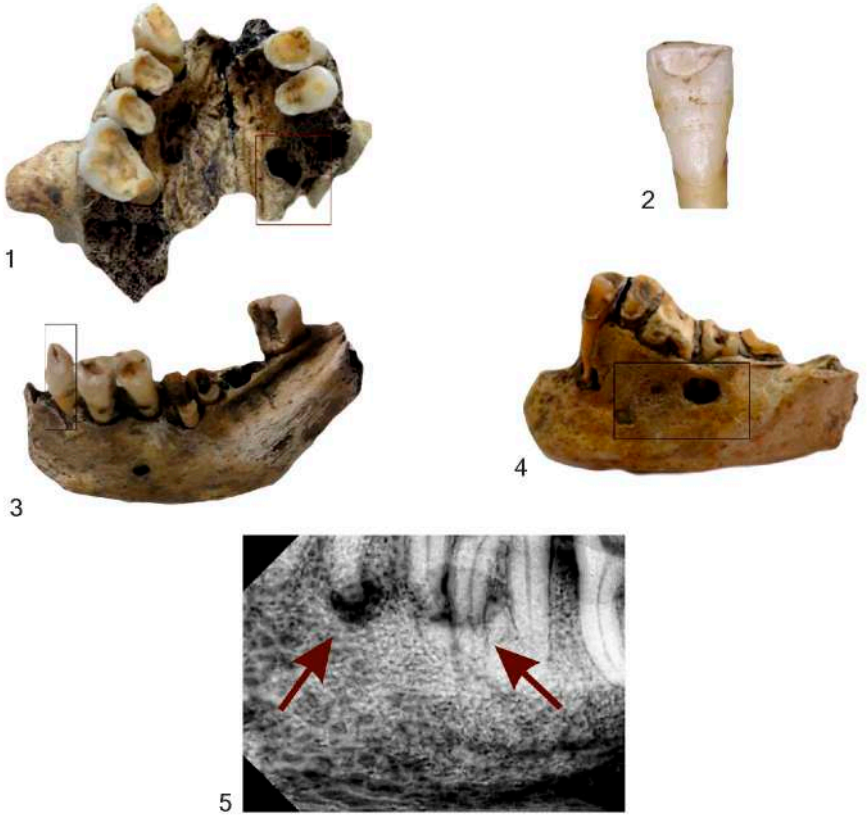


Pl. XIII. 1–2. SK 201, archaeological context and anatomical layout; 3–4. SK 233, archaeological context and anatomical layout.
Pl. XIII. 1–2. SK 201, contextul arheologic și reconstituirea anatomică; 3–4. SK 233, contextul arheologic și reconstituirea anatomică.



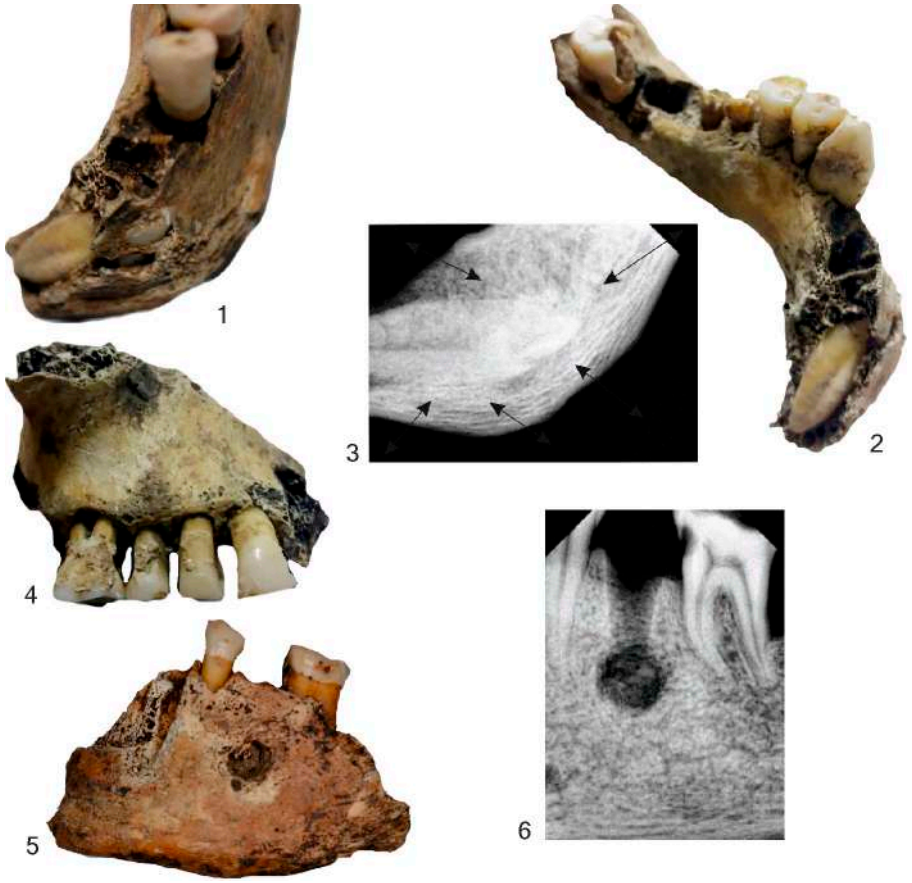
Pl. XIV. Epigenetic traits. 1. Retained metopic suture as seen on the frontal bone of SK 122; 2. Two zygomatico-facial foramina seen on the zygomatic bones of SK 142 and SK 157; 3. Lambdoid ossicles as seen on the skull of SK 122; 4. Shovel-shaped incisors as seen on the maxillary dentition of SK 105.

Pl. XIV. Trăsături epigenetice. 1. Sutură metopică, vizibilă pe osul frontal al SK 122; 2. Două foramene zigomatico-faciale, vizibile pe oasele zigomatice ale SK 142 și SK 157; 3. Osicule lambdoide, observate pe craniul SK 122; 4. Incisivi de tip „lopățică", vizibili pe dentiția maxilară a SK 105.



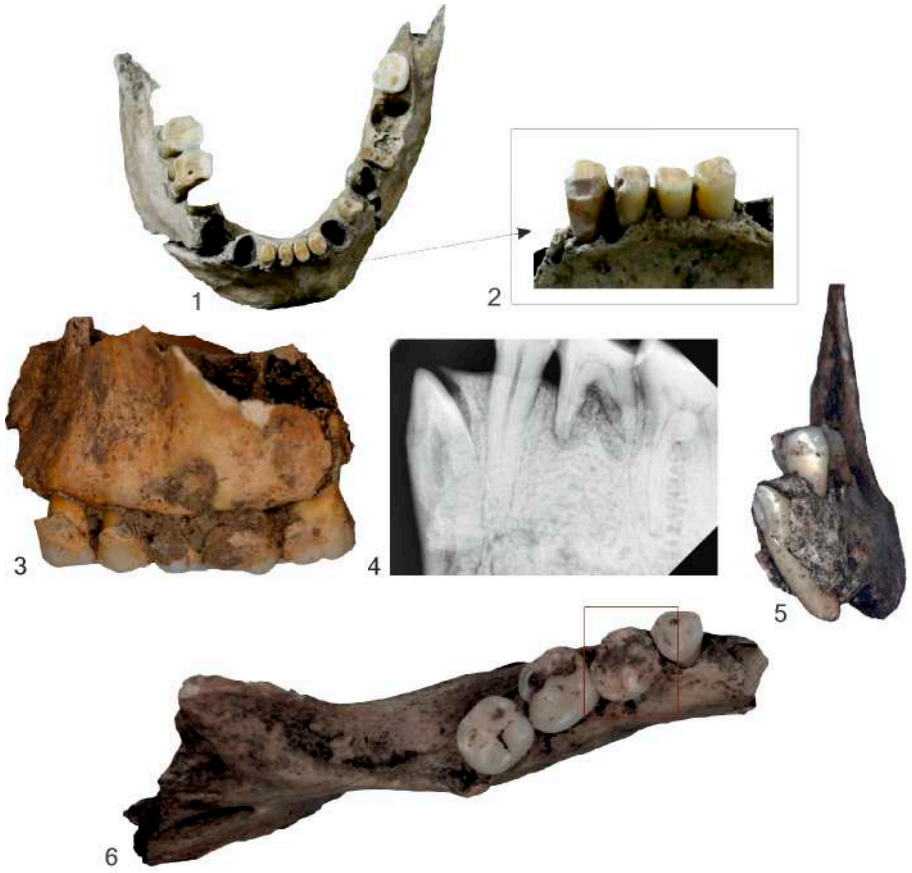
Pl. XV. Dental pathologies. 1. Abscess on the right maxillary molar – SK 132; Antemortem tooth loss – maxillary second molars; 2. Chipping, left lateral mandibular incisor – SK 142; 3. Dental caries, periodontitis – SK 132; Mesio-lingual rotation, canine – SK 132; Dental caries, mandibular first and third molars – SK 132; 4–5. Mandible – SK 107, periapical abscesses, second premolar, first molar; calculus, periodontitis; wear on the crowns, new bone formation, sign of active infection; X-ray, radiolucent areas, periapical abscesses.

Pl. XV. Patologii dentare. 1. Abces molar drept maxilar – SK 132; Pierderi *antemortem*, ambii molari II maxilari; 2. Ciobire, incisiv lateral mandibular stâng – SK 142; 3. Carii dentare, parodontită – SK 132; Rotire mesio-lingual, canin – SK 132; Carii la molari mandibulari unu și trei – SK 132; 4–5. Mandibulă SK 107, abcese periapicale, premolar doi, molar unu; tartru, parodontită, uzură dentară, formare de os nou, semn de infecție activă; Radiografia evidențiază zone radiolucente, abcese periapicale – SK 107.



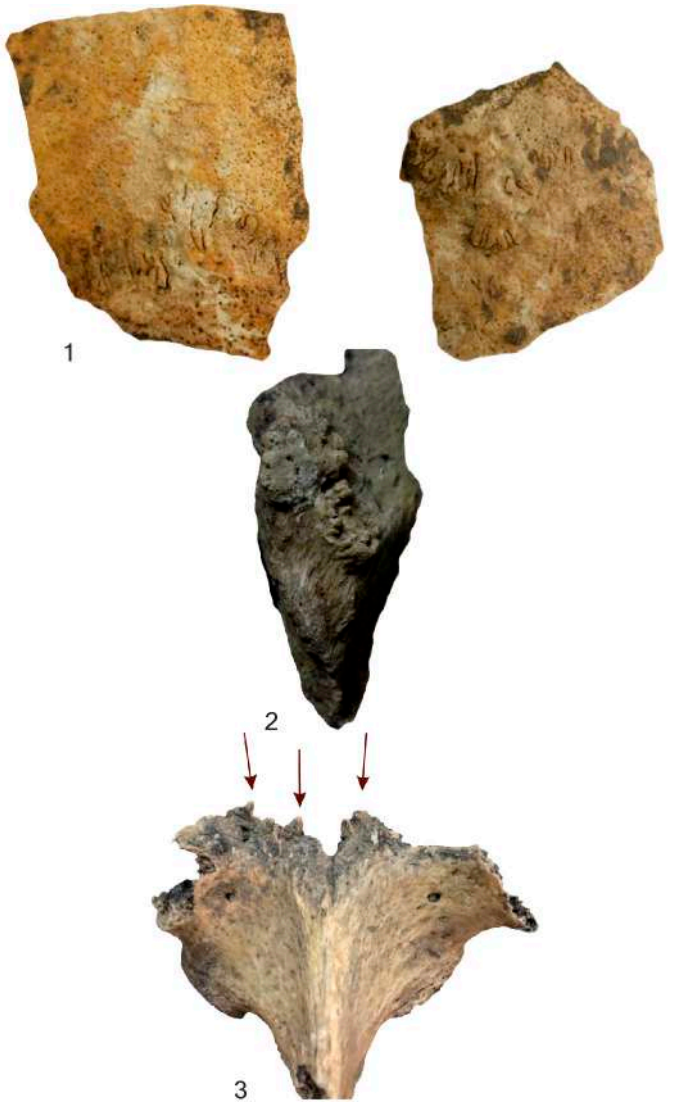
Pl. XVI. Dental pathologies. 1. Dental impaction on the left mandibular canine, obliquely angled and protruding the mandibular bone – SK 132; 2. Dental caries on the interproximal facet of the third molar, periodontitis, supragingival calculus – SK 132; 3. X-ray with a well-defined radiopaque area at the impacted mandibular canine – SK 132; 4. Supragingival calculus, maxilla – SK 132; 5. Periapical abscess, the second mandibular premolar – SK 200; 6. X-ray with a radiolucent area at the apex the second premolar – SK 200.

Pl. XVI. Patologii dentare. 1. Impactare canin mandibular stâng – SK 132; canin înclinat oblic și protruziv în mandibulă; 2. Carii dentare pe fața interproximală a celui de-al treilea molar, parodontită și depuneri de tartru supragingival – SK 132; 3. Radiografie cu o zonă radiopacă bine delimitată, la caninul mandibular impactat – SK 132; 4. Depuneri de tartru supragingival, maxilar – SK 132; 5. Abces periapical, al doilea premolar mandibular – SK 200; 6. Radiografie cu o zonă radiolucidă, la alveola premolarului doi – SK 200.



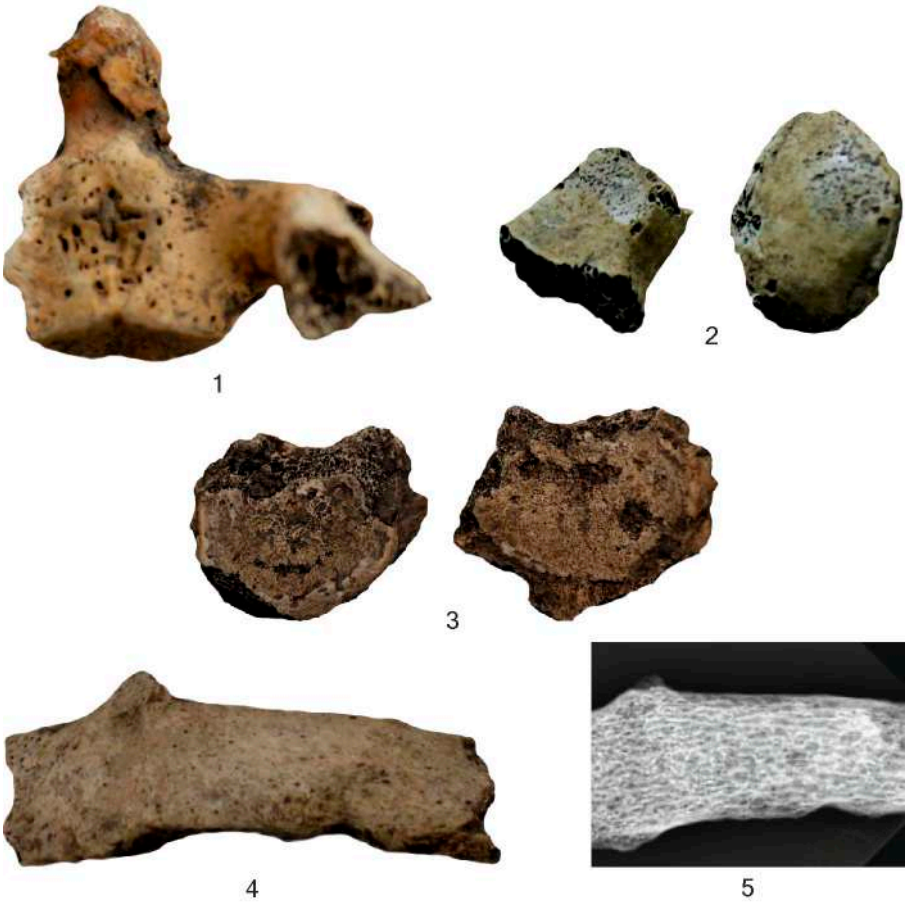
Pl. XVII. Dental pathologies. 1–2. Extramasticatory wear on the incisors of SK 152; antemortem tooth loss of the left first molar – Sk 152; 3. Supragingival calculus on the maxillary dentition of SK 233; 4–6. Impaction and retention of deciduous dentition – SK 190; 4. Impaction of the left mandibular canine – SK 190; 5. X-ray displaying severe crowding of the retained first decidual molar and the permanent one; note the radiolucent area surrounding the roots of the first deciduous molar, likely consistent with resorption due to retention, or a developing inflammation – SK 190; 6. Retention of the first deciduous molar – SK 190.

Pl. XVII. Patologii dentare. 1–2. Uzură extramasticatorie, expunere de dentină la incisivii SK 152; pierderea *antemortem* a primului molar stâng – Sk 152; 3. Depuneri de tartru supragingival pe dentiția maxilarului – SK 233; 4–6. Impactare, retenție dentiție deciduală – SK 190; 4. Impactare canin mandibular stâng – SK 190; 5. Radiografie ce arată o aglomerare la primul molar decidual și la cel definitiv; se observă o zonă radiolucidă la rădăcinile primului molar decidual, probabil datorată resorbției din cauza retenției sau unui proces inflamator în curs de dezvoltare – SK 190; 6. Retenție de prim molar decidual mandibular – SK 190.



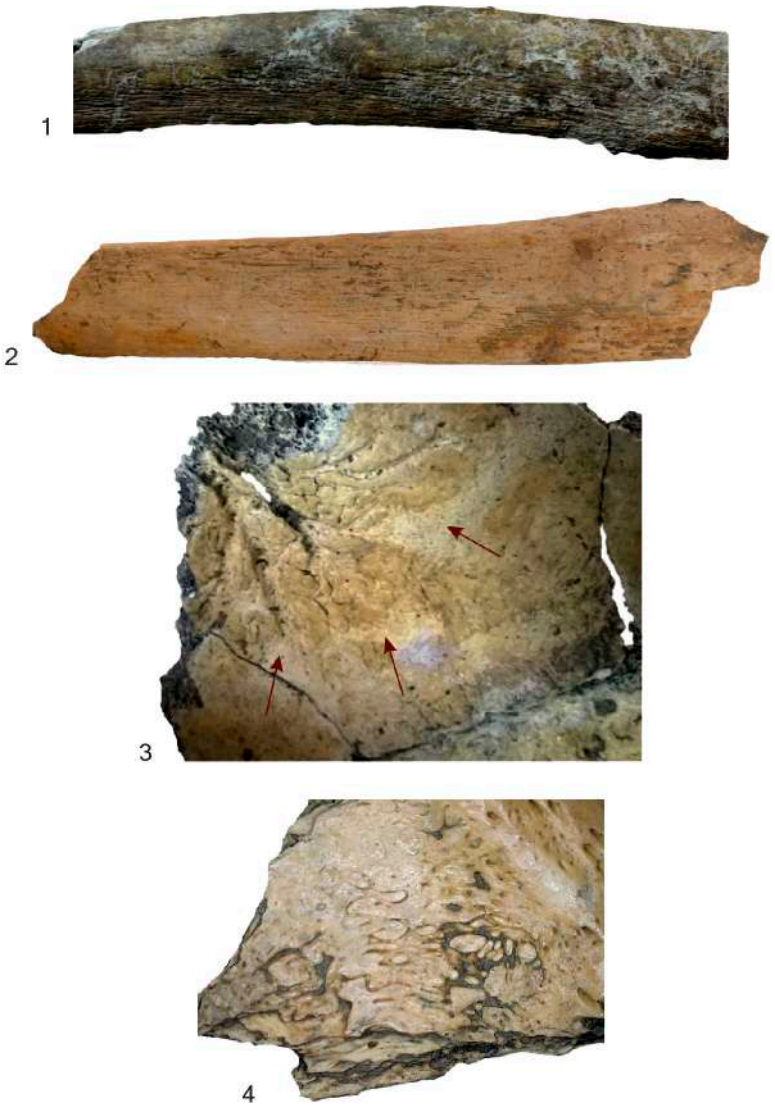
Pl. XVIII. 1. Craniosynostosis as seen on the lambdoid suture of SK 107; 2. Entheses on the anterior iliac spine of SK 157, site for the sartorius muscle; 3. Ossification of the ligamentum flavum as seen on the thoracic vertebrae of SK 157 (note the bony excrescences at the attachment sites of the ligamentum flavum).

Pl. XVIII. 1. Craniosinostoză observată pe sutura lambdoidă a SK 107; 2. Enteze pe linia iliacă anterioară a SK 157, aferentă mușchiului *sartorius*; 3. Osificarea ligamentului *flavum*, vizibilă pe vertebrele toracice ale SK 157 (excrescențe osoase de la zonele de atașare ale ligamentului *flavum*).



Pl. XIX. 1. The odontoid process of the second cervical vertebra of SK 119 displaying osteophytes and lipping; 2. Osteoarthritis clearly marked by eburnation and porosities on the carpal bones of SK 152; 3. Marginal osteophytes on the thoracic vertebrae of SK 152; 4. Healed fracture on a central rib belonging to SK 152; 5. X-ray showing clear cortical irregularity at the shaft with a change in the continuity of the rib's outline (note the dense callus formation, with increased radiopacity in the area).

Pl. XIX. 1. Procesul odontoid al celei de-a doua vertebre cervicale a SK 119, prezentând osteofite și *lipping*; 2. Osteoartrită, evidențiată prin eburnare și porozități pe oasele carpiene ale SK 152; 3. Osteofite marginale pe vertebrele toracice ale SK 152; 4. Fractură vindecată pe o coastă centrală, aparținând SK 152; 5. Radiografie ce evidențiază iregularități corticale clare la nivelul diafizei, cu modificări ale continuității conturului coastei, cu formarea densă de calus osos, decelat prin radiopacitate crescută.



Pl. XX. 1. Tibia belonging to SK 157 showing an active healing infection (mixture of woven and lamellar bone); 2. SK 116 showing an active infection on the tibia (lamellar bone); 3. Endocranial modifications on the left parietal of SK 122; 4. Endocranial modifications, "hair-on-end" type on the left parietal of SK 133.

Pl. XX. 1. Tibia SK 157, prezentând o infecție în proces activ de vindecare (cu formare de țesut osos fibrilar și lamelar); 2. SK 116, cu o infecție activă pe tibie (țesut lamelar); 3. Modificări endocraniene pe parietalul stâng al SK 122; 4. Modificări endocraniene, de tip „hair-on-end", pe parietalul stâng al SK 133.



Pl. XXI. 1. Cribra orbitalia as seen in SK 233; 2. Cribra orbitalia as seen in SK 201; 3. Cribra orbitalia as seen in SK 142 (detail).
Pl. XXI. 1. *Cribra orbitalia*, vizibilă la SK 233; 2. *Cribra orbitalia*, vizibilă la SK 201; 3. *Cribra orbitalia*, vizibilă la SK 142 (detaliu).